Microtubules and Intermediate Filaments

Chien, 2025

An actin filament is flexible, has a helical repeat every 37 nm, ranges from 5-9 nm in diameter.

The outer diameter of a microtubule is between 23 and 27 nm while the inner diameter is between 11 and 15 nm.

IF proteins is conserved alpha-helical rod shape, formation of filaments roughly 8 to 12 nm in diameter (10 nm).

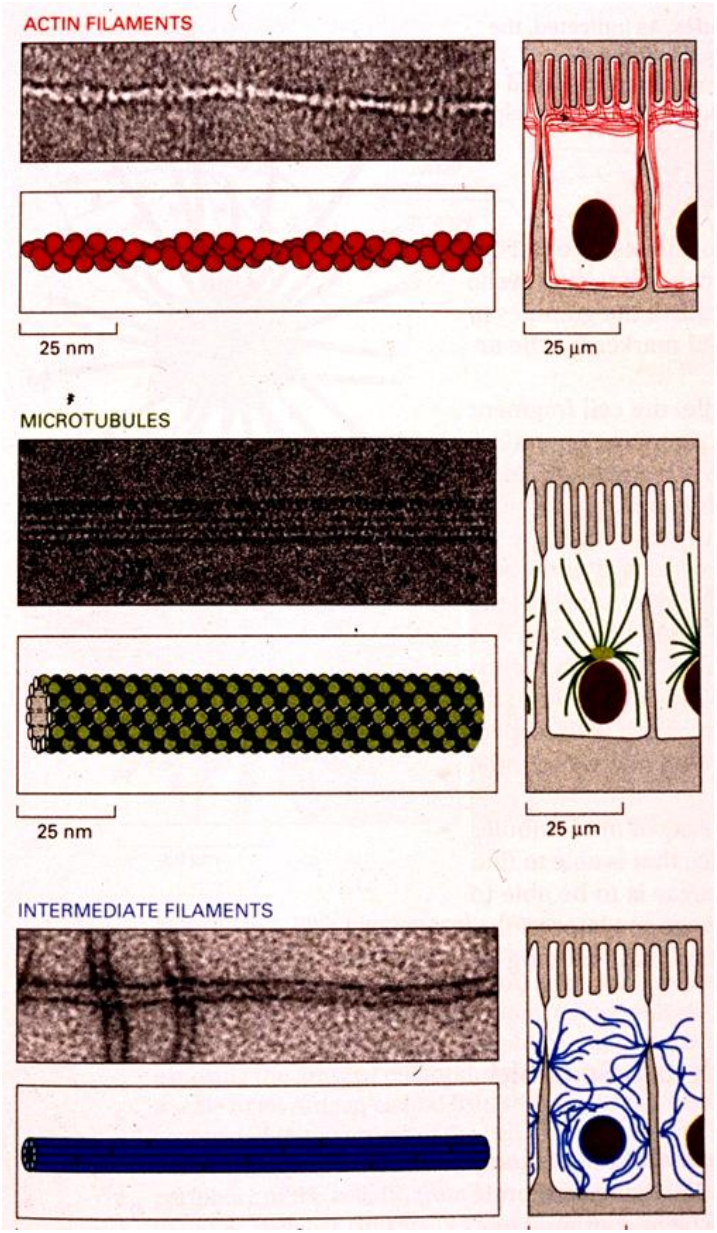

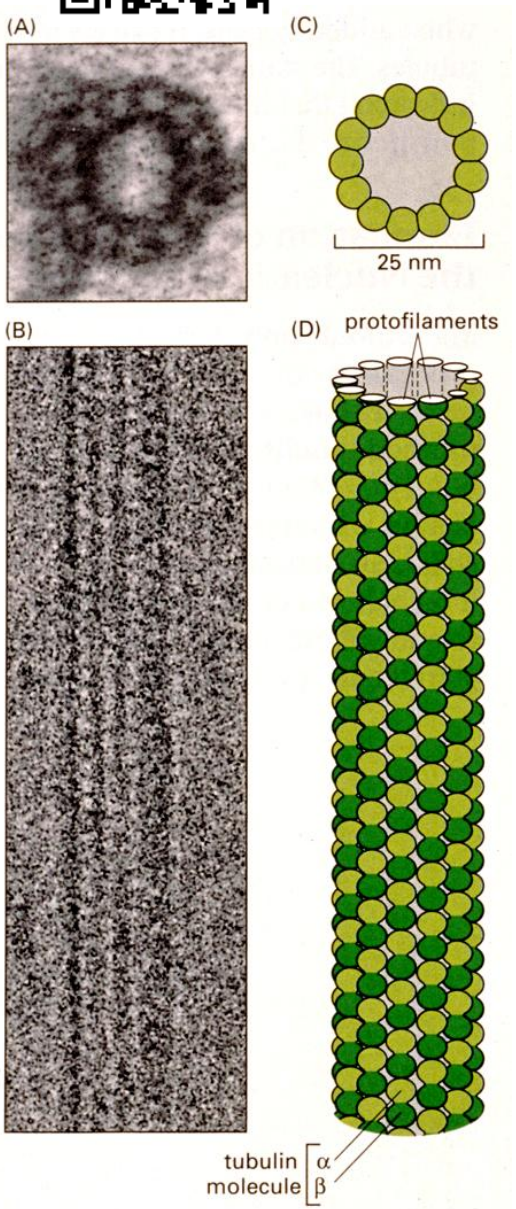

Cytoskeletons in the culture cell

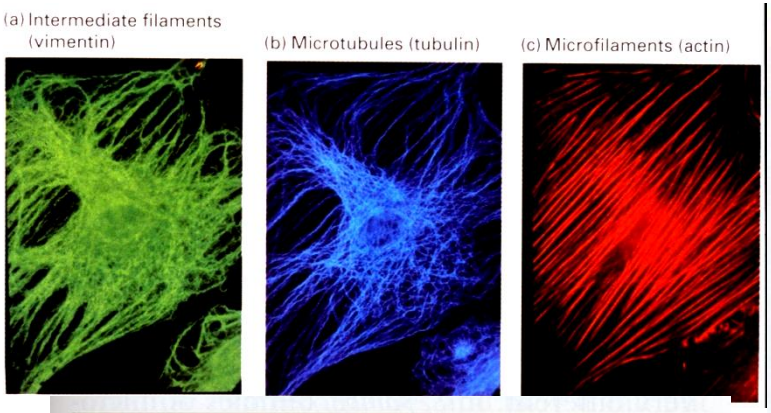

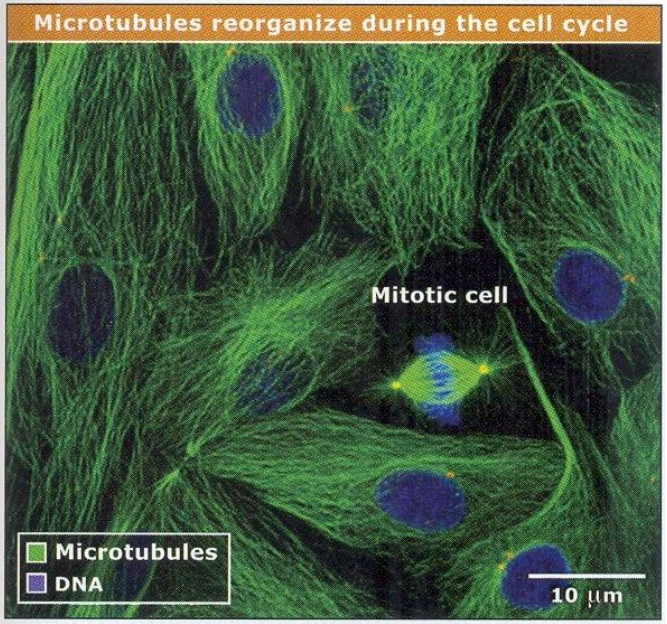

FIGURE 7.6 A field of about a dozen cells is shown, with their microtubules and chromosomes visualized by fluorescence microscopy. One mitotic cell—with its microtubules assembled into a very clear mitotic spindle—is surrounded by interphase cells. The reorganization of microtubules that takes place as a cell enters mitosis is dramatic but requires only a few minutes. Photo courtesy of Lynne Cassimeris, Lehigh University.

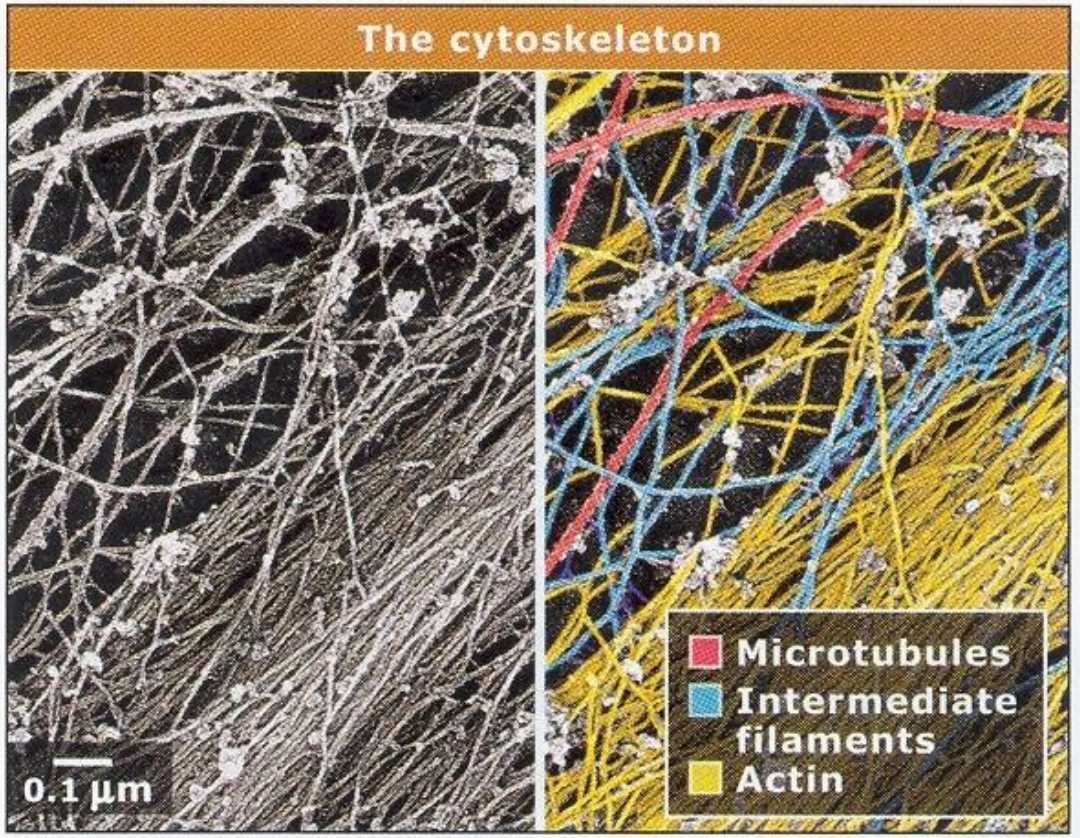

FIGURE 7.3 A small region of a fibroblast cell viewed by electron microscopy (left panel). Numerous filaments are visible. In the right panel, the three types of cytoskeletal polymers present in eukaryotic cells have been colored so that they can be easily distinguished from one another. Photos courtesy of Tatyana Svitkina. Reprinted from *J. Struct. Biol.*, vol. 115, Svitkina, T., et al., *Improved Procedures* . . ., pp. 290-303. Copyright 1995, with permission from Elsevier.

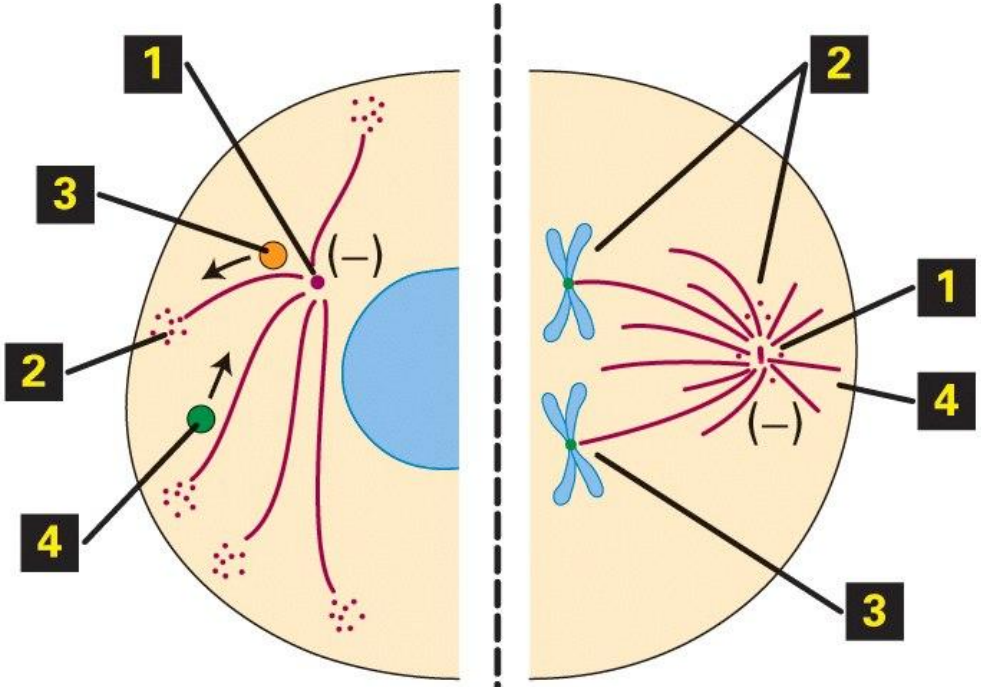

Interphase cell

Mitotic cell

CYTOSKELETAL COMPONENT	CELL FUNCTION
1 MTOC, spindle pole	Organizing cell polarity
2 Microtubule dynamics	Chromosome movements MT assembly
3 Kinesin motors	(+) end–directed vesicle and chromosome transport
4 Dynein motors	(–) end–directed vesicle transport spindle assembly

Microtubules

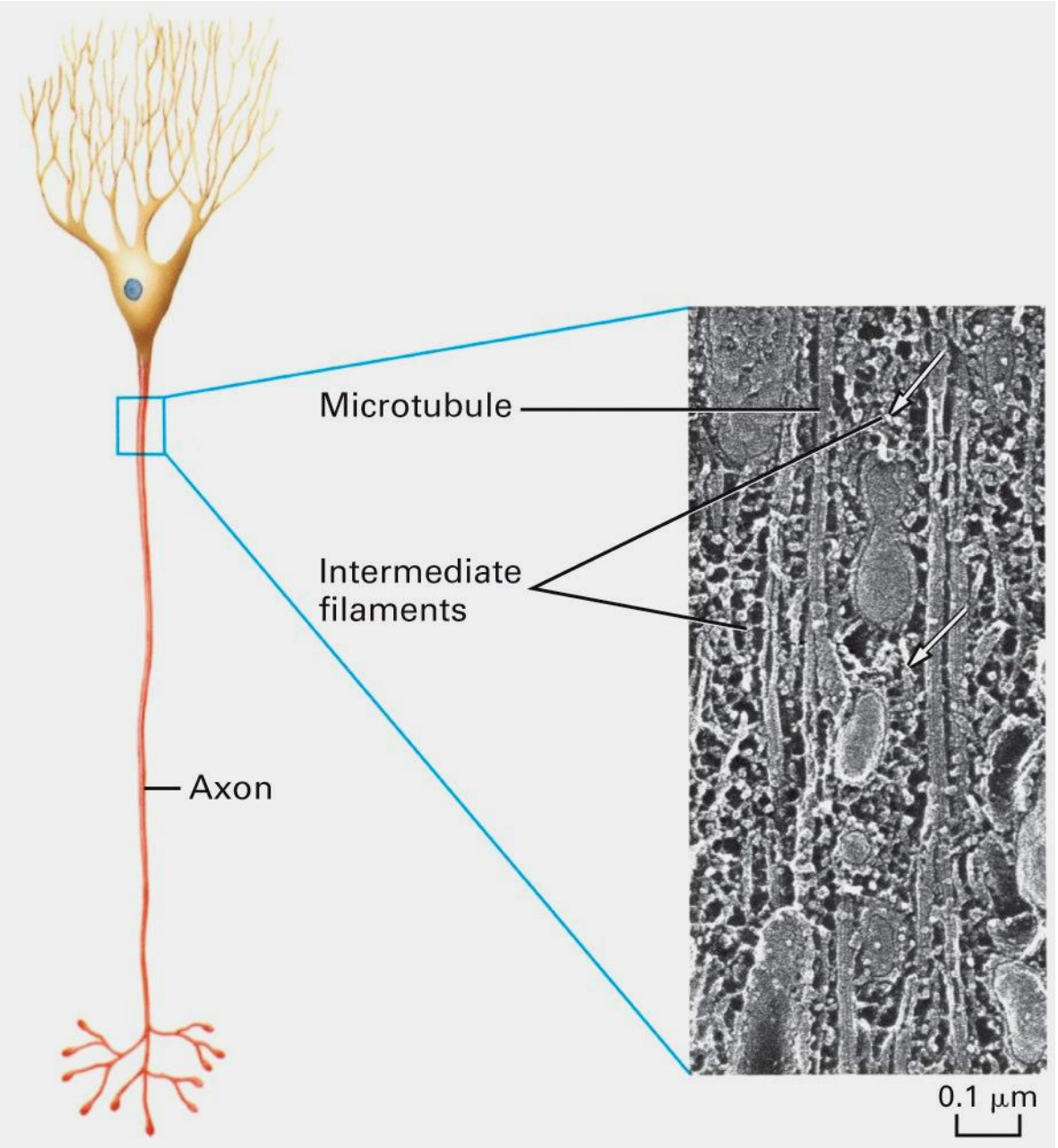

Cilia

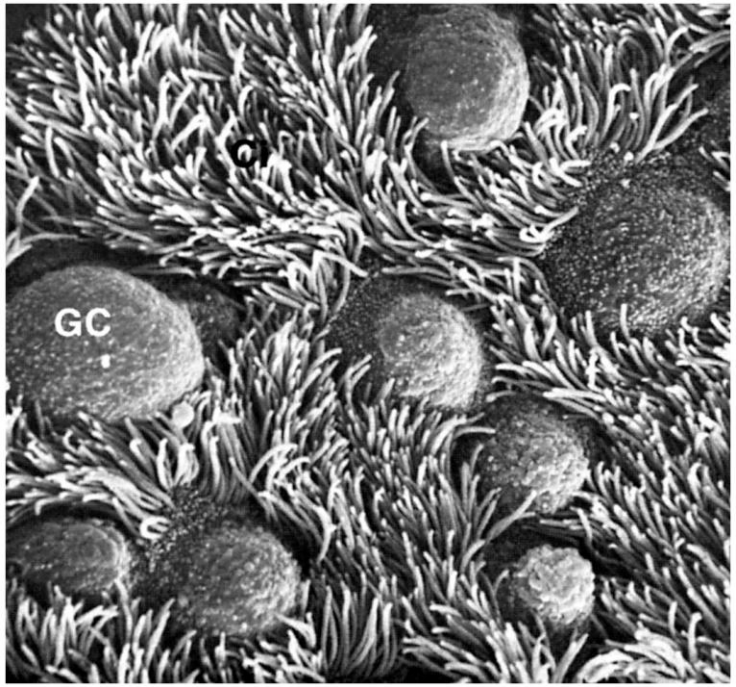

Mitotic spindle

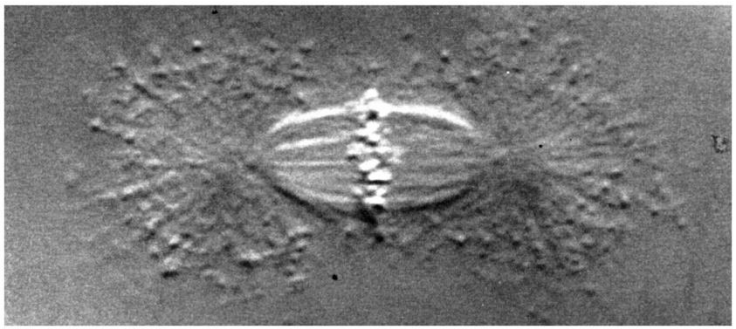

Microtubules in the RBC of toadfish

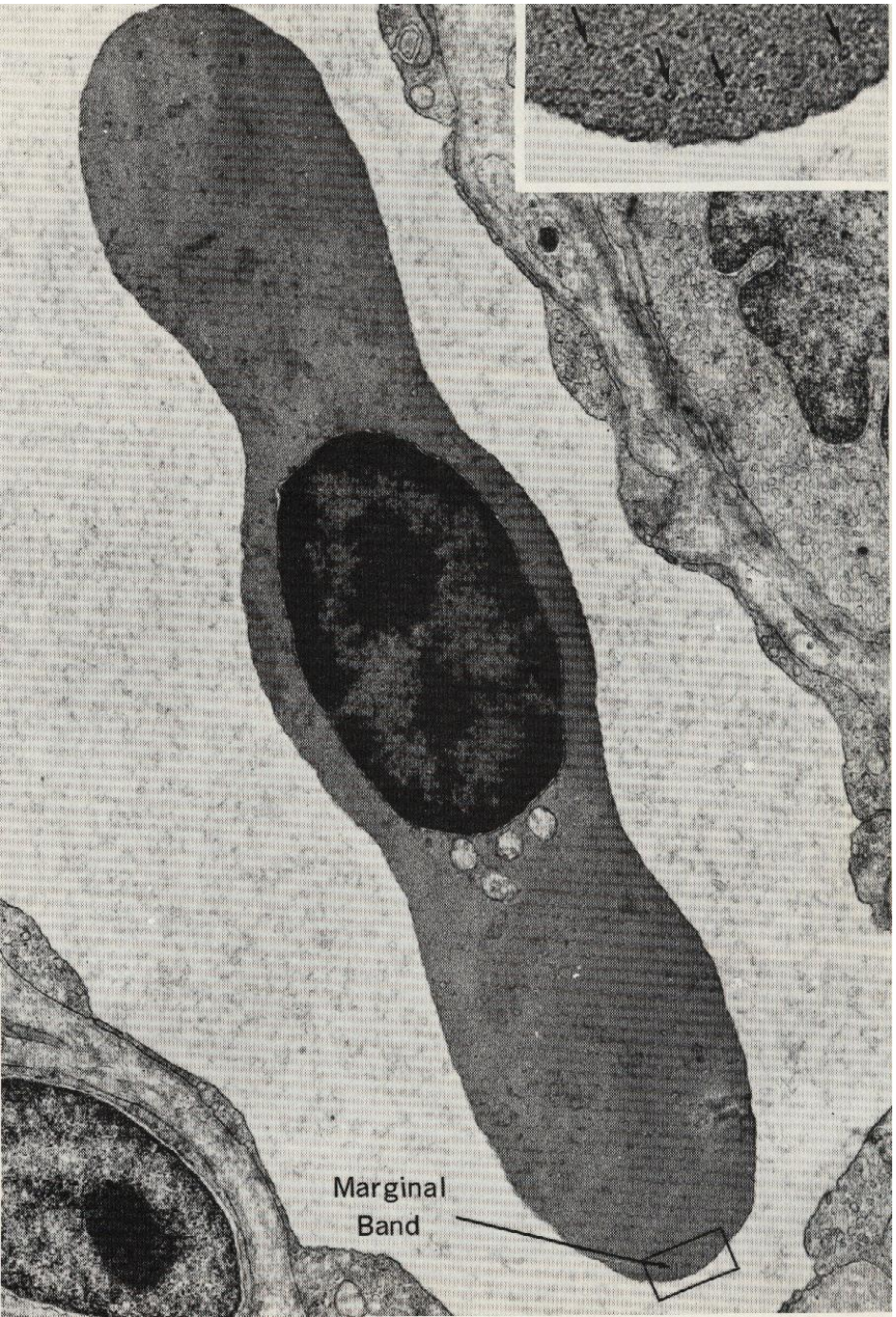

Microtubules in the blood platelet

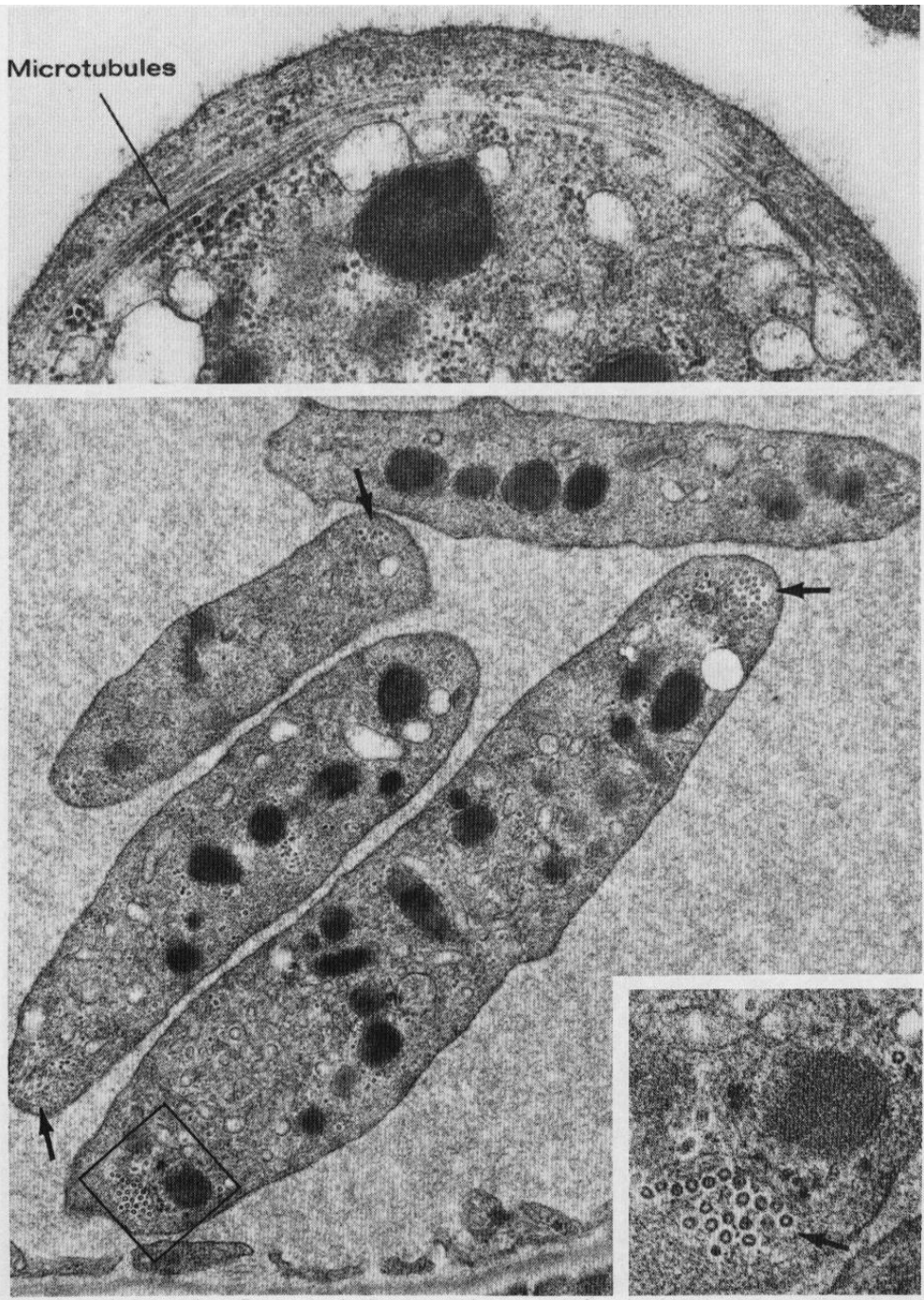

Tubulin structures

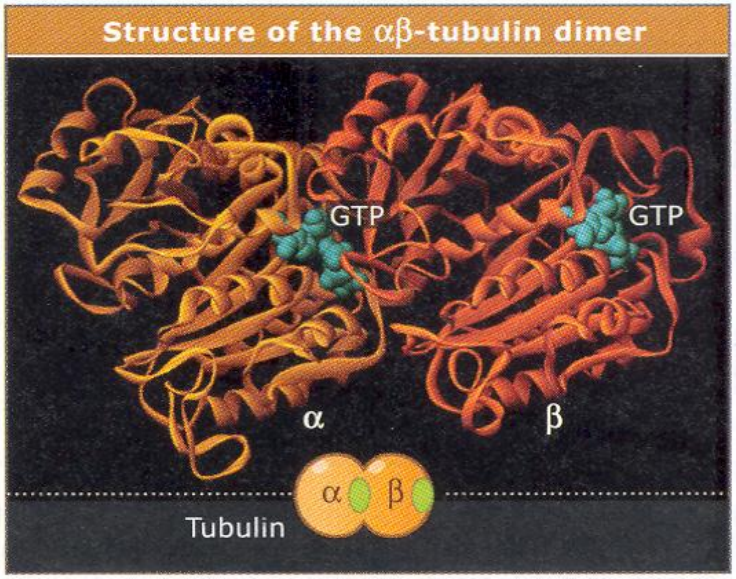

FIGURE 7.11 The three-dimensional structure of the tubulin heterodimer, the basic building block of a microtubule. In gold and copper colors are the polypeptide backbones of the two protein subunits, and in green are the two molecules of GTP that are bound to each heterodimer. Note the similarity in the stuctures of the two subunits, and that they are arranged head-to-tail in the complex. At the bottom is a schematic drawing that shows how the dimer will be represented in the figures in the chapter. Modified from Nogales, E., Wolf, S. G., and Downing, K. H. *Nature*. 1998. 391: 199-203.

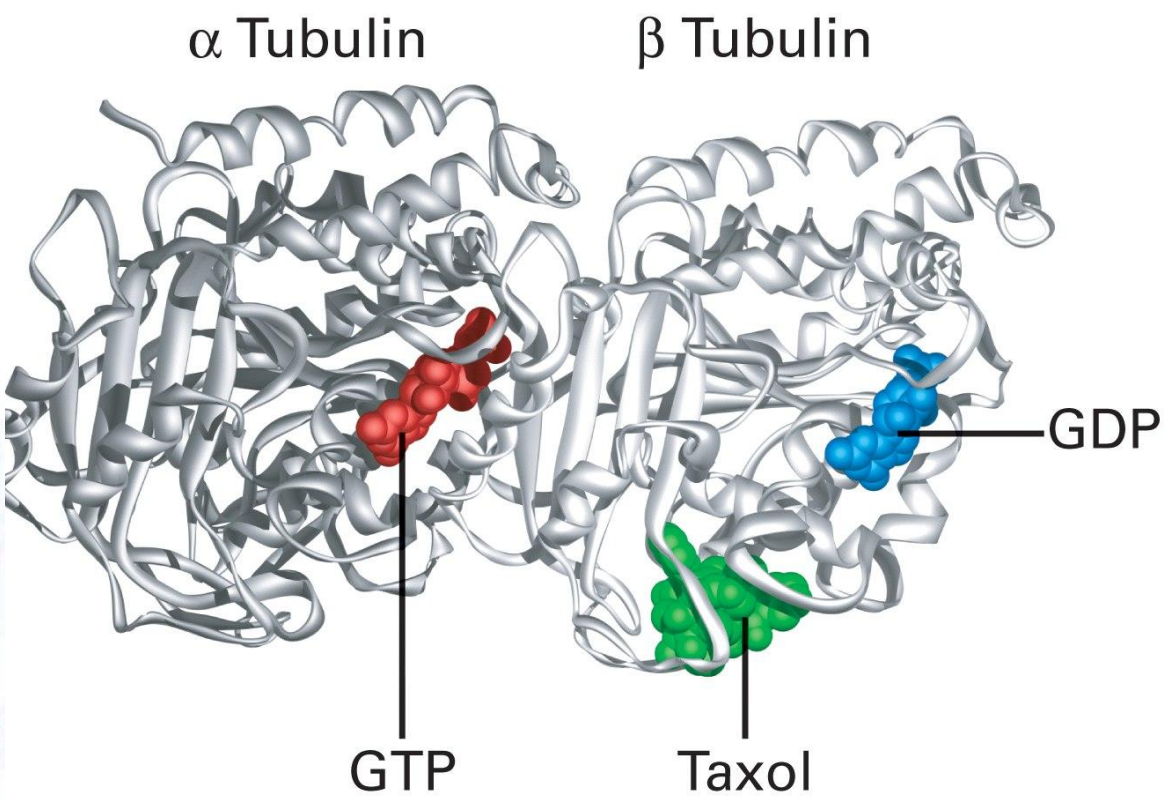

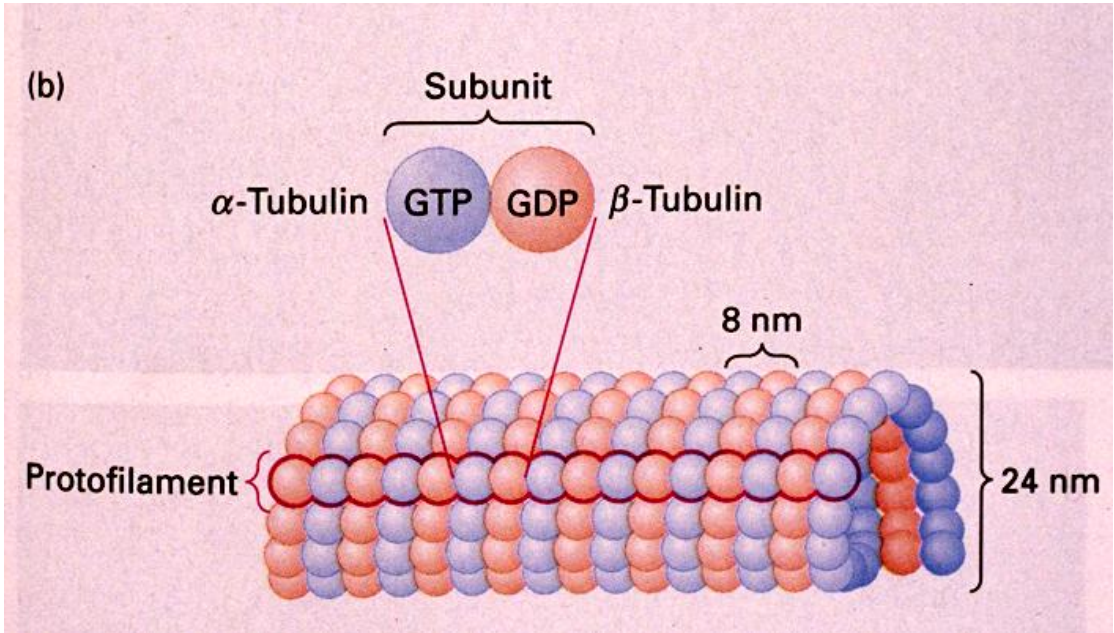

Microtubule structure (Subunit)

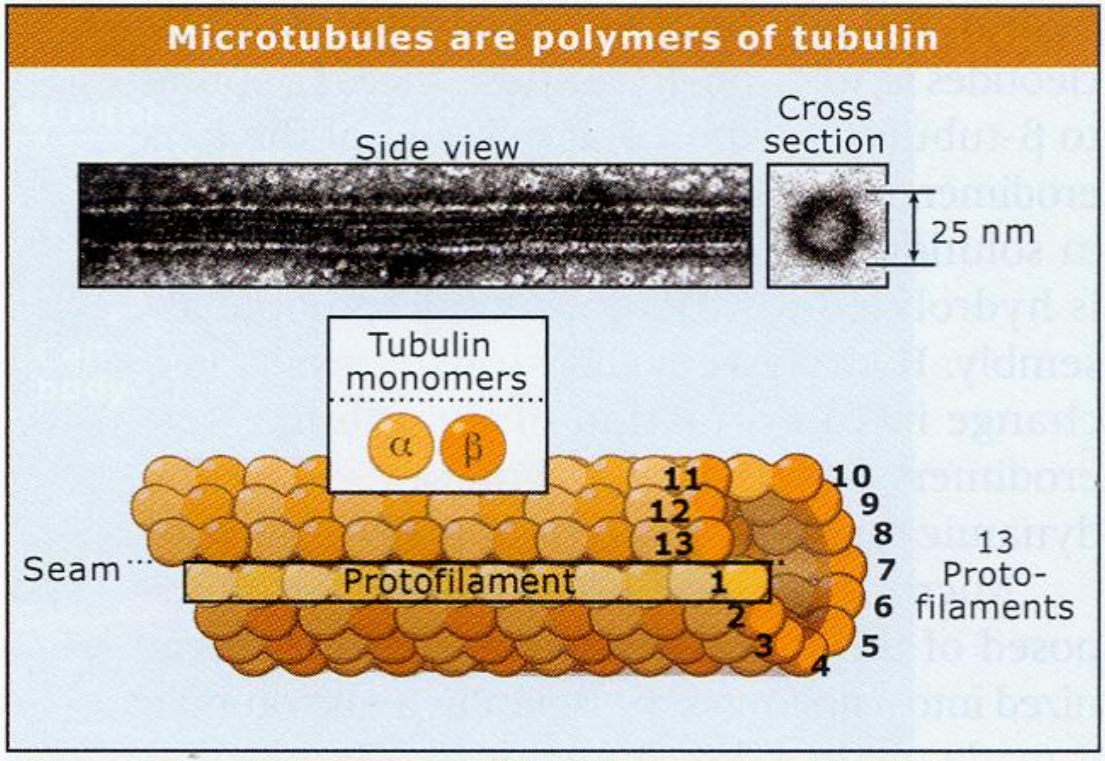

FIGURE 7.12 The structure of a small segment of a microtubule. The individual tubulin heterodimers are aligned end-to-end in straight protofilaments, and the protofilaments are arranged side-by-side to form a hollow tube. All of the heterodimers have the same orientation, with the β subunit toward one end of the microtubule and the α subunit toward the other. At the top are electron micrographs of microtubules assembled from pure tubulin. Photo courtesy of Lynne Cassimeris, Lehigh University (left) and micrograph provided by Harold Erickson, Duke University School of Medicine (right).

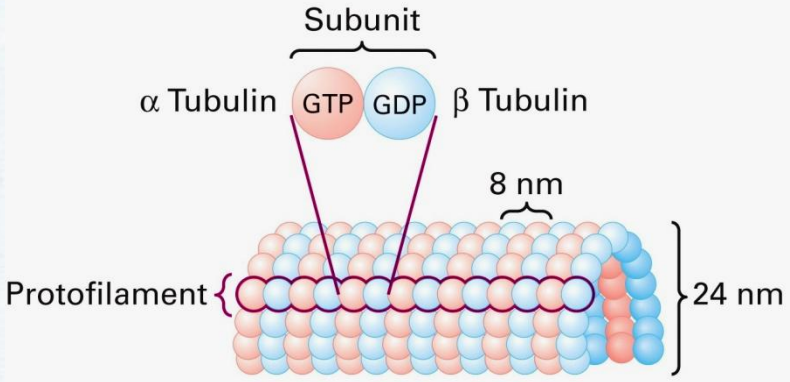

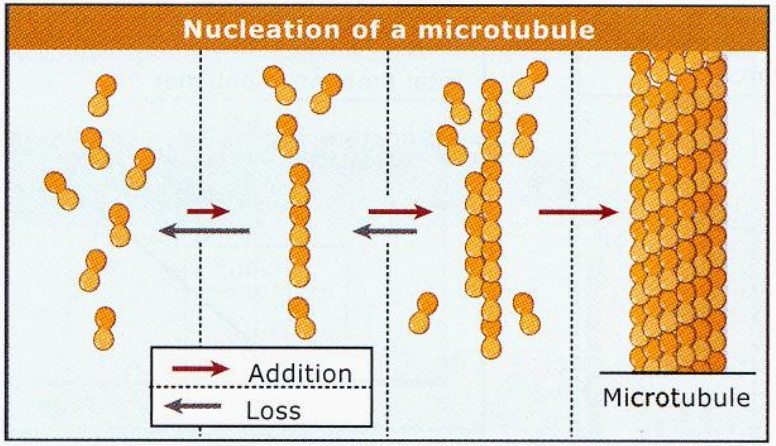

FIGURE 7.16 A simplified view of microtubule nucleation. A small number of dimers can associate, but the complex usually falls apart. In rare instances, however, additional dimers add on and dimers associate side-by-side. Once a complex of 6-12 dimers is formed, it is likely to continue growing. A small sheet of protofilaments results that will eventually close into a short microtubule, often called a "seed."

Arrangement of protofilaments in singlet, doublet, and triplet microtubules

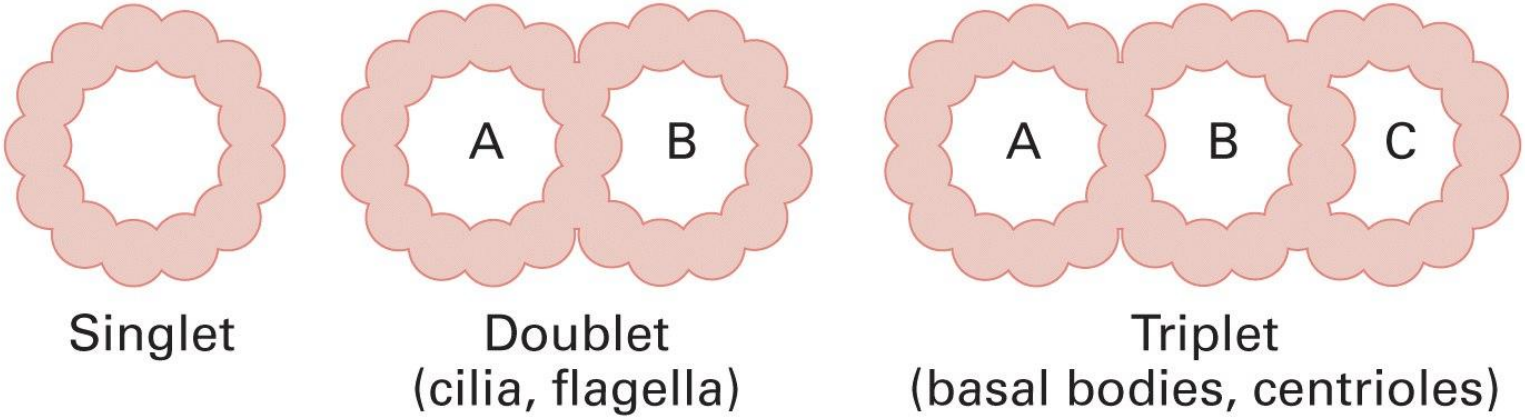

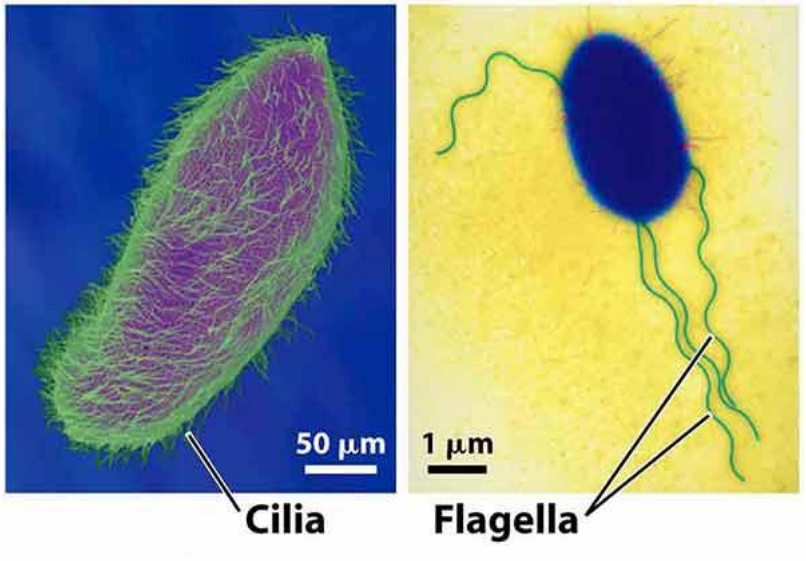

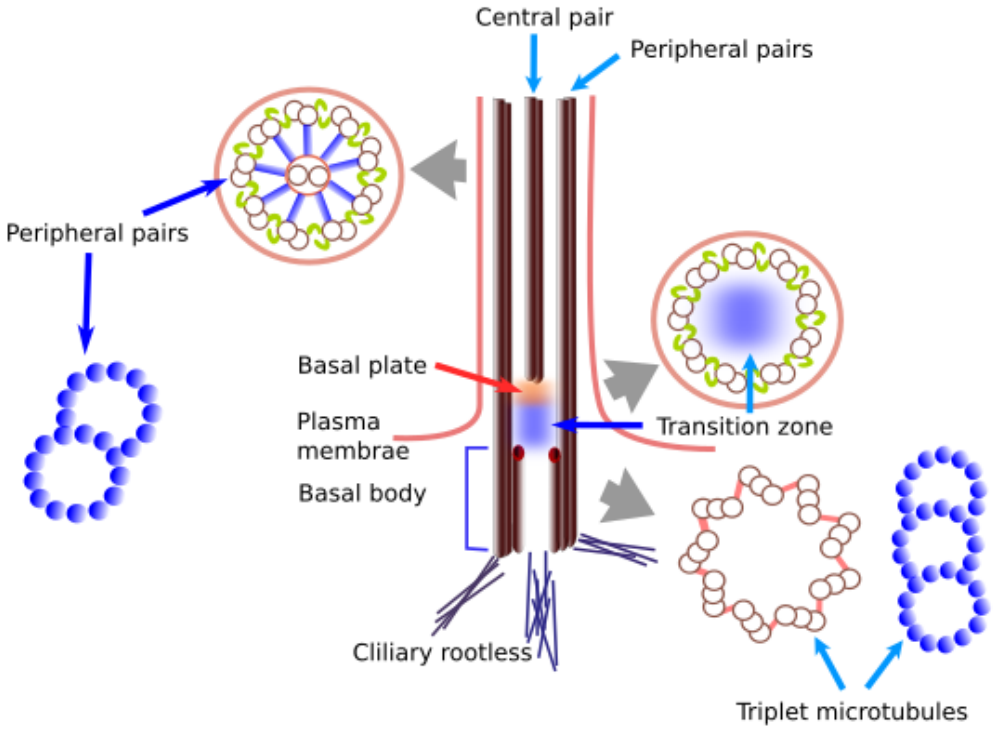

Cilia & flagella

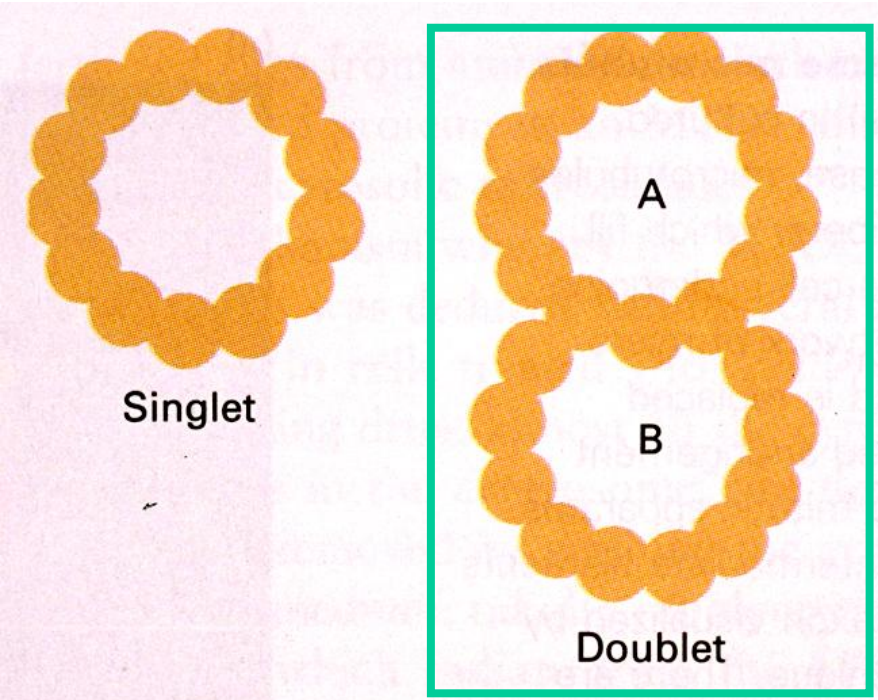

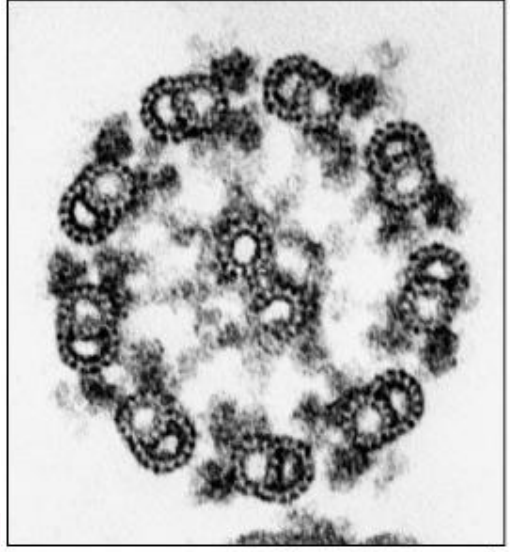

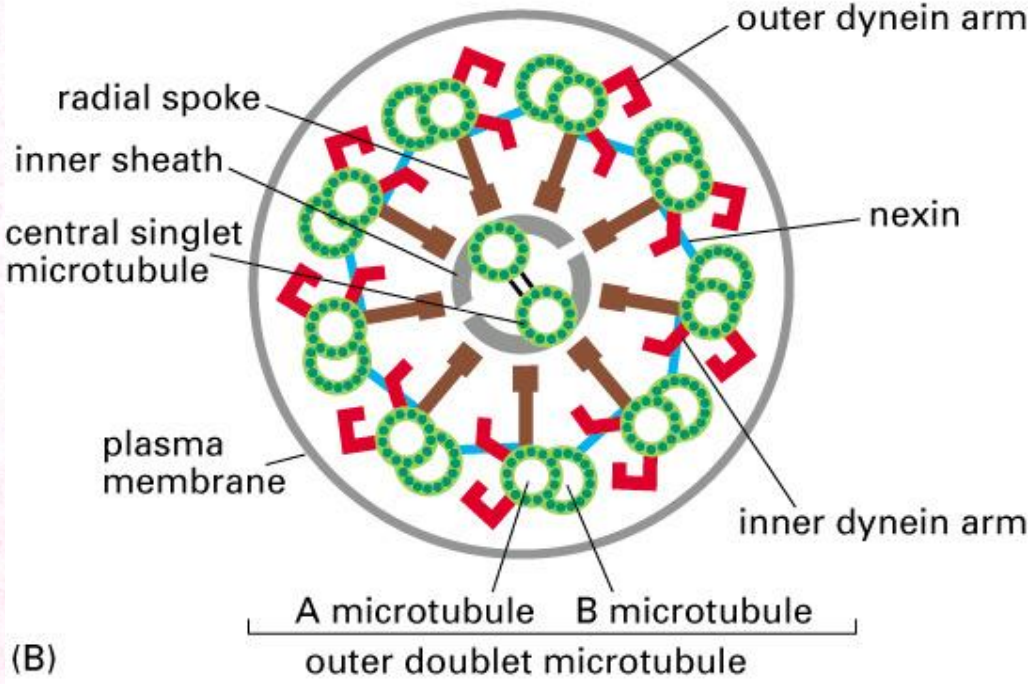

Figure 16–77. Molecular Biology of the Cell, 4th Edition.

Microtubule-organizing center (MTOC) Centrosome: Centrioles

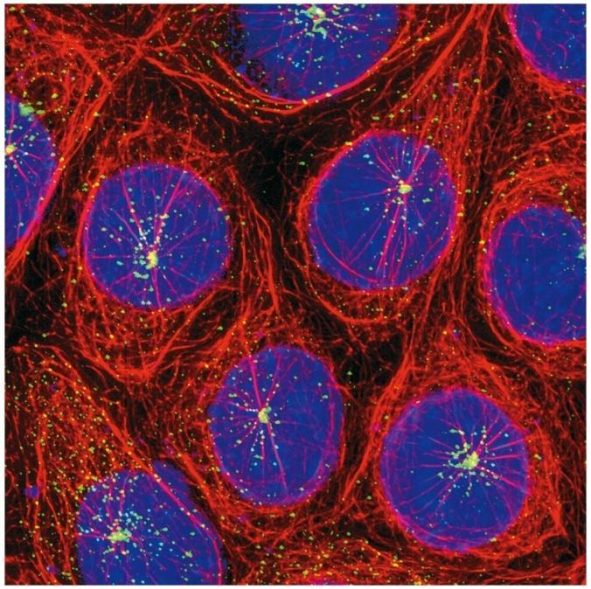

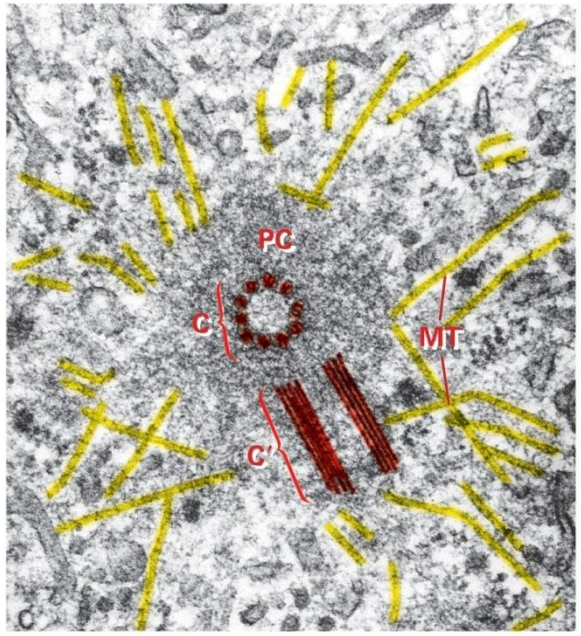

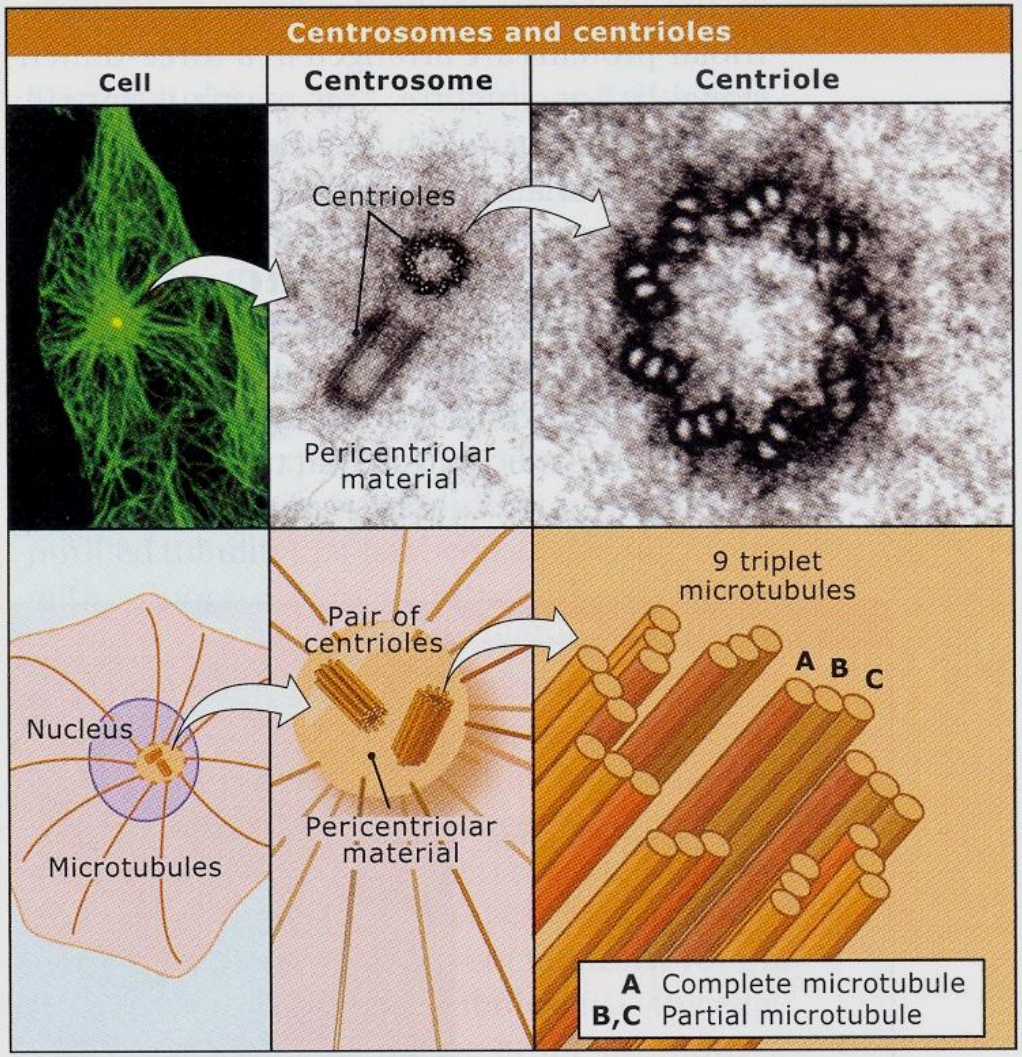

FIGURE 7.24 At the top left is a fluorescence micrograph of a whole cell with its microtubules labeled in green and its centrosome in yellow. Microtubules radiate from the centrosome. In the upper middle and right are electron micrographs of a whole centrosome and one of its two centrioles. The micrograph of the centrosome shows how the centrioles are arranged at right angles to one another. The pericentriolar material appears in the micrograph as a granular material immediately surrounding the two centrioles. Note how much clearer the cytoplasm is at the top and bottom of the picture. Photos courtesy of Lynne Cassimeris, Lehigh University.

Orientation of cellular microtubules

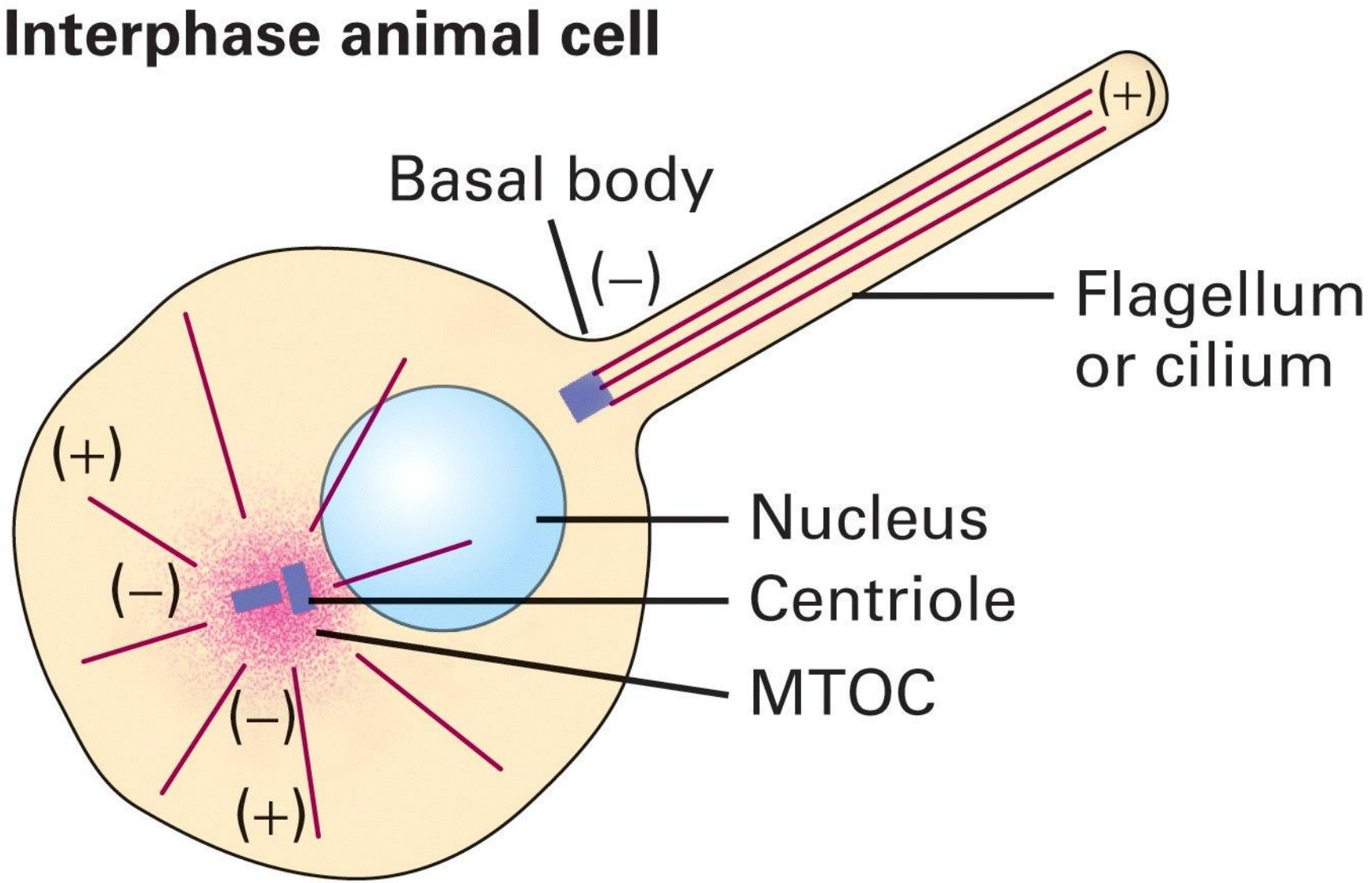

Orientation of cellular microtubules

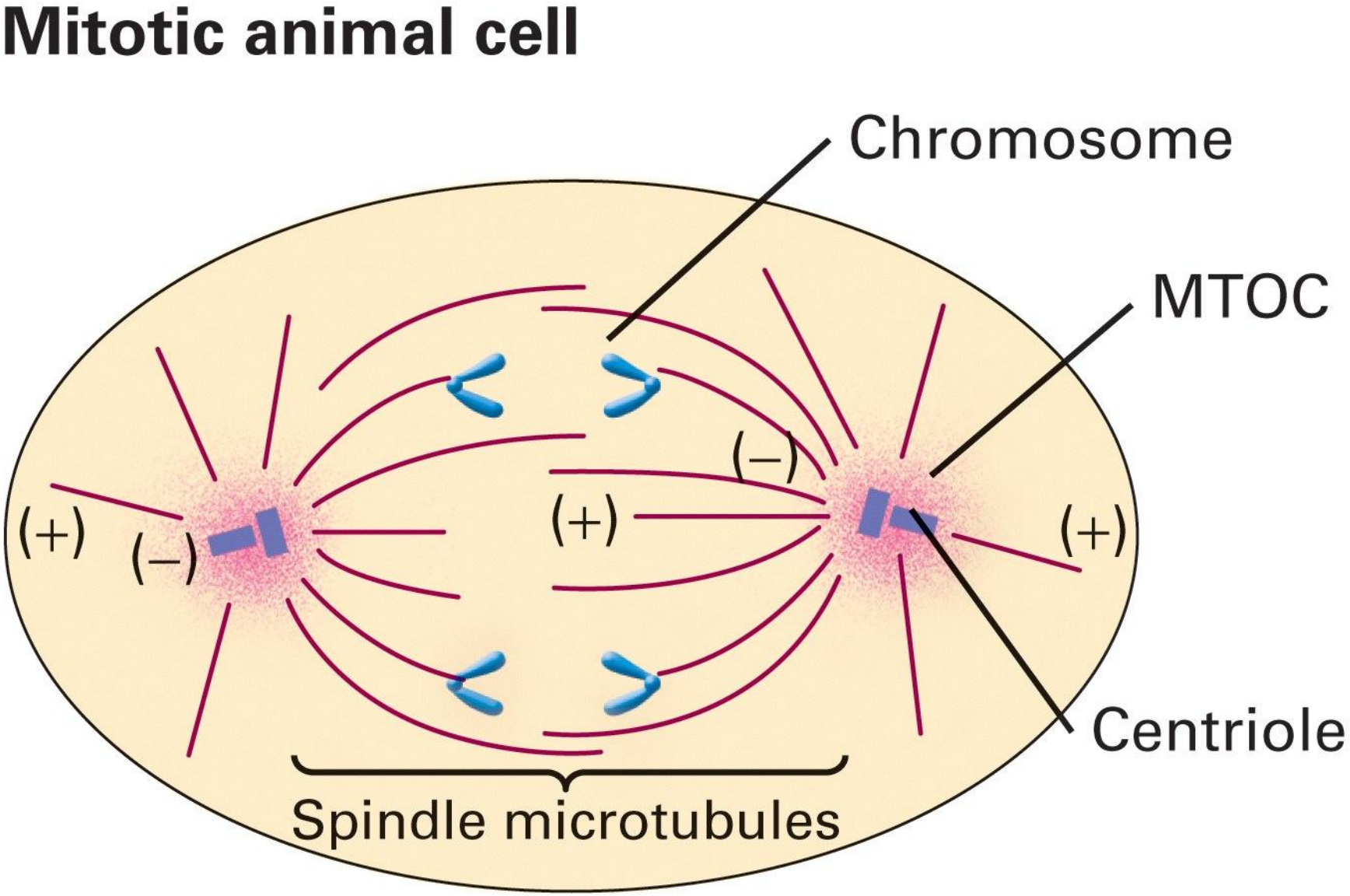

Orientation of cellular microtubules

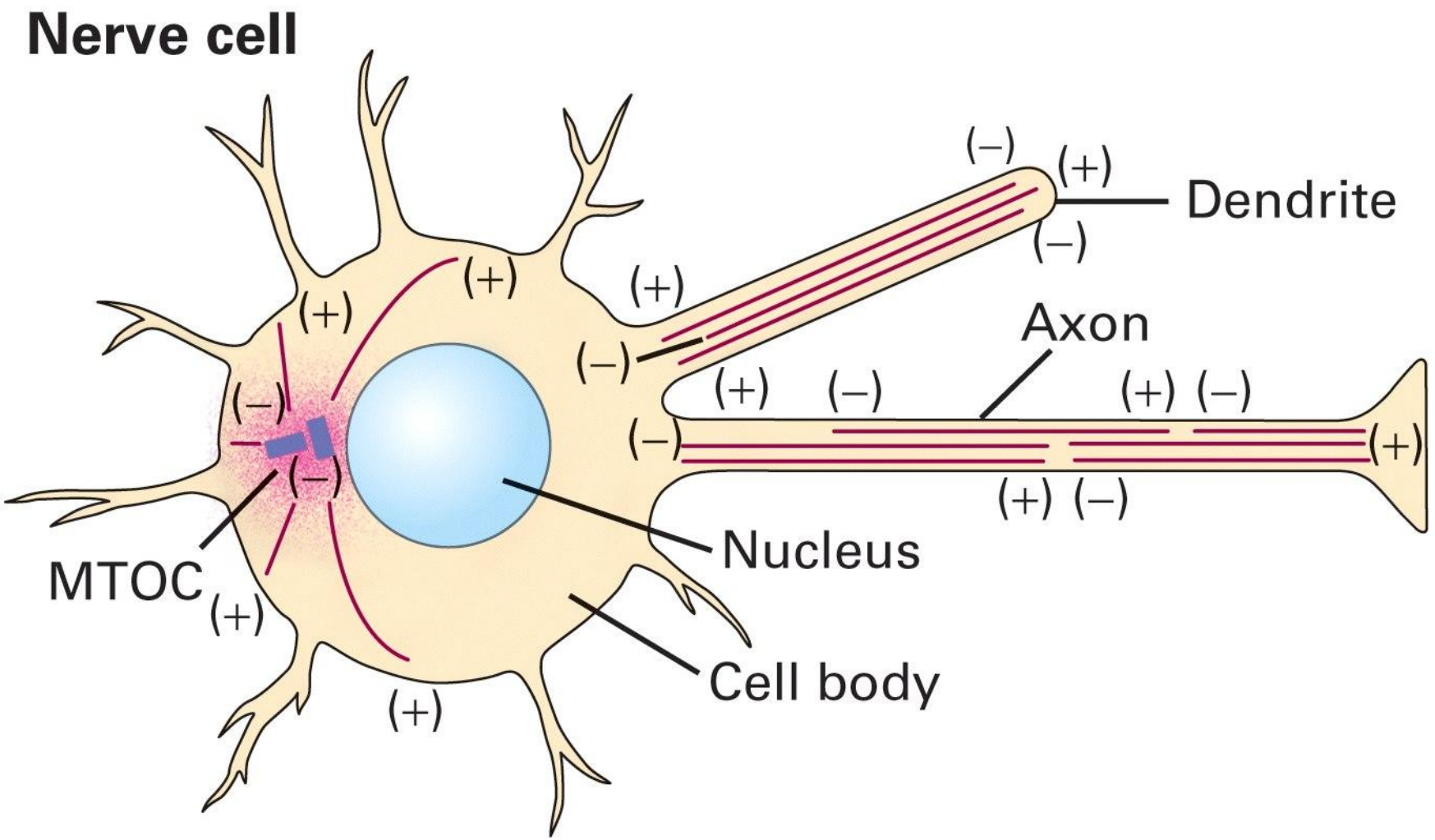

The disassembly and assembly of microtubules in inter-phase cultured cells can be induced either by adding and subsequently removing colccemid or by cooling to 0 ˚C and subsequently rewarming to 37 ˚C.

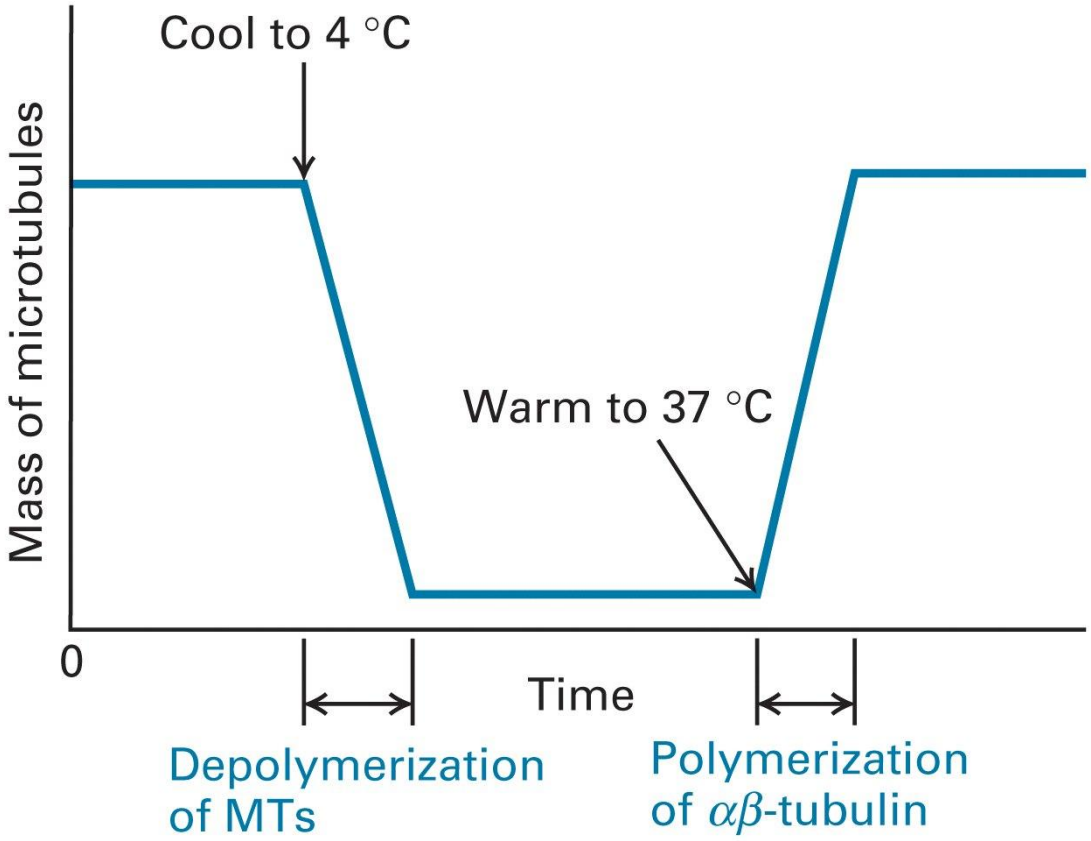

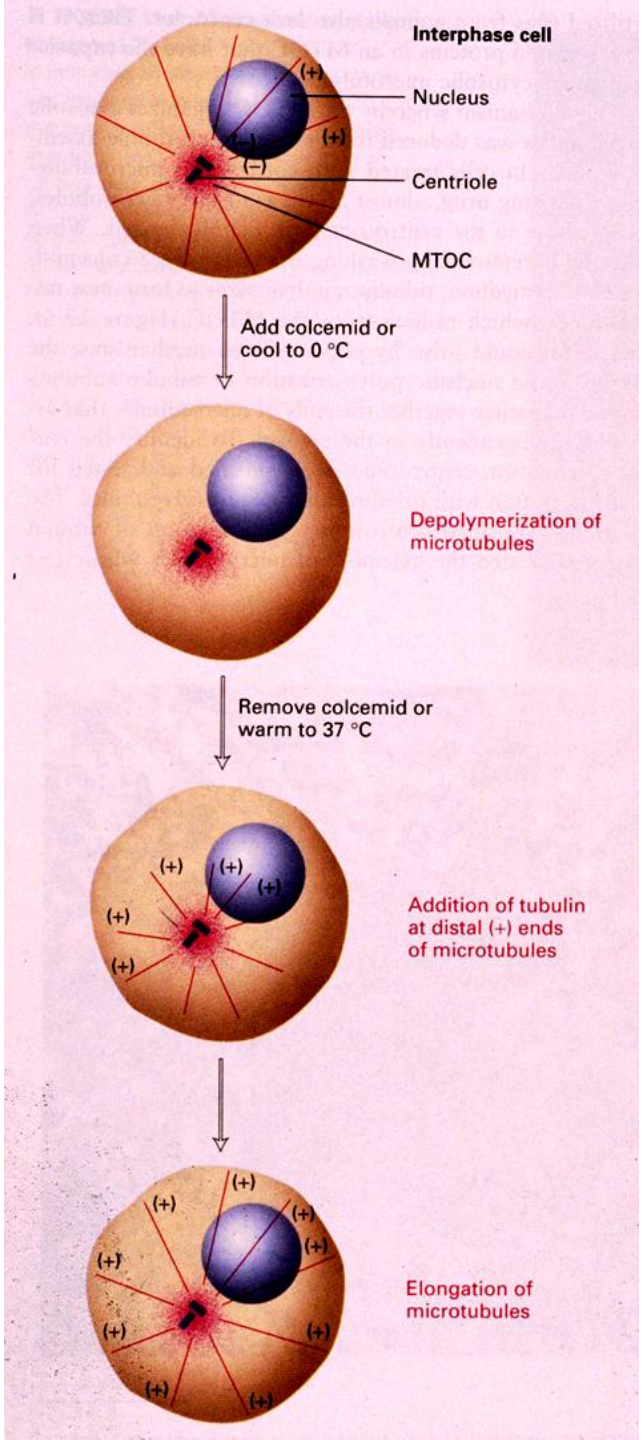

Effect of temperature and tubulin concentration on microtubule assembly and disassembly

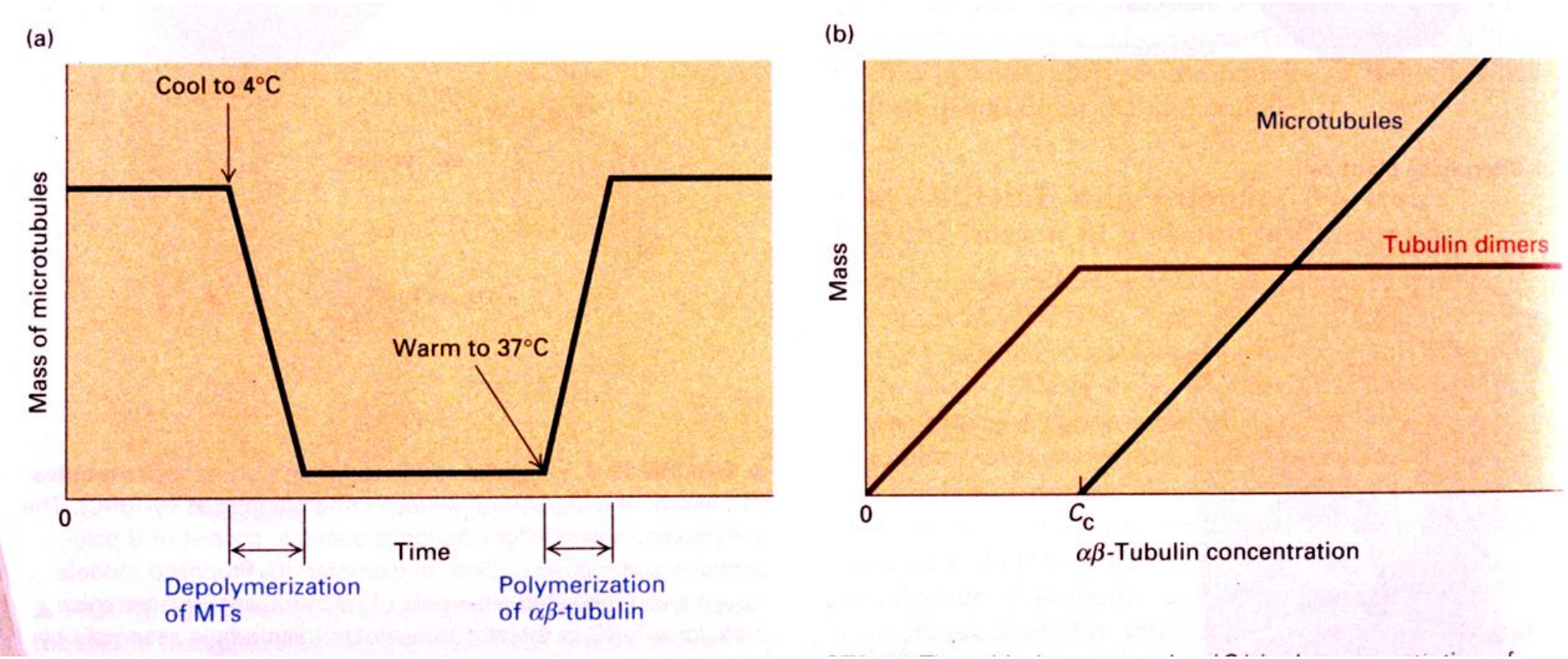

Assembly of microtubules (MT dynamics

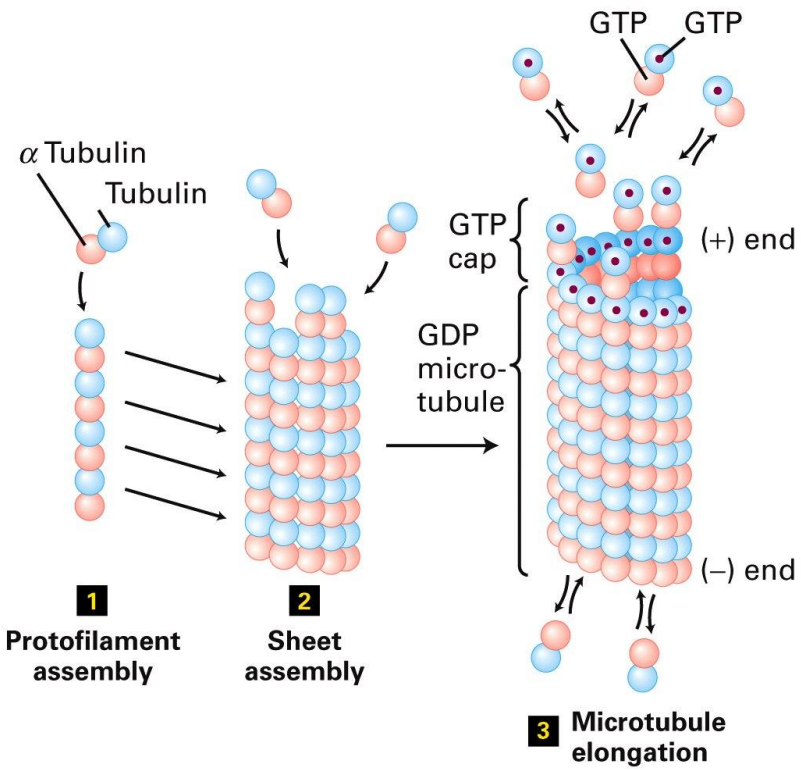

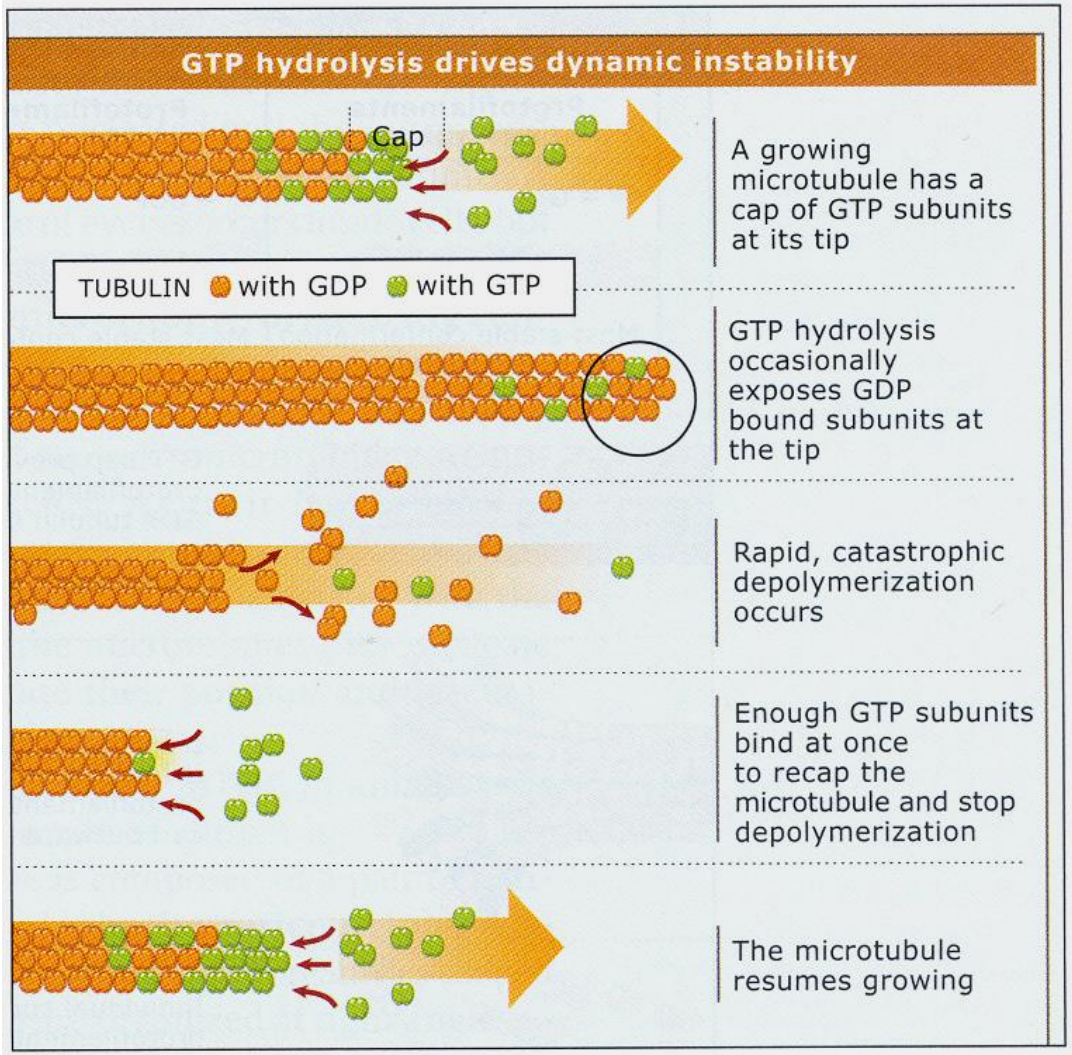

FIGURE 7.21 A schematic view of events at the end of a dynamic microtubule. The GTP bound to β-tubulin is hydrolyzed shortly after a tubulin dimer adds to a microtubule, creating a small cap of GTP-bound subunits at the microtubule's end as it grows. As long as the cap is present the microtubule will grow. However, if GDP-bound subunits ever become exposed at its end, the microtubule will begin to depolymerize very rapidly. The microtubule can be rescued if GTP subunits bind as it is depolymerizing. Depolymerization is fast enough, and rescue rare enough, so that a large fraction of a microtubule can depolymerize before it is rescued.

TABLE 16–2 Drugs That Affect Actin Filaments and Microtubules

ACTIN-SPECIFIC DRUGS	
Phalloidin	binds and stabilizes filaments
Cytochalasin	caps filament plus ends
Swinholide	severs filaments
Latrunculin	binds subunits and prevents their polymerization
MICROTUBULE-SPECIFIC DRUGS	
Taxol	binds and stabilizes microtubules
Colchicine, colcemid	binds subunits and prevents their polymerization
Vinblastine, vincristine	binds subunits and prevents their polymerization
Nocodazole	binds subunits and prevents their polymerization

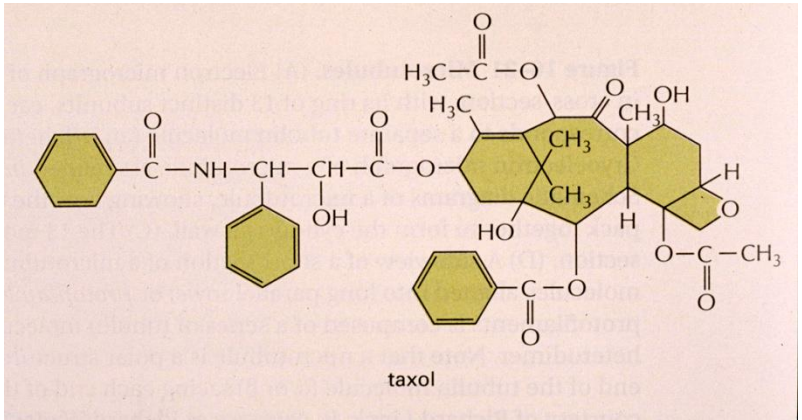

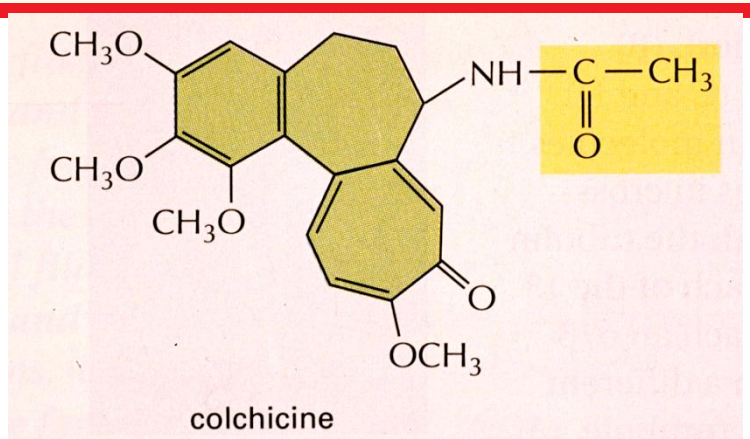

Taxol: Stabilization of microtubules

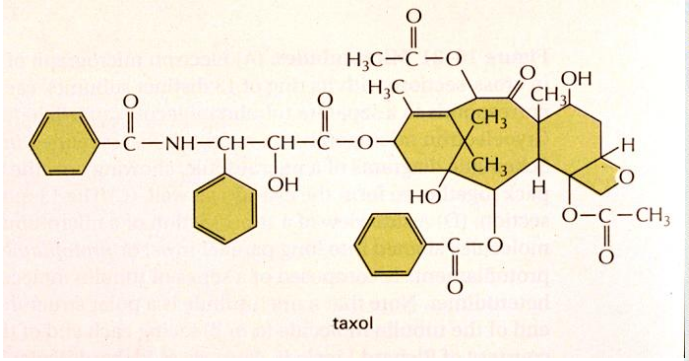

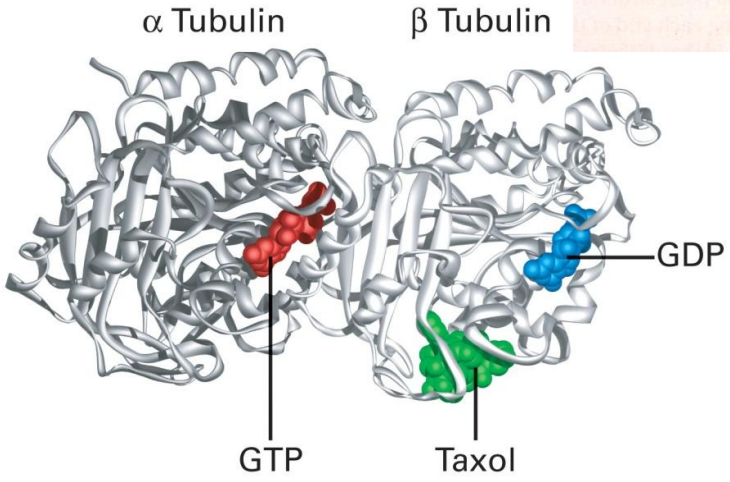

Colchine binds tubulin irreversibly with high-affinity

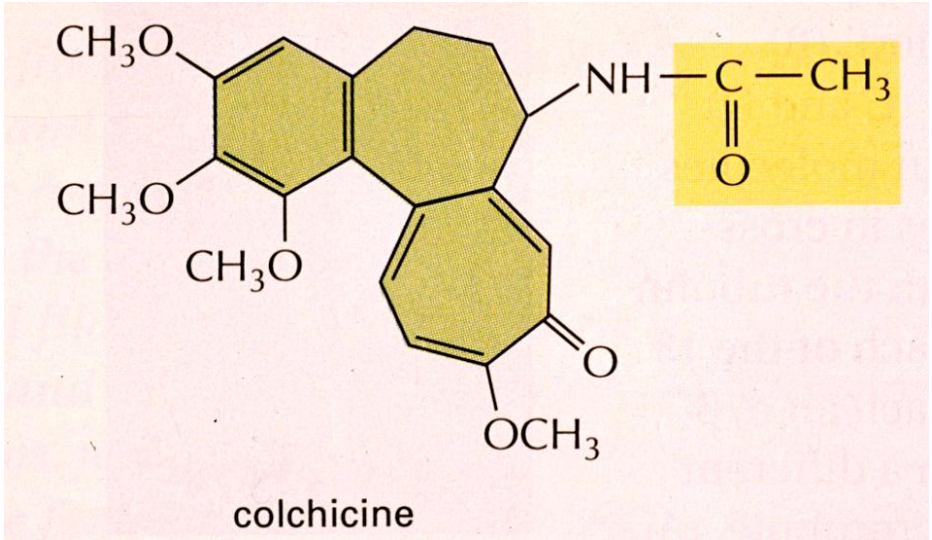

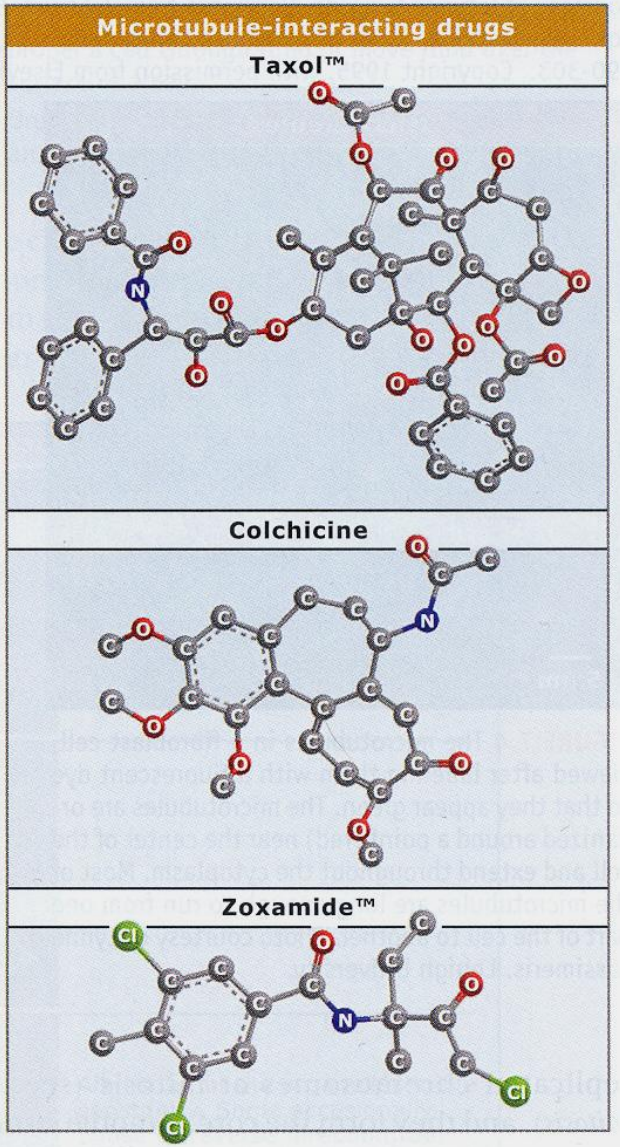

FIGURE 7.5 The structures of three small organic molecules that disrupt microtubule assembly or disassembly. Paclitaxel (Taxol™) and colchicine are natural products produced by specific plants (the Pacific yew tree and the meadow saffron, respectively). Zoxamide™ is a man-made molecule discovered by screening a large collection of small molecules for those with the ability to interfere with microtubules.

Taxol-
treatment

Nocodazol-
treatment

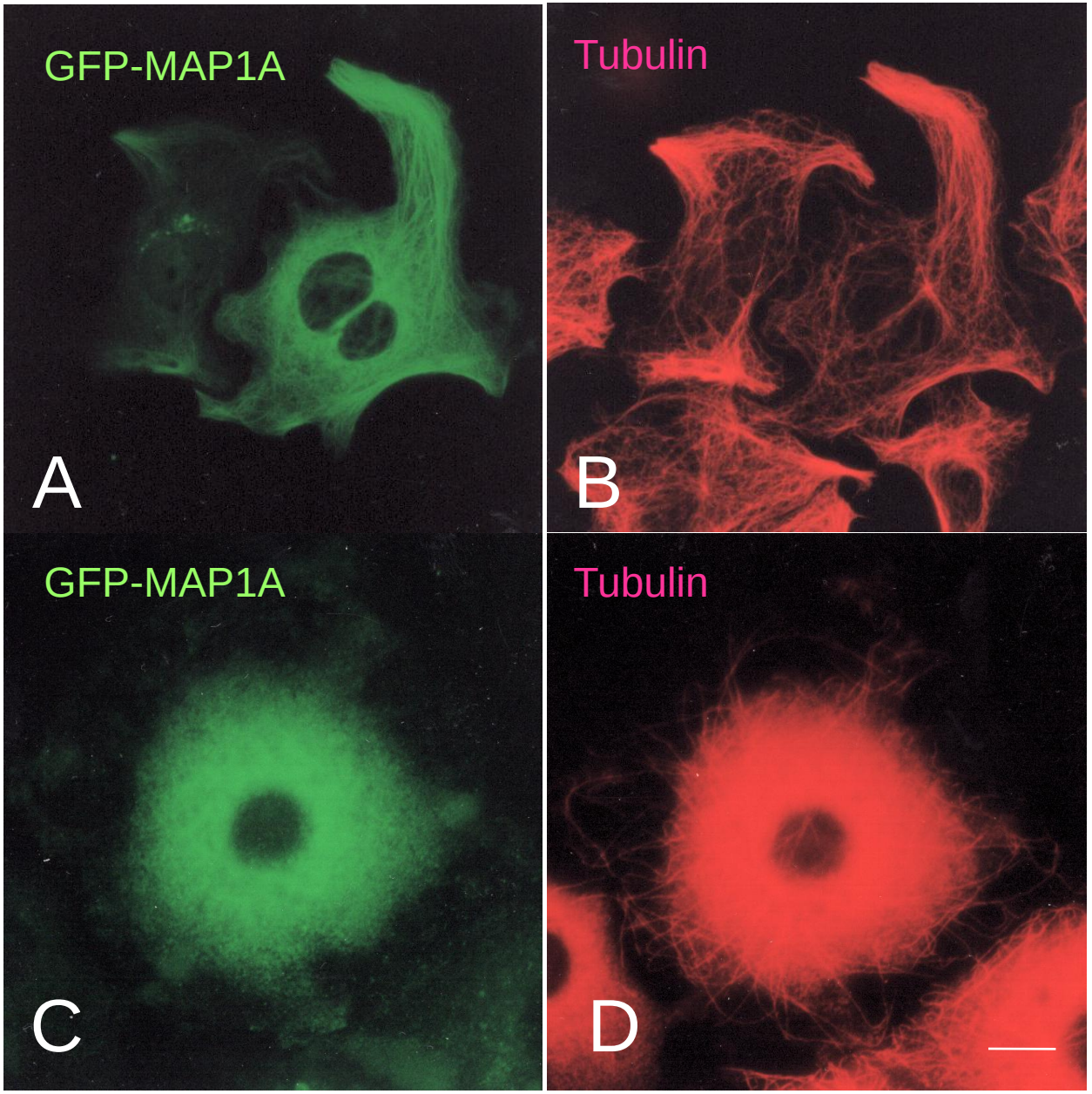

TABLE 20-1 Proteins That Modulate Microtubule (MT) Dynamics

Protein	MW	Location	Function
MICROTUBULE-STABILIZING PROTEINS			
MAP1	250,000–300,000 (heavy chain)	Dendrites and axons; non-neuronal cells	Assembles and stabilizes MTs
MAP2	42,000 and 200,000	Dendrites	Assembles and cross-links MTs to one another and to intermediate filaments
MAP4	210,000	Most cell types	Stabilizes MTs
Tau	55,000–62,000	Dendrites and axons	Assembles, stabilizes, and cross-links MTs
CLIP170	170,000	Most cell types	Cross-links MTs to endosomes and chromosomes
MICROTUBULE-DESTABILIZING PROTEINS			
Katanin	84,000	Most cell types	Microtubule severing
Op18 (stathmin)	18,000	Most cell types	Binds tubulin dimers

Protein	MW	Domain Organization*	Location
TYPE I			
MAP1A	300,000 heavy chain		Dendrites and axons
MAP1B	255,000		Dendrites and axons
TYPE II			
MAP2a	280,000		Dendrites
MAP2b	200,000		Dendrites
MAP2c	42,000		Embryonic dendrites
MAP4	210,000		Non-neuronal cells
Tau	55,000–62,000		Dendrites and axons

**Yellow, microtubule-binding domain; pink, projection domain; green, 18 amino acid repeats.*

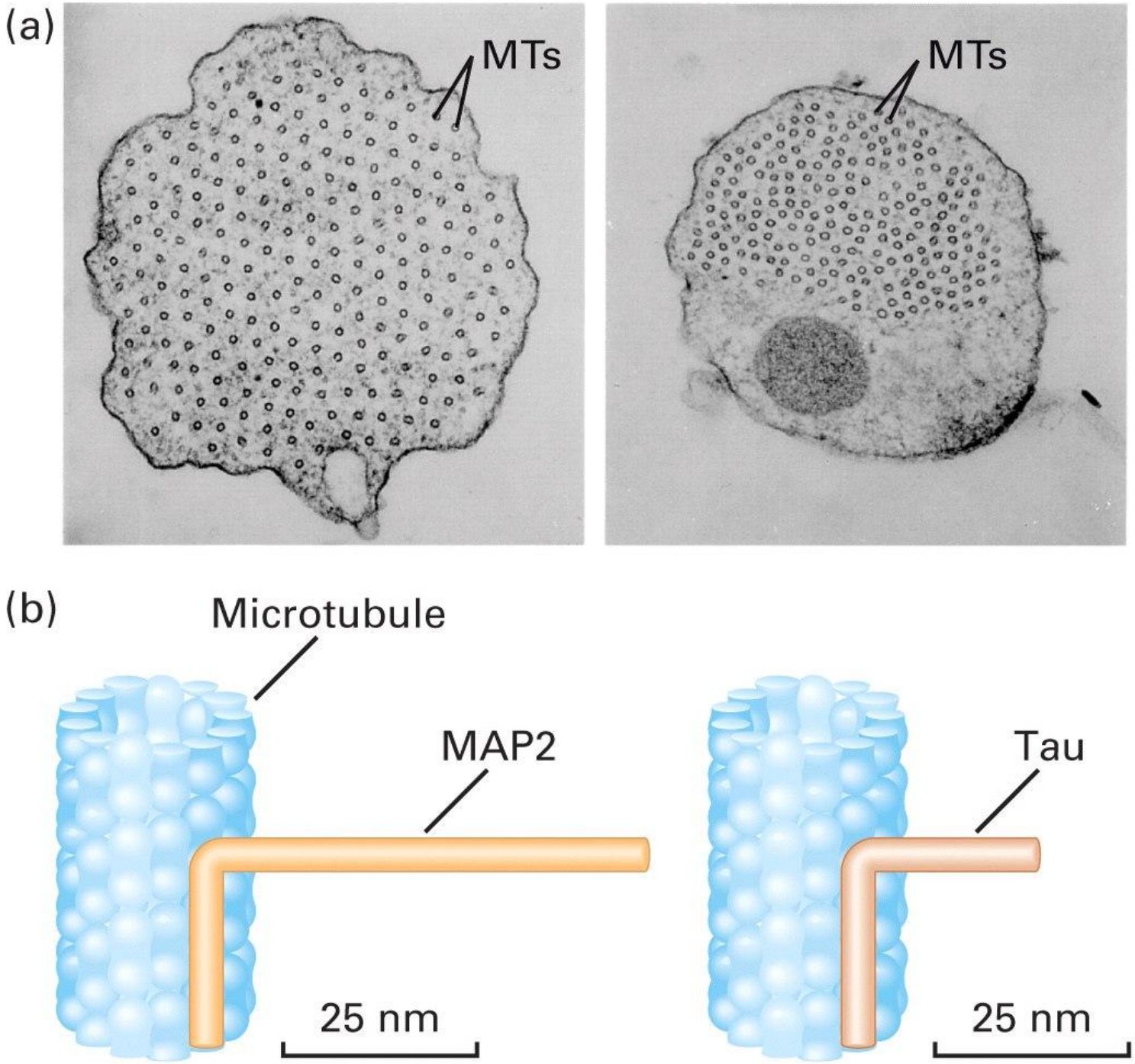
(a)
MTs
MTs
(b)
Microtubule
MAP2
Tau
25 nm
25 nm

MAP2A and Tau

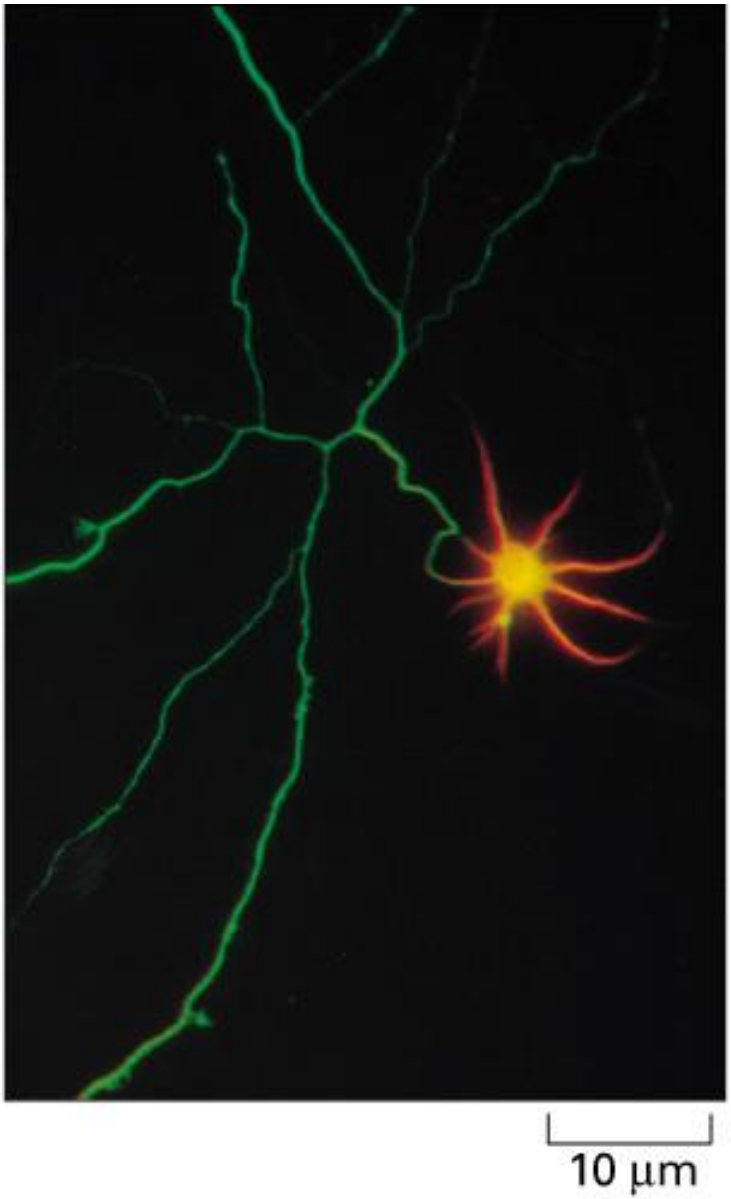

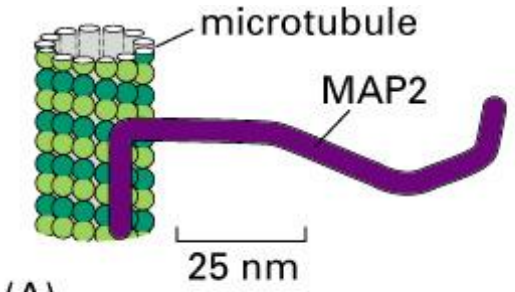

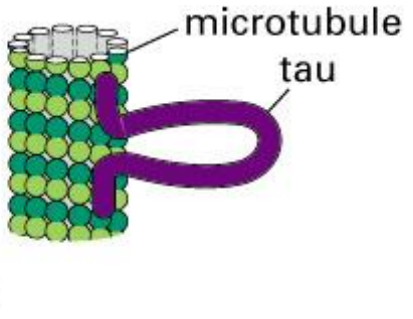

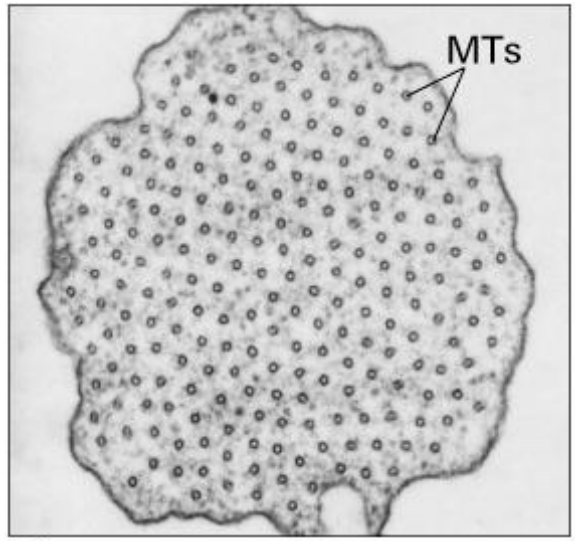

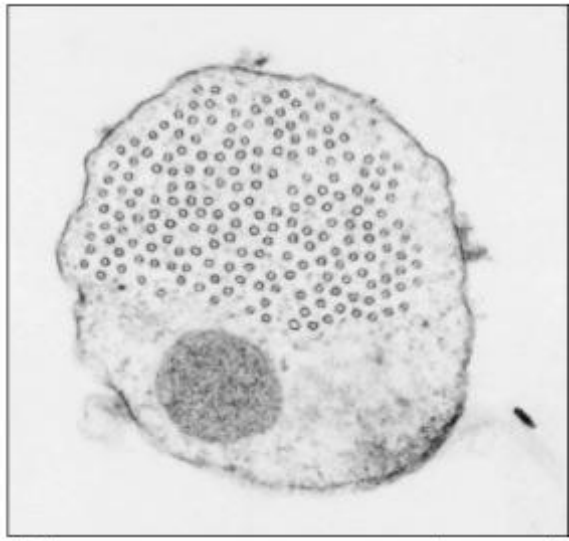

Figure 16–33. Molecular Biology of the Cell, 4th Edition.

Figure 16–32. Molecular Biology of the Cell, 4th Edition.

Immunocytochemical staining of transfected COS7 cells

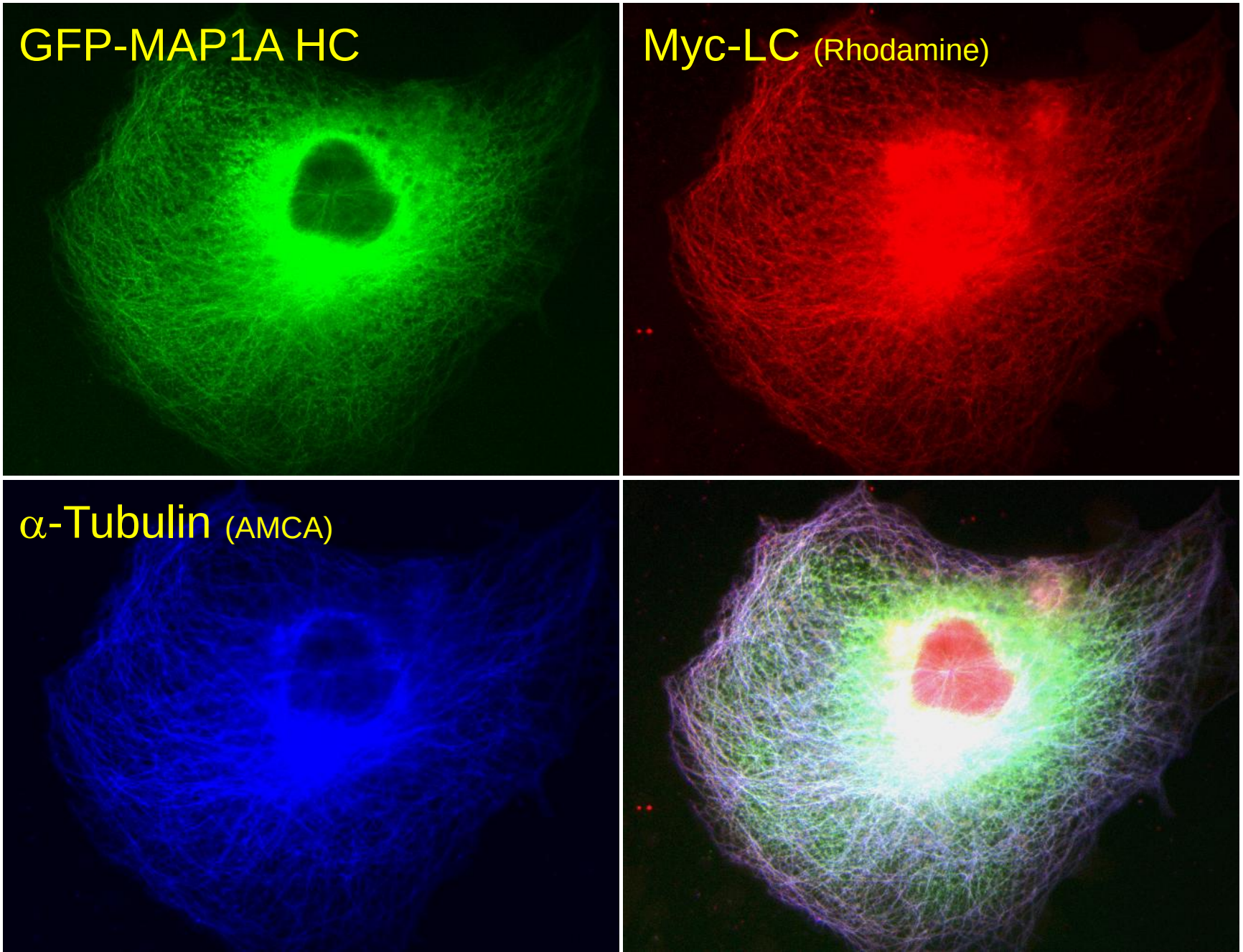

Tau proteins:
Paired helical filaments

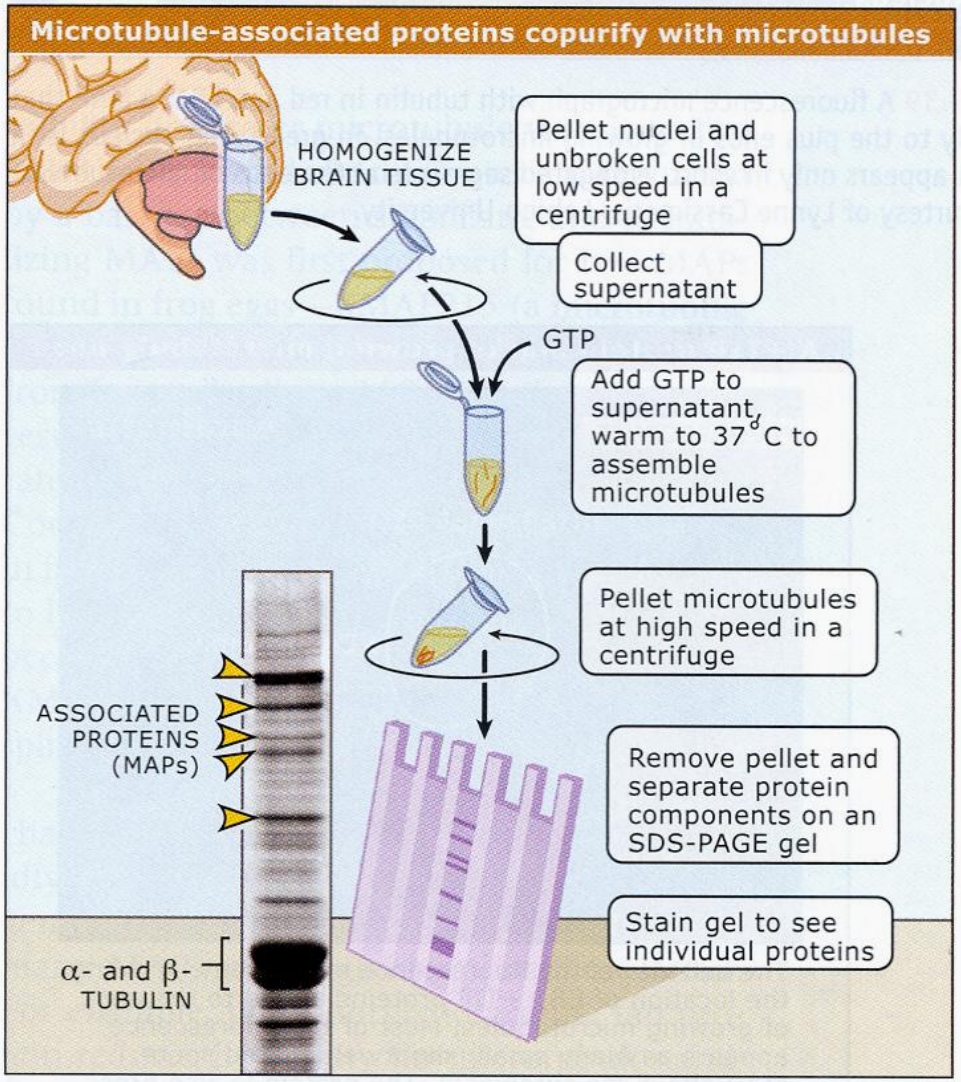

FIGURE 7.38 How the first MAPs were identified. Brain was used because of the large quantity of microtubules in neurons. Brain was homogenized under conditions in which the microtubules would depolymerize. Centrifugation then removed any large material and left only soluble proteins in the supernatant, including a large concentration of tubulin that resulted from all the microtubules in the brain tissue. When the tubulin was polymerized and the microtubules collected with a second centrifugation, many proteins in addition to α- and β-tubulin were also present. Photo courtesy of Lynne Cassimeris, Lehigh University.

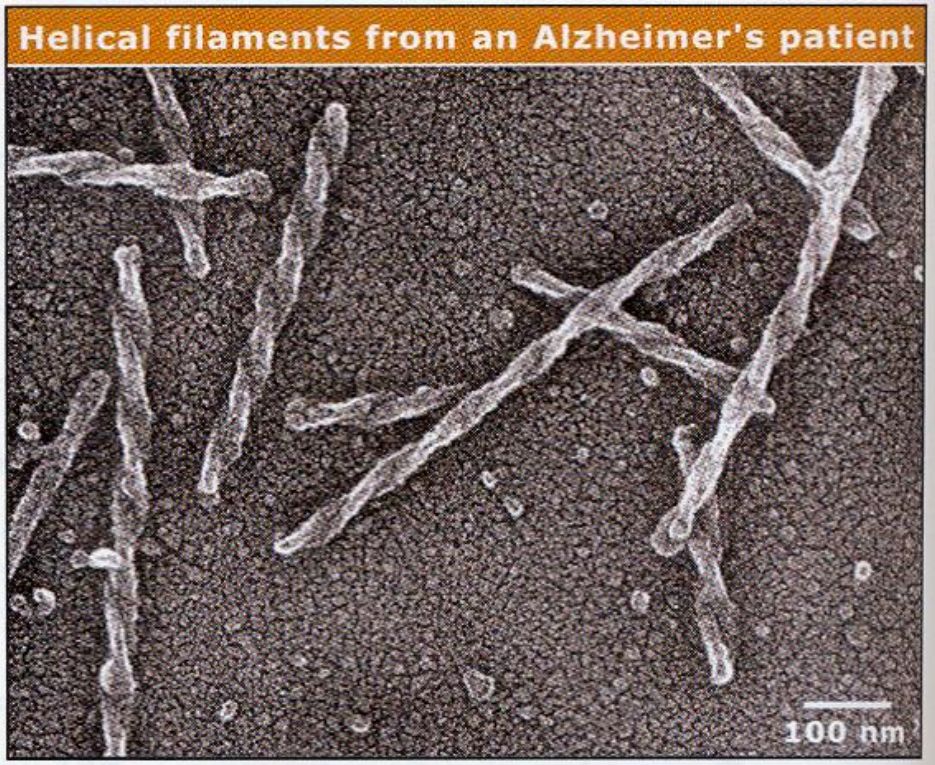

FIGURE 7.44 Tau protein, a MAP present in neuronal tissue, is hyperphosphorylated and aggregates into paired helical filaments during the neural degeneration associated with Alzheimer's disease. Here, purified filaments are viewed by electron microscopy. Photo courtesy of Denah Appelt and Brian Balin, Philadelphia College of Osteopathic Medicine, 1994.

Tau and Neuronal degeneration

Over-phosphorylated and aggregated in the cell body and axons

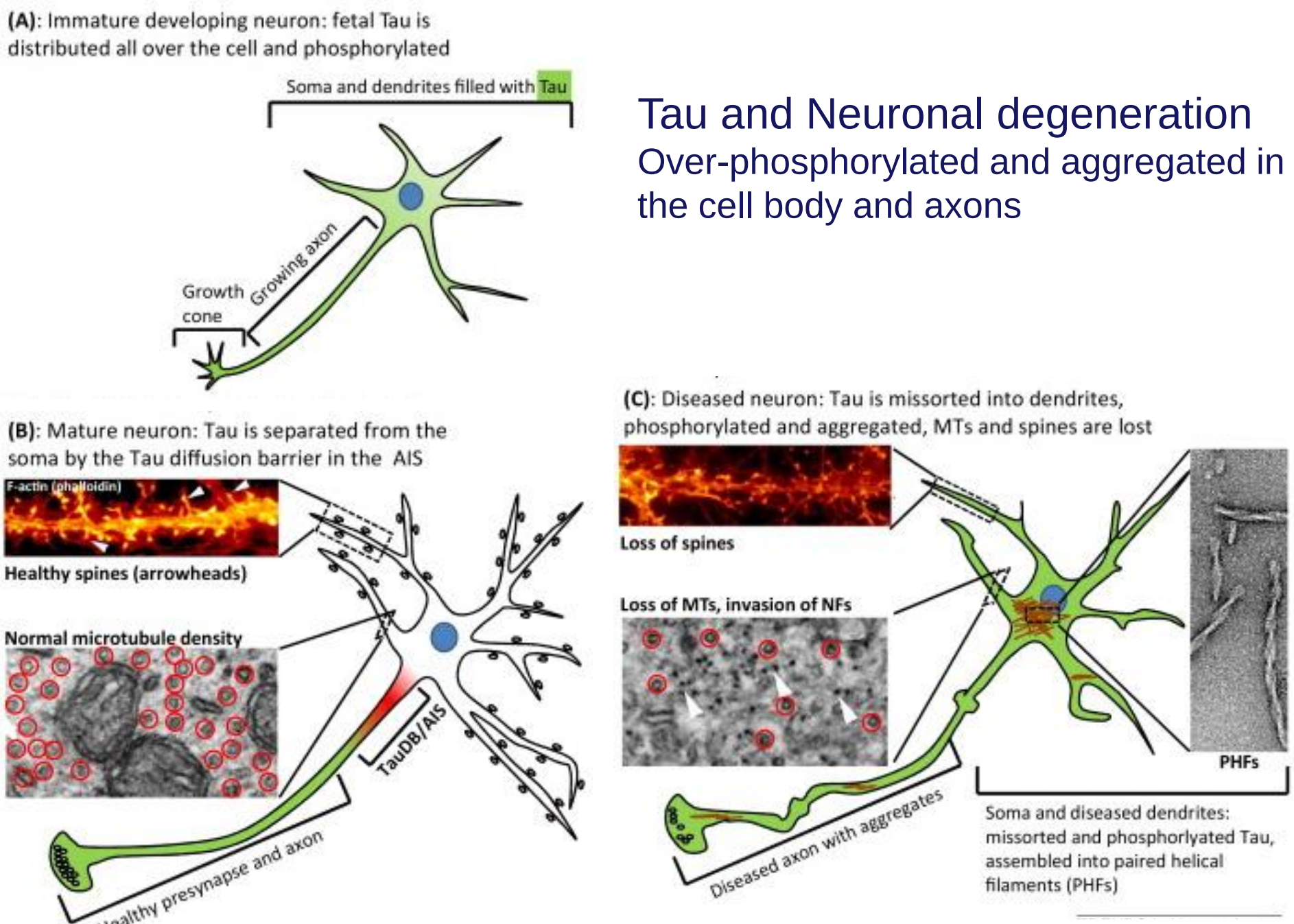

Trends in Neurosciences December 2014, Vol. 37, No. 12

Pathological missorting of Tau in Alzheimer disease (AD) and physiological missorting in hibernating animals. In AD (left) and during hibernation (right), Tau becomes missorted and phosphorylated, dendrites retract. In AD, missorting and phosphorylation are followed by aggregation of Tau and dysfunction of the neuron. In hibernation, Tau missorting, phosphorylation, and reduced dendritic arborization are completely reversible. Tau-based therapy could target pretangle stages of missorting and prevent or reverse missorting, phosphorylation, aggregation, and spreading of Tau.

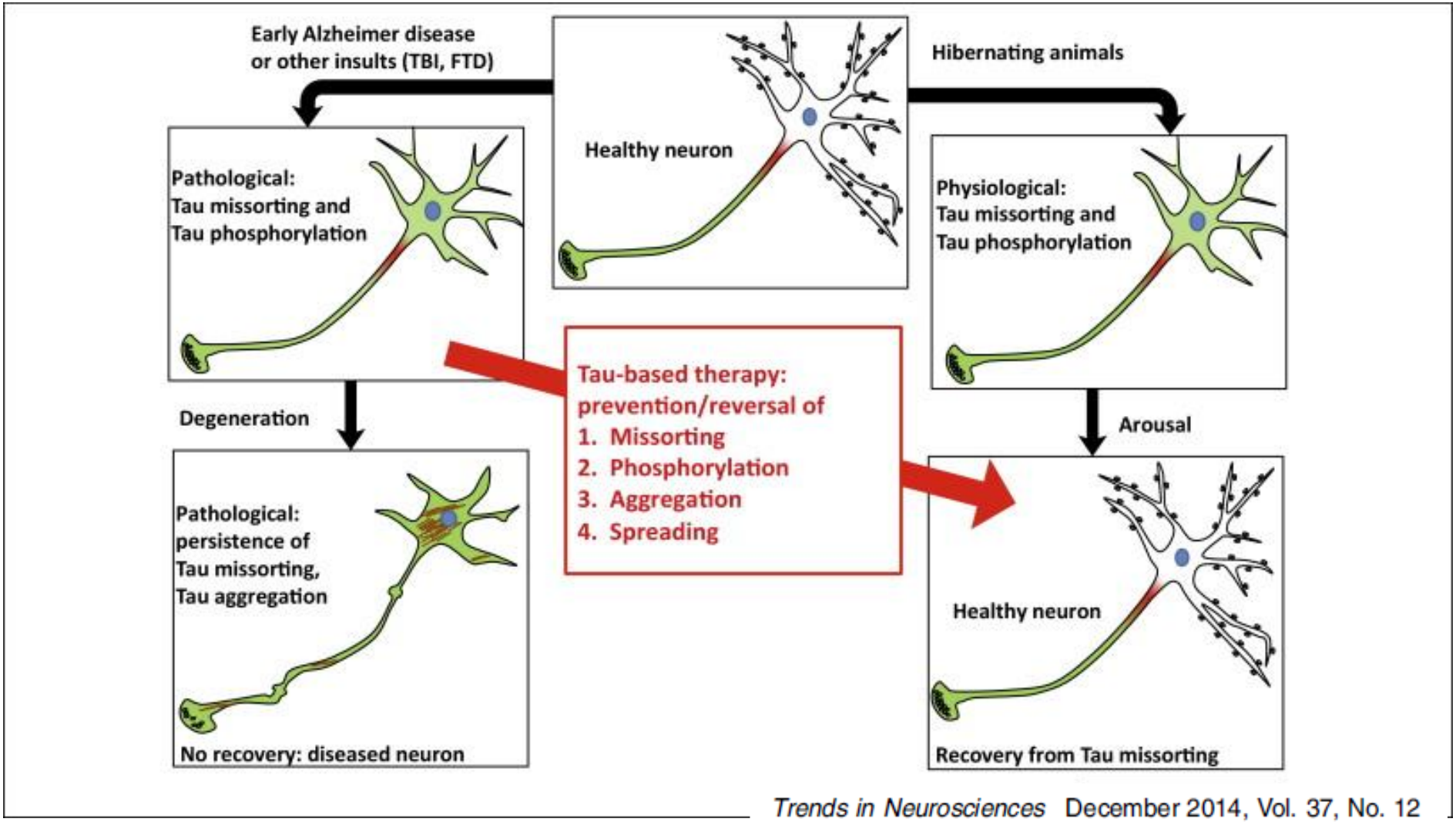

Trends in Neurosciences December 2014, Vol. 37, No. 12

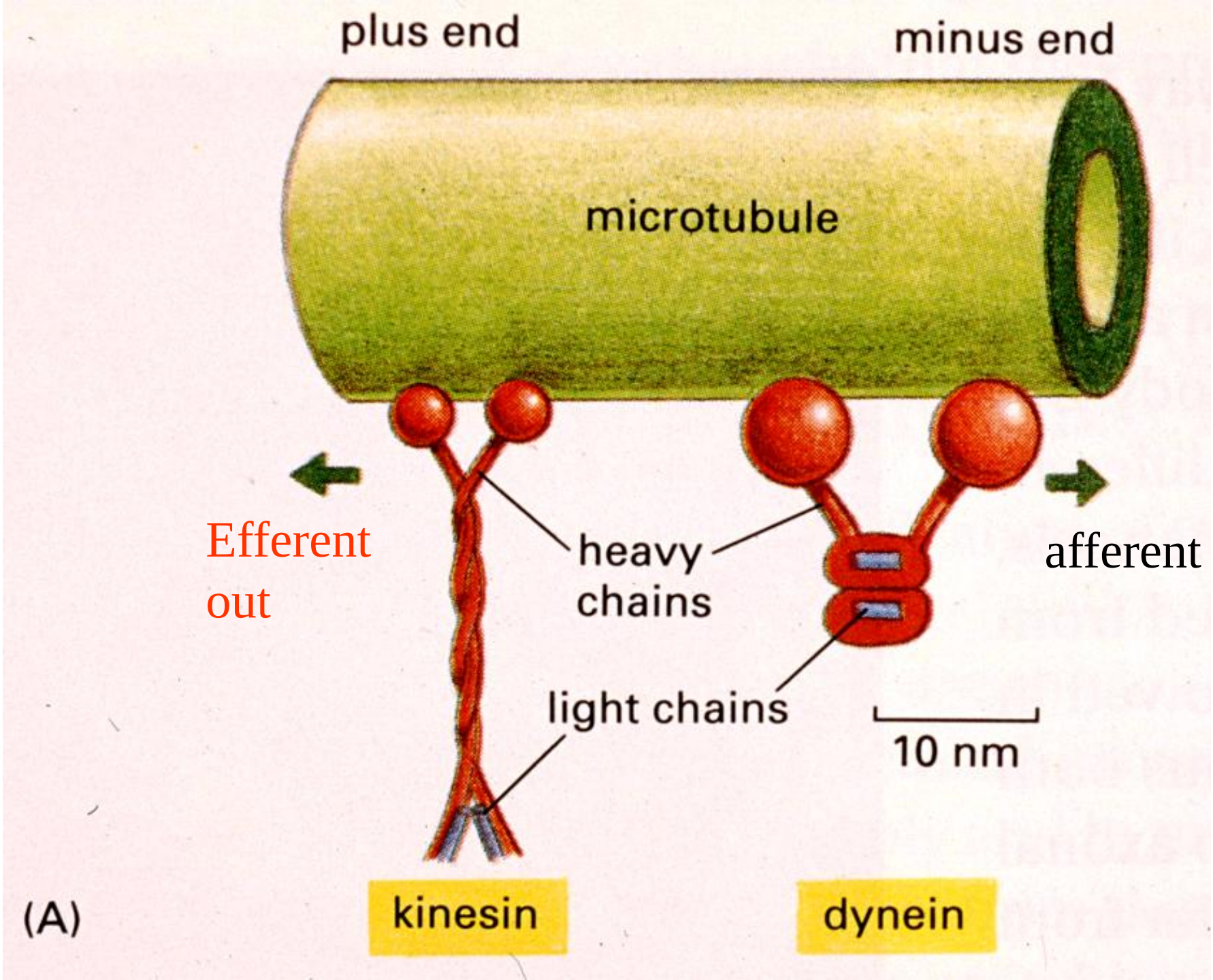
plus end
minus end
microtubule
Efferent
out
heavy
chains
afferent
light chains
10 nm
(A)
kinesin
dynein

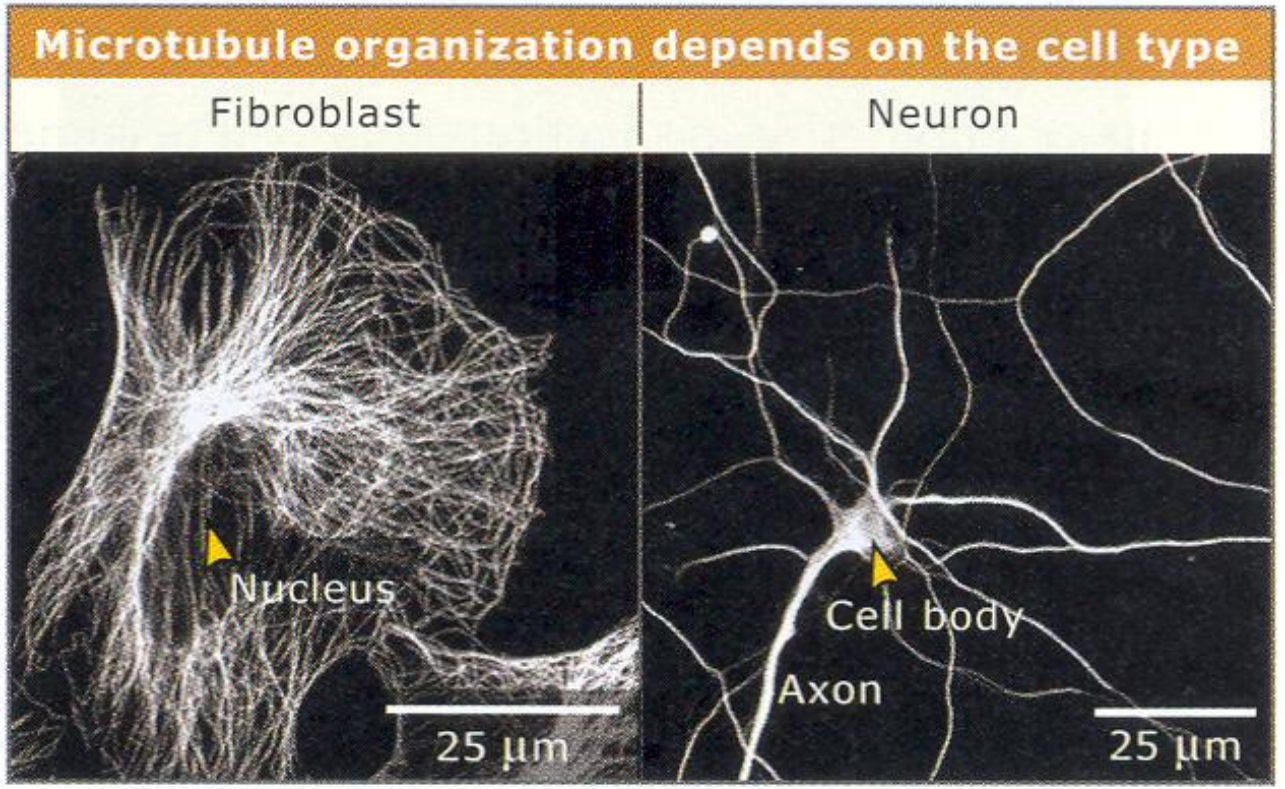

Kinesin: Efferent out

Dynein: Afferent in

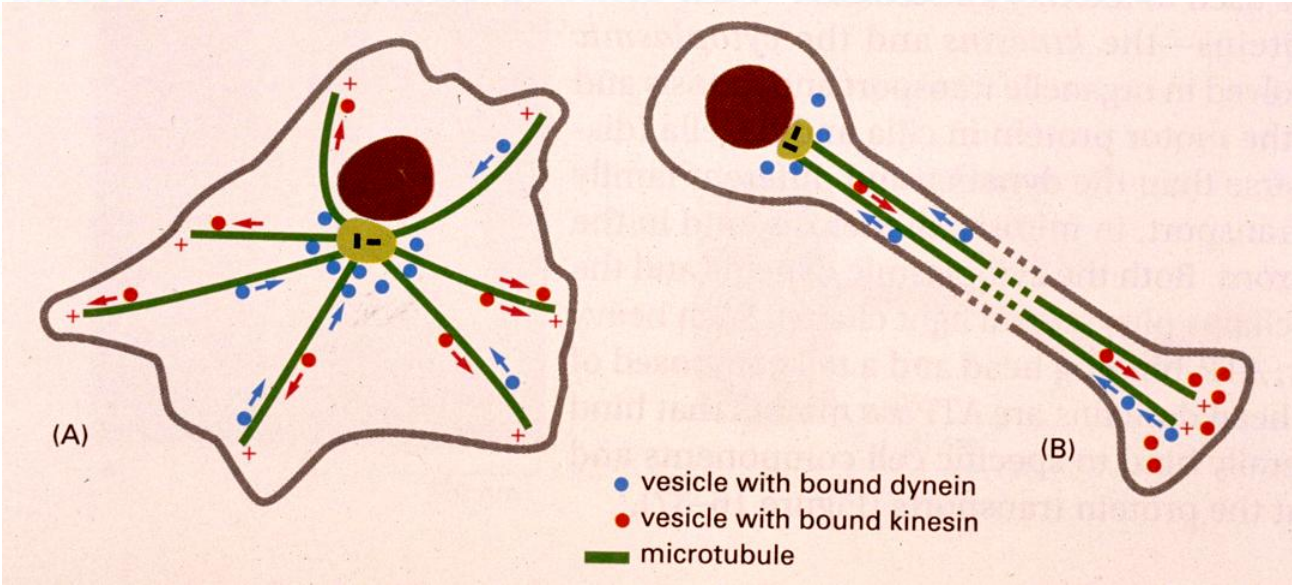

Structure of Kinesin and Dynein

Kinesin structure

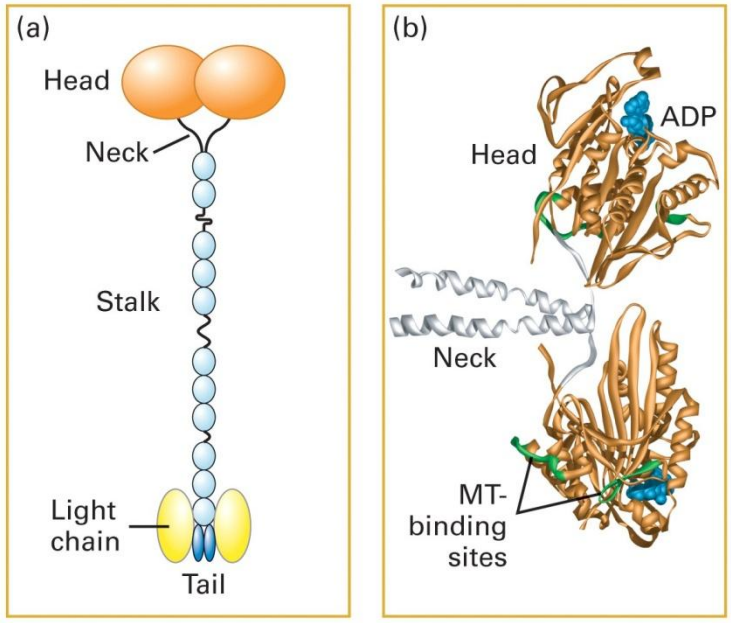

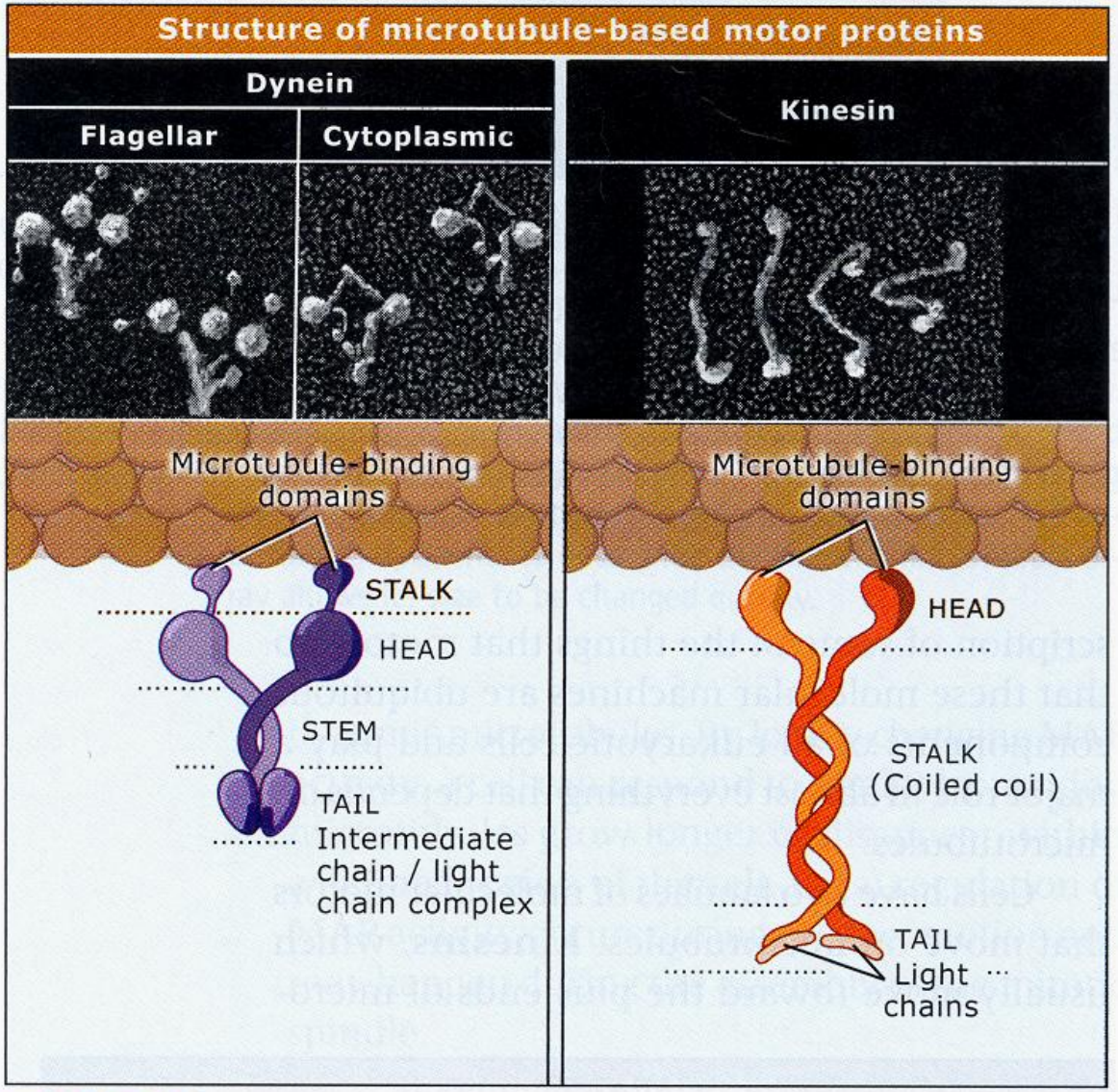

FIGURE 7.49 Structures of microtubule-based motor proteins are shown by rotary shadowing and electron microscopy (top panels). Schematic representations of motors bound to microtubules are shown in the lower panels. Each motor is made up of two or more large polypeptides (heavy chains) and several smaller polypeptides (intermediate and light chains). Photos courtesy of John Heuser, Washington University, School of Medicine.

Vesicle transport

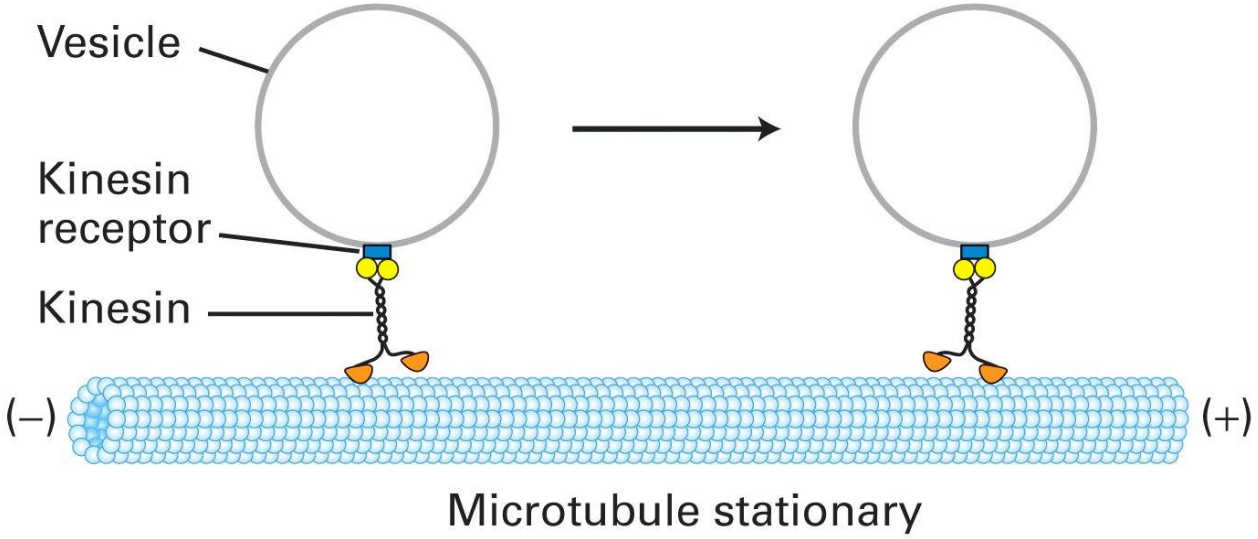

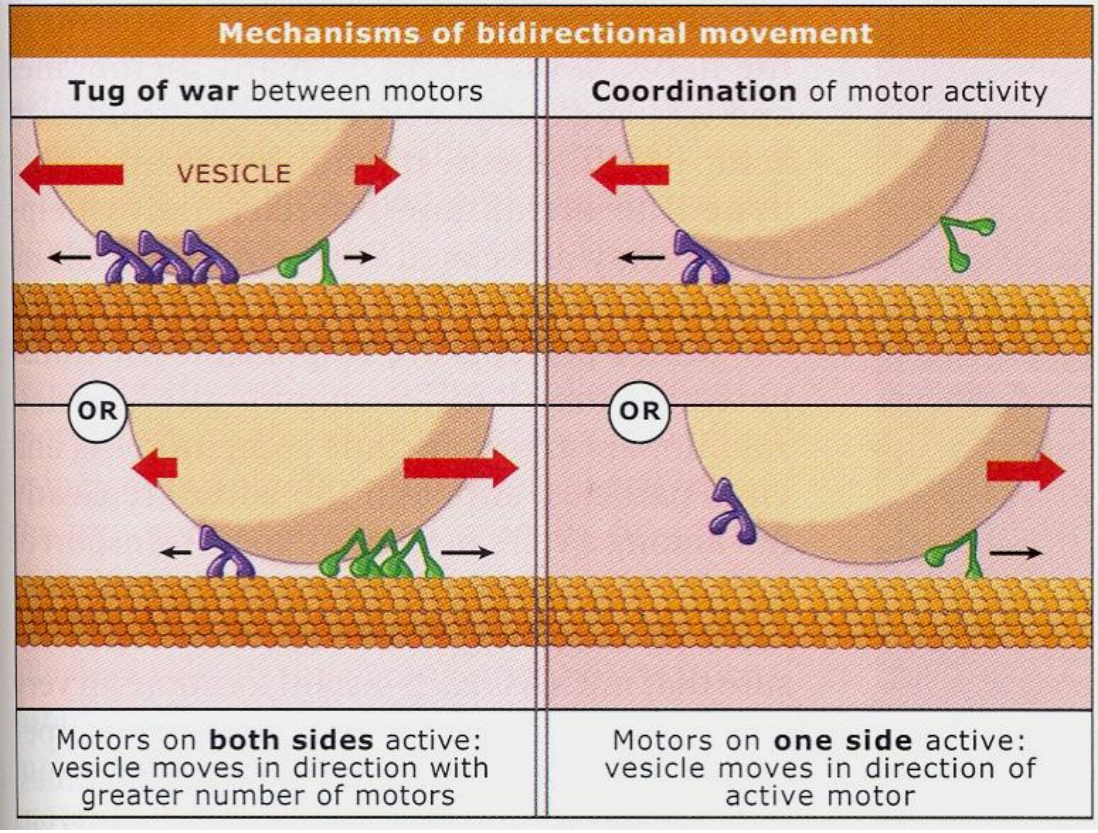

FIGURE 7.54 Possible ways to generate bidirectional movement of a cargo along a microtubule. In each case, both plus end- and minus end-directed motors are bound to the vesicle surface. On the left they are active at the same time, and the one able to generate the larger pulling force (probably because it is present in a larger number) would determine the direction of vesicle movement. On the right the motors are coordinated so that only motors that pull in one direction are active at a time. Current evidence suggests that cells use the mechanism on the right, but how the motors are coordinated is not yet understood.

TABLE 20-2 Functional Classes of Microtubule Motor Proteins

Class	Common Members	Cargo	Direction of Movement*
Cytosolic motors	Kinesins (I, KIFIA, KIFIB)	Cytosolic vesicles/organelles	(+)
	Cytosolic dynein	Cytosolic vesicles/organelles	(−)
	Kinesin II	Cytosolic vesicles/organelles	(+)
Mitotic motors	Kinesin BimC (bipolar)	Spindle and astral MTs	(+)
	Chromokinesins	Chromosomes (arms)	(+)
	MCAK	Kinetochores	(+)
	CENP-E	Kinetochores	(+)
	Kinesin Ncd	Spindle and astral MTs	(−)
	Cytosolic dynein	Kinetochores, centrosomes, cell cortex near spindle poles	(−)
Axonemal motors	Outer-arm and inner-arm dyneins†	Doublet microtubules in cilia and flagella	(−)

*Movement of motor protein toward the (+) end or (−) end of microtubules.
† Outer-arm dyneins have three heavy chains, and inner-arm dyneins have two heavy chains.

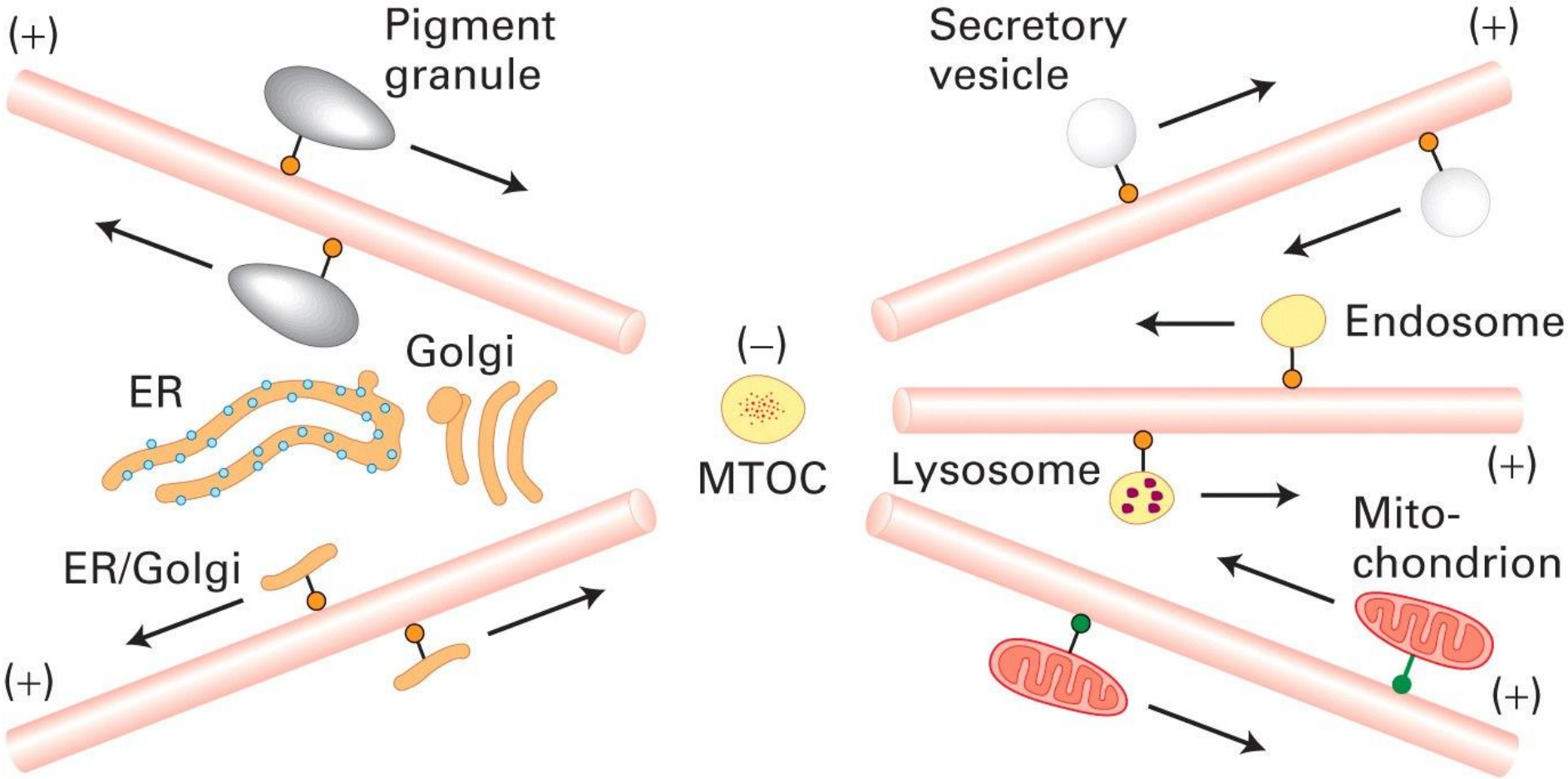
(+)
Pigment granule
Golgi
ER
(–)
MTOC
ER/Golgi
(+)
Secretory vesicle
(+)
Endosome
Lysosome
(+)
Mito-chondrion
(+)
Cytosolic dyneins
Cytosolic kinesins

Cargoes for vesicle

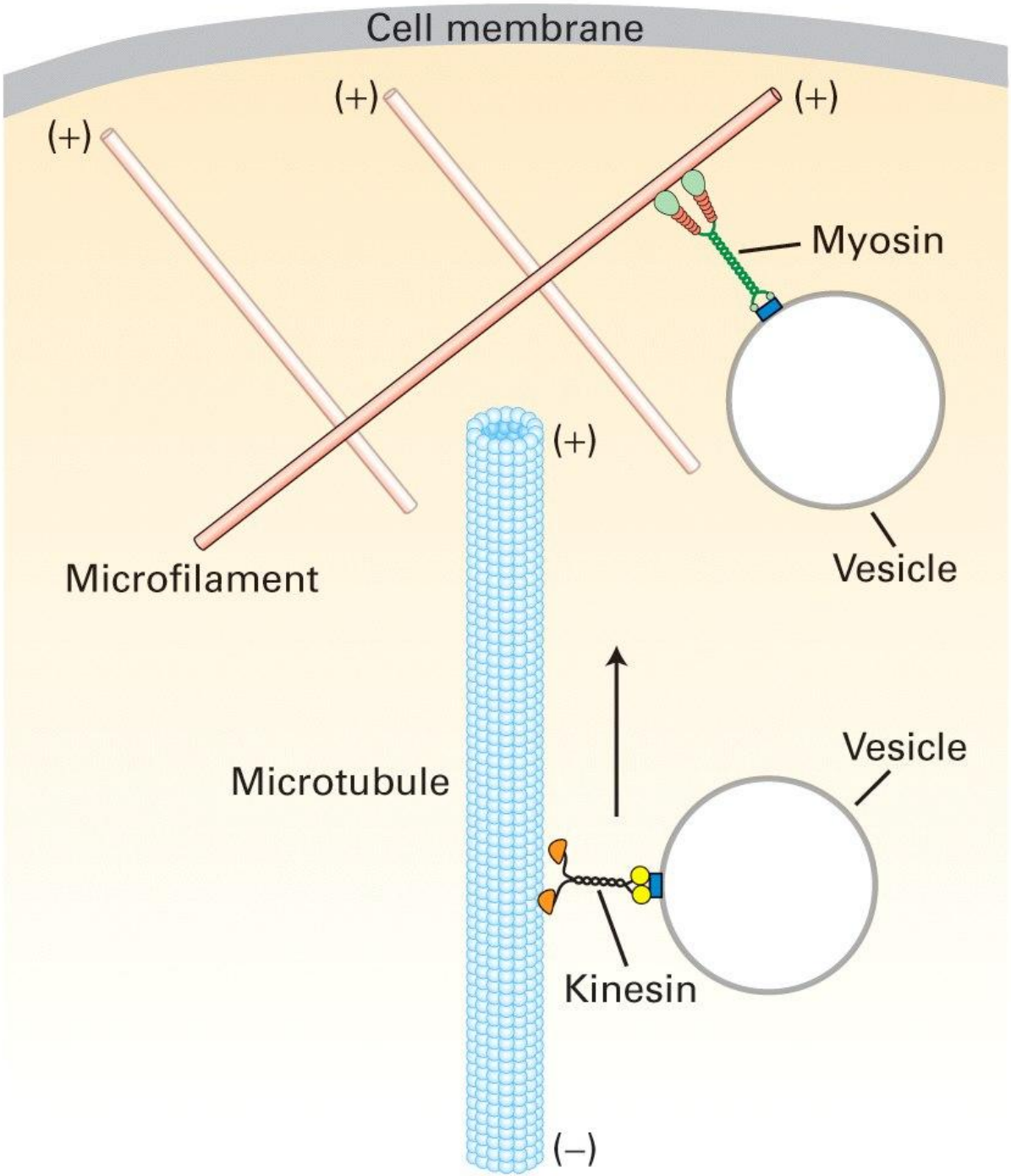

10 nm intermediate Filaments

Polymerization of intermediate filaments

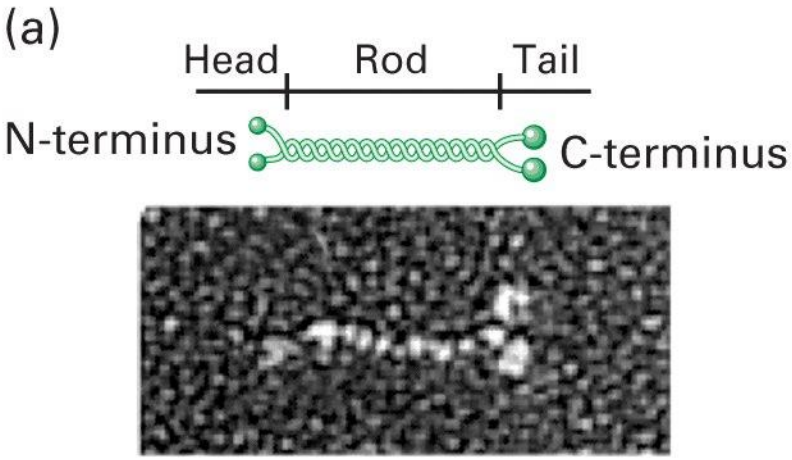

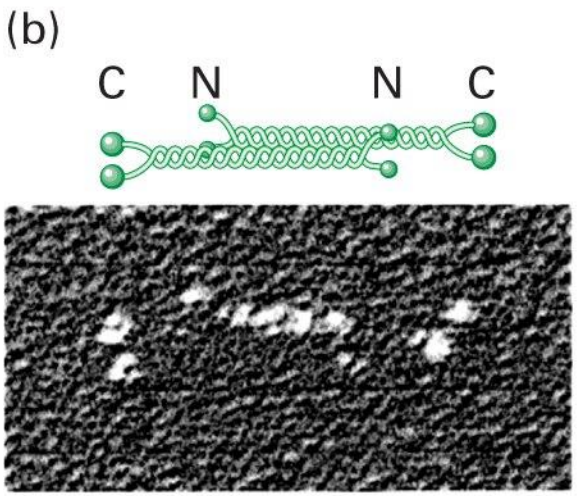

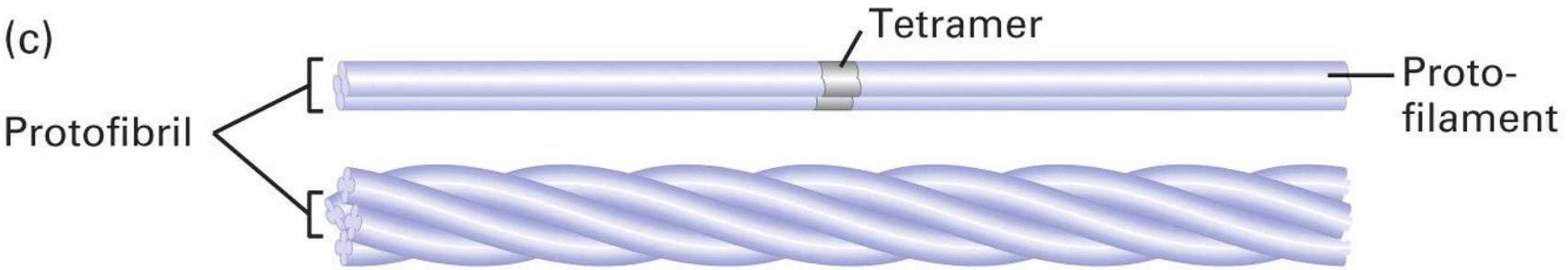

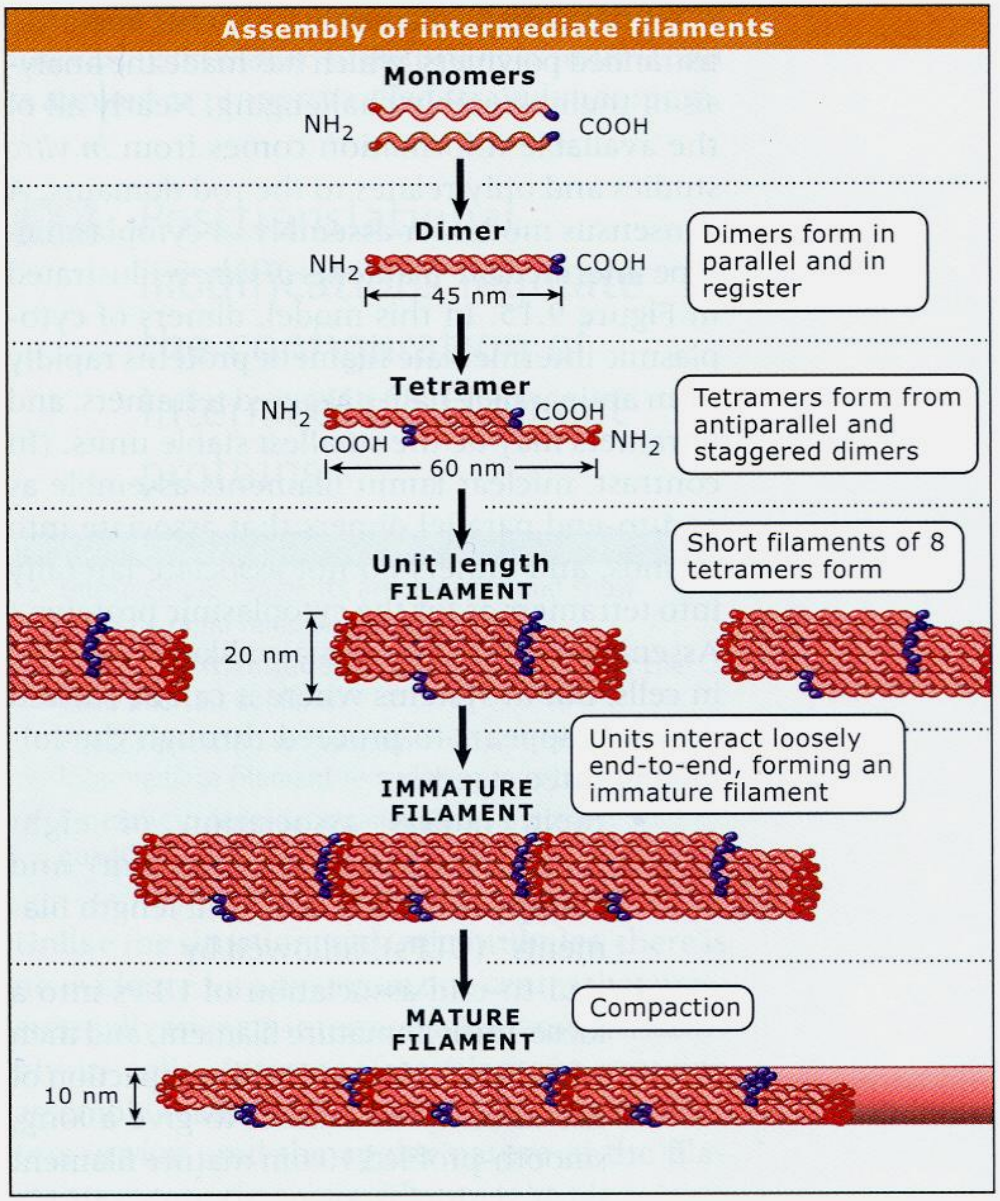

FIGURE 9.15 Consensus model for assembly of intermediate filaments from monomeric proteins. Assembly into dimers is immediate and necessary to prevent protein degradation. Tetramers are the most likely minimal state of proteins *in vivo*. For simplicity, nonhelical domains are not shown. Helix boundary motifs are indicated as red (N-terminal) and blue (C-terminal) ends of rod domains.

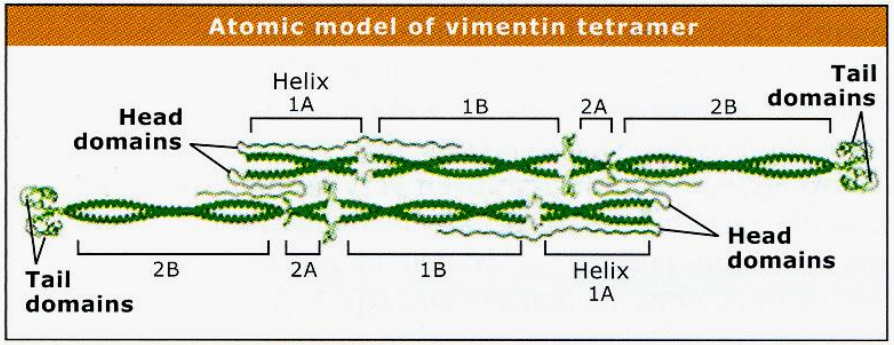

FIGURE 9.16 Atomic model of the homopolymeric type III protein vimentin, based on crystallographic modeling of parts of the protein complemented by homology modeling of the rest. When the protein assembles into filaments, the head domains probably associate with rod domains in the regions indicated. Reprinted, with permission, from the *Annual Review of Biochemistry*, Volume 73. © 2004 by Annual Reviews (www.annualreviews.org). Photo courtesy of Harald Herrmann, German Cancer Research Center, and Ueli Aebi, M. Muller Institute, Basel.

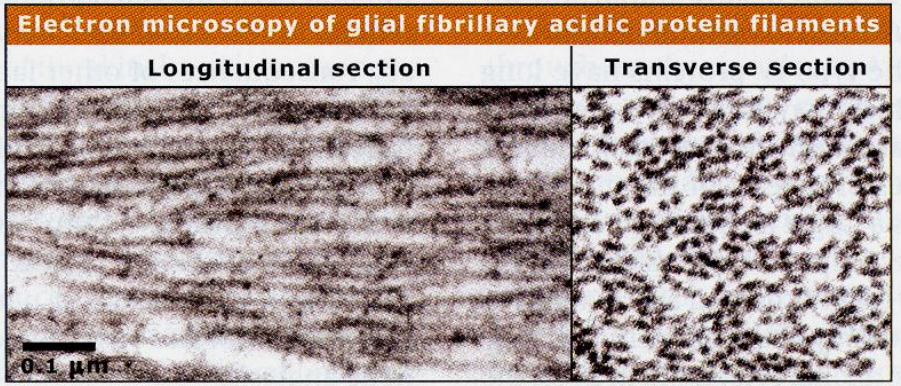

FIGURE 9.13 Electron micrographs of glial fibrillary acidic protein (GFAP) filaments in astrocytes of the spinal cord. Photos reproduced from Eliasson, C., et al. *J. Biol. Chem.* 1999. 274: 23996-24006. Copyright © 1999 by ASBMB. Photos courtesy of Dr. Milos Pekny and Dr. Claes-Henric Berthold, Sahlgrenska Academy, Göteborg University.

TABLE 19-4 Primary Intermediate Filaments in Mammals

IF Protein	MW (10^{-3})*	Filament Form	Tissue Distribution
NUCLEAR LAMINS			
Lamin A	70	Homopolymer	Nucleus
Lamin B	67	Homopolymer	Nucleus
Lamin C	67	Homopolymer	Nucleus
KERATINS†			
Acidic keratins	40–57	Heteropolymers	Epithelia
Basic keratins	53–67	Heteropolymers	Epithelia
TYPE III INTERMEDIATE FILAMENTS			
Vimentin	57	Homo- and heteropolymers	Mesenchyme (fibroblasts)
Desmin	53	Homo- and heteropolymers	Muscle
Glial fibrillary acidic protein	50	Homo- and heteropolymers	Glial cells, astrocytes
Peripherin	57	Homo- and heteropolymers	Peripheral and central neurons
NEUROFILAMENTS			
NF-L	62	Homopolymers	Mature neurons
NF-M	102	Heteropolymers	Mature neurons
NF-H	110	Heteropolymers	Mature neurons
Internexin	66	—	Developing CNS

*Intermediate filaments show species-dependent variations in molecular weight (MW).
†More than 15 isoforms of both acidic and basic keratins are known.

Keratin Pairs: Type II & Type I

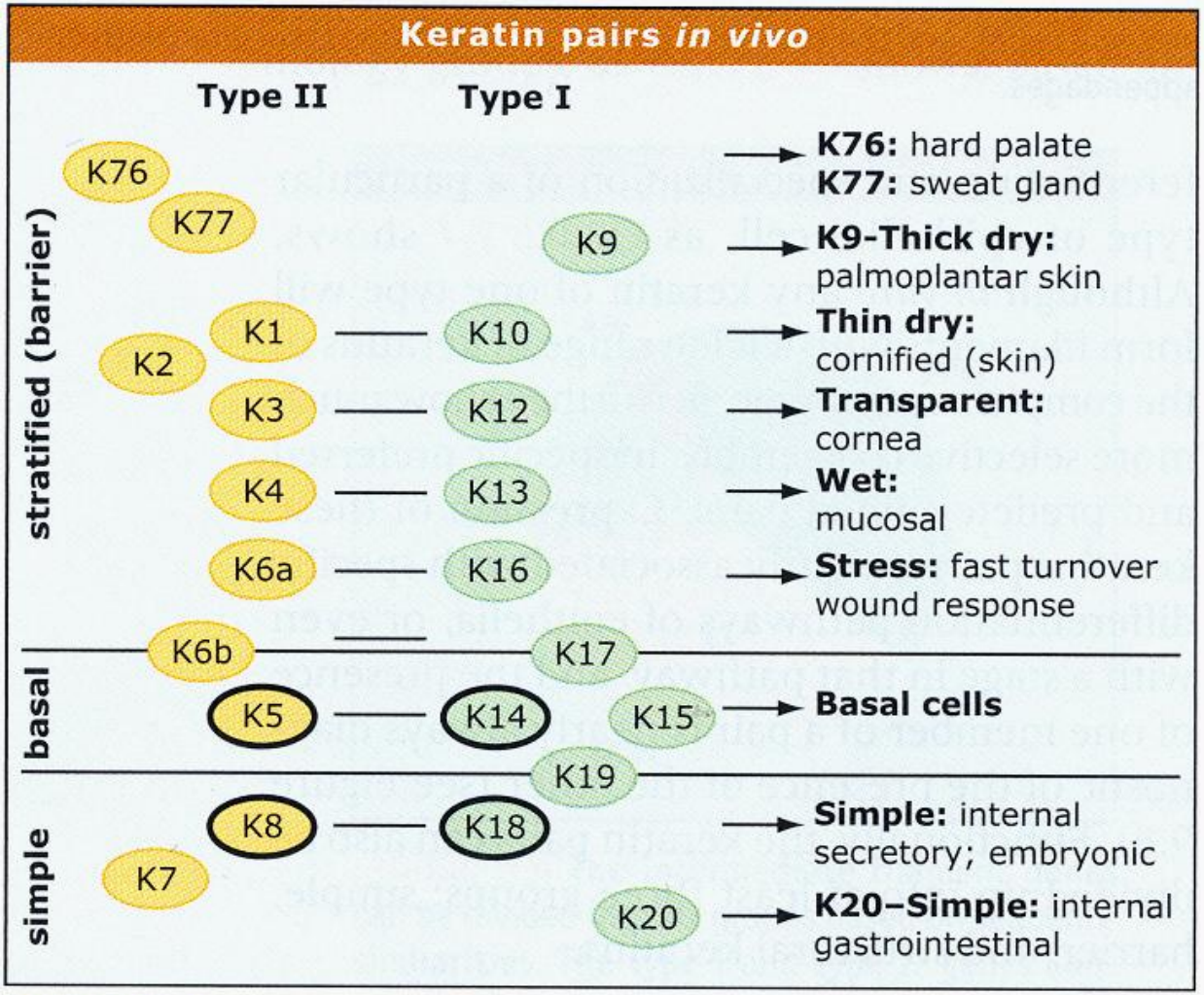

FIGURE 9.7 Keratins are expressed as tissue-specific pairs of type I/type II proteins. Each keratin pair is characteristic of a particular type of epithelial differentiation. Bold rings indicate the primary keratins.

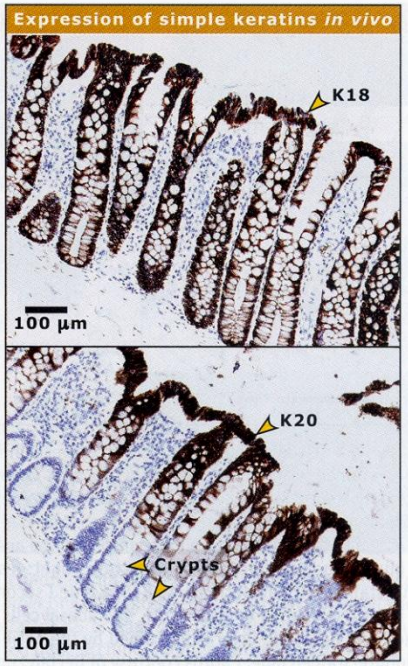

FIGURE 9.9 Detection of simple keratins in the epithelial lining of the large intestine by immunohistochemistry. The locations of two type I keratins, K18 and K20, are revealed by immunoperoxidase staining with two specific monoclonal antibodies. Keratins are stained brown, with blue haematoxylin counterstain. The primary keratin K18 is present in all simple epithelia, whereas K20 is specific for certain gastrointestinal differentiation lineages and seen here to be restricted to the later parts of the progressively differentiating epithelium as cells move upward from the bottom of the crypt. Photos courtesy of Declan Lunny and Birgit Lane, School of Life Sciences, University of Dundee.

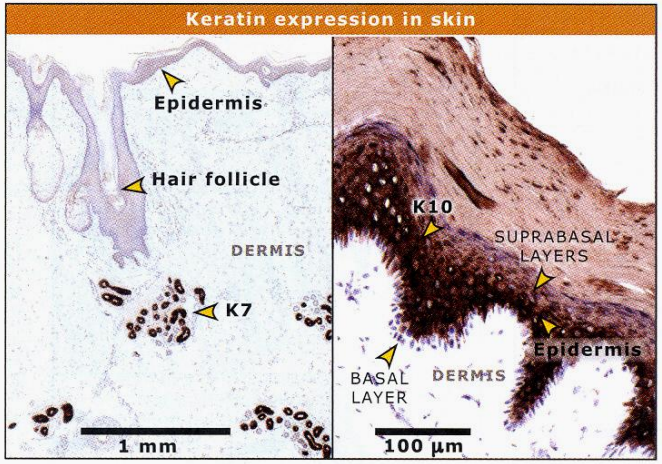

FIGURE 9.10 Tissue specificity of keratin expression in skin. Left: Tissue section stained with an antibody to K7, a type II simple keratin, highlights only the secretory cells of the sweat gland (dark brown, using indirect immunoperoxidase staining). The stratified squamous barrier epithelium of the epidermis is unrecognized by the antibody, only stained pale blue by the haematoxylin counterstain. Right: A section of thick epidermis stained with an antibody to K10, a type I secondary or tissue-specific keratin expressed in postmitotic suprabasal cells of cornified barrier tissues. The basal cell layer is unstained by the antibody, and the nuclei are counterstained blue. Photos courtesy of Declan Lunny and Birgit Lane, School of Life Sciences, University of Dundee.

Summary of the major consensus patterns of keratin expression in epidermis and epidermal appendages.

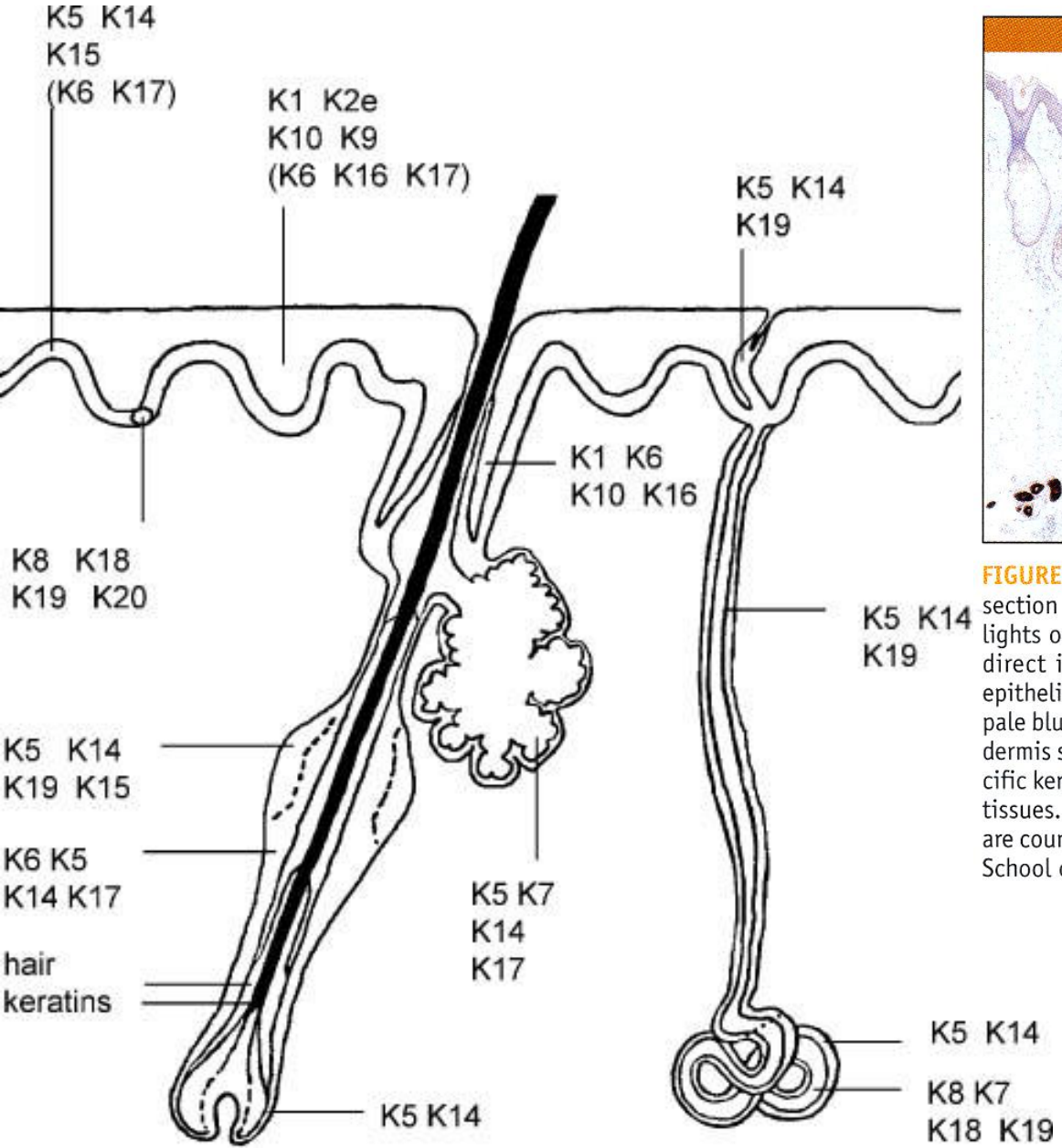

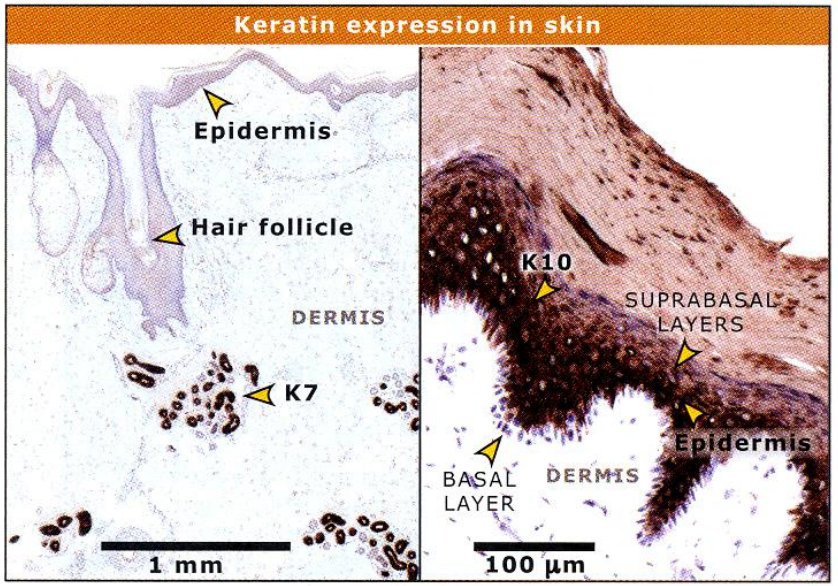

FIGURE 9.10 Tissue specificity of keratin expression in skin. Left: Tissue section stained with an antibody to K7, a type II simple keratin, highlights only the secretory cells of the sweat gland (dark brown, using indirect immunoperoxidase staining). The stratified squamous barrier epithelium of the epidermis is unrecognized by the antibody, only stained pale blue by the haematoxylin counterstain. Right: A section of thick epidermis stained with an antibody to K10, a type I secondary or tissue-specific keratin expressed in postmitotic suprabasal cells of cornified barrier tissues. The basal cell layer is unstained by the antibody, and the nuclei are counterstained blue. Photos courtesy of Declan Lunny and Birgit Lane, School of Life Sciences, University of Dundee.

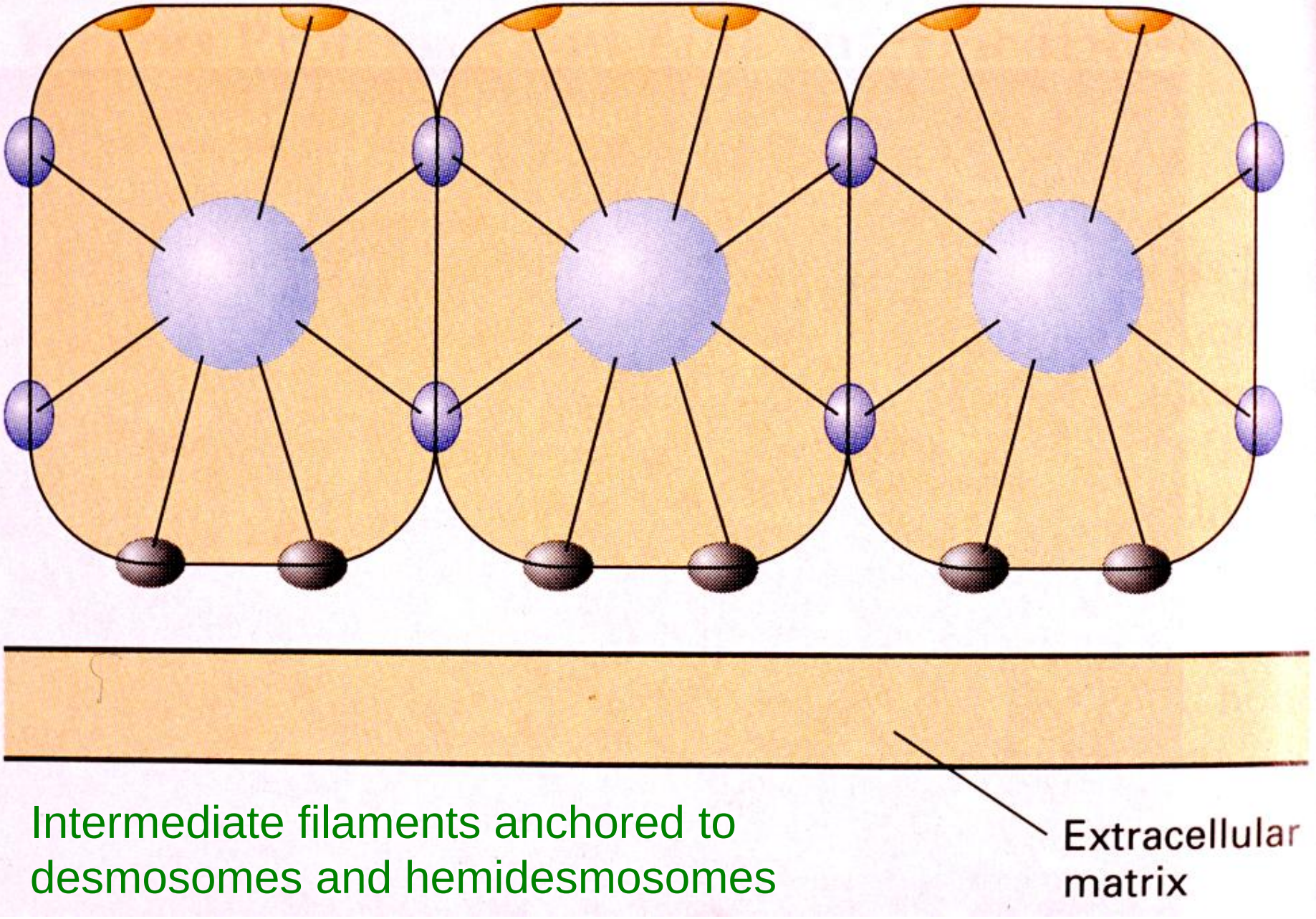

Intermediate filaments anchored to
desmosomes and hemidesmosomes

Keratin filaments in epidermis

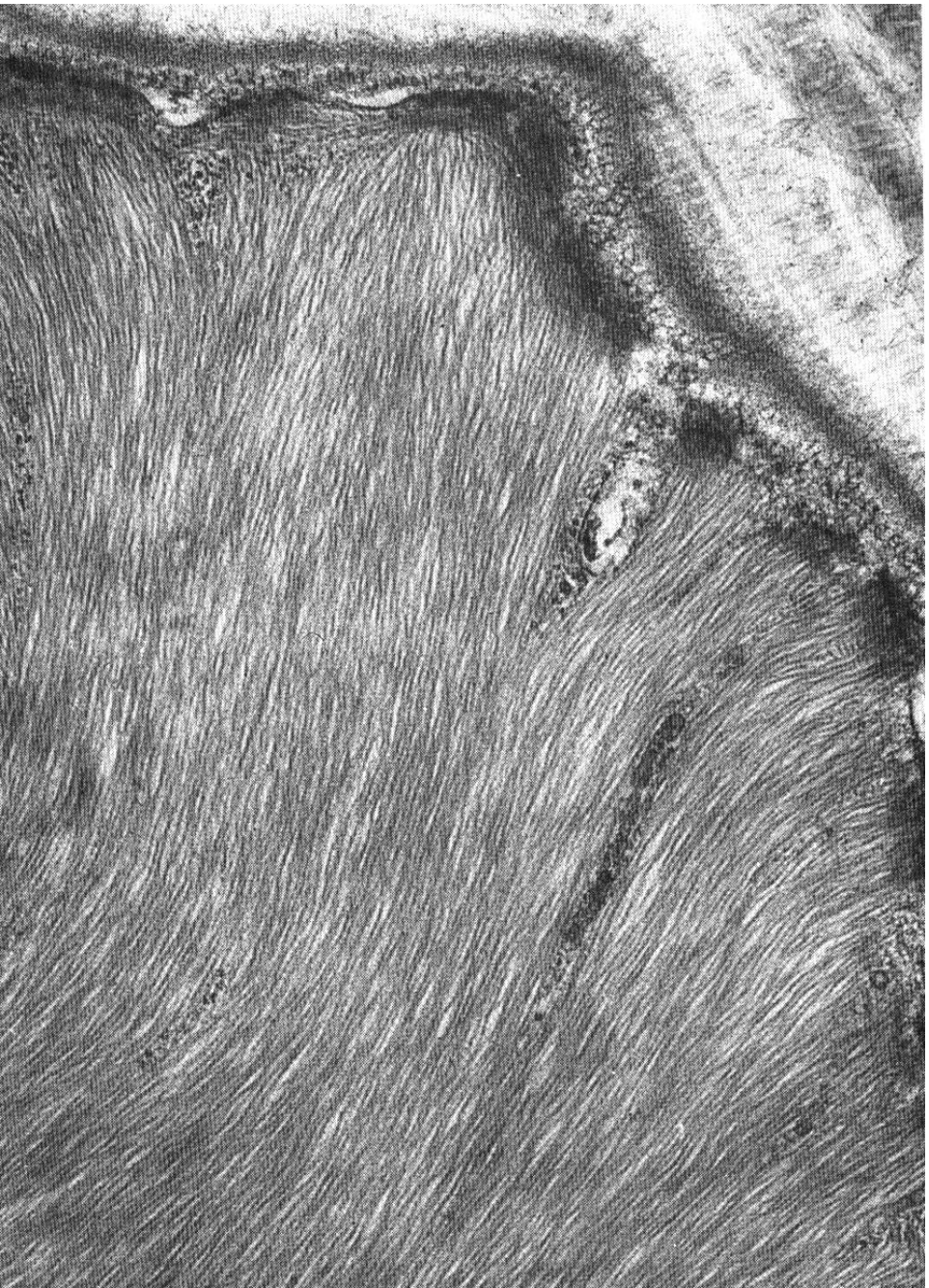

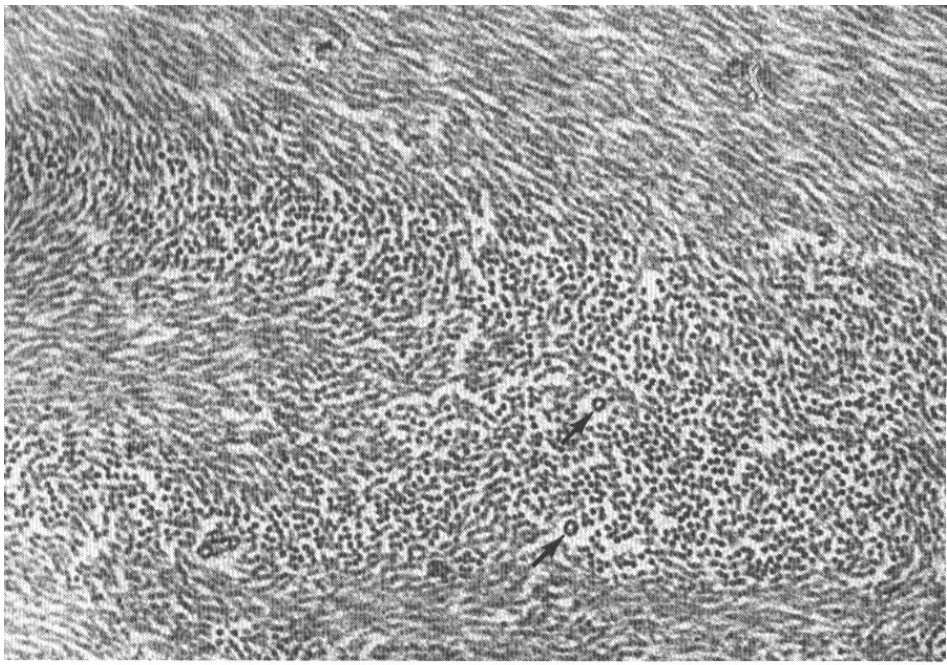

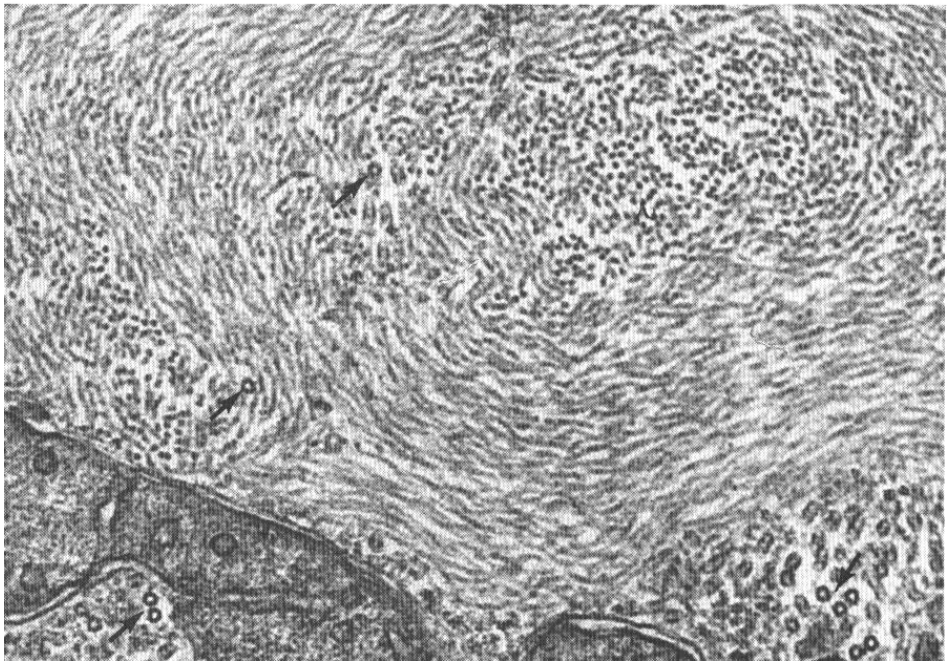

K14 knockout mice

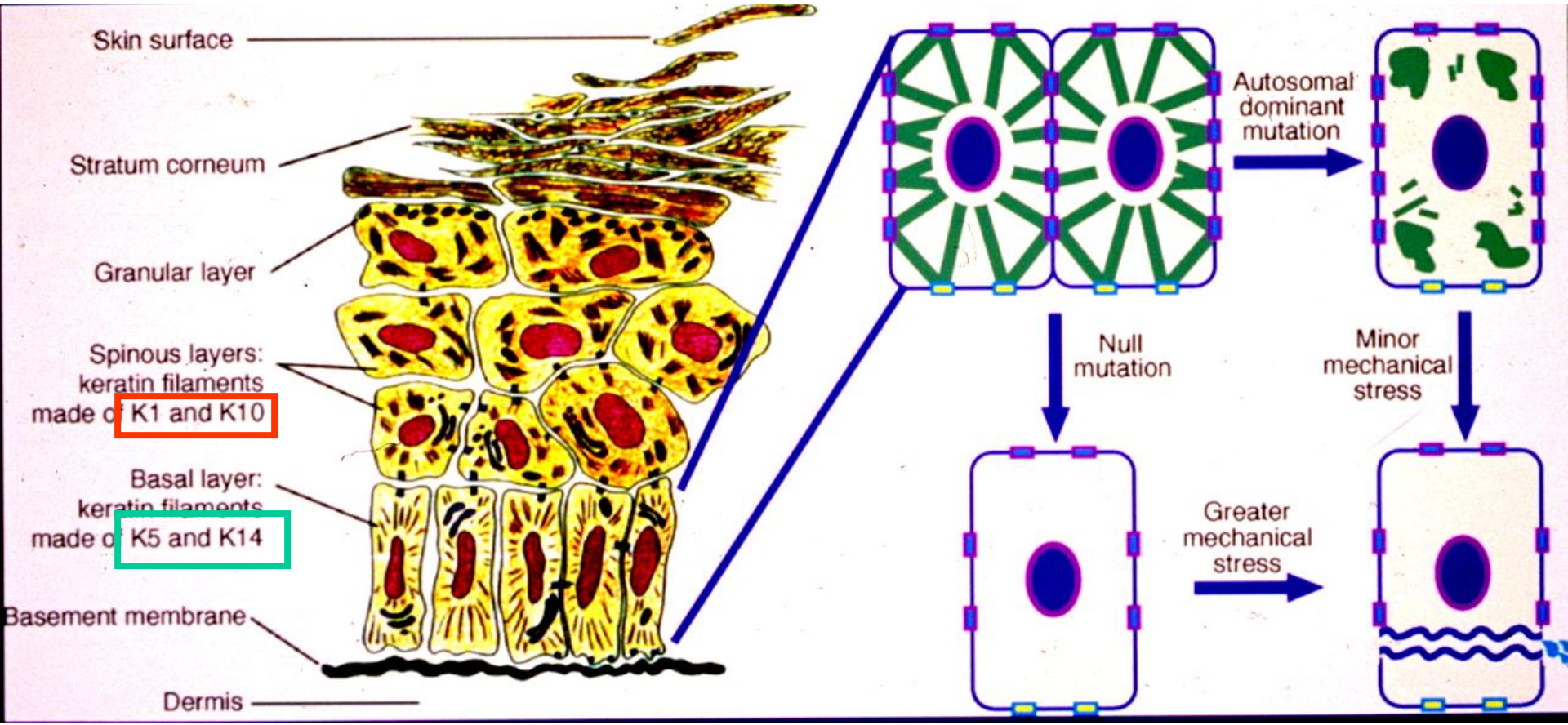

Epidermolysis bullosa simplex K14 mutant

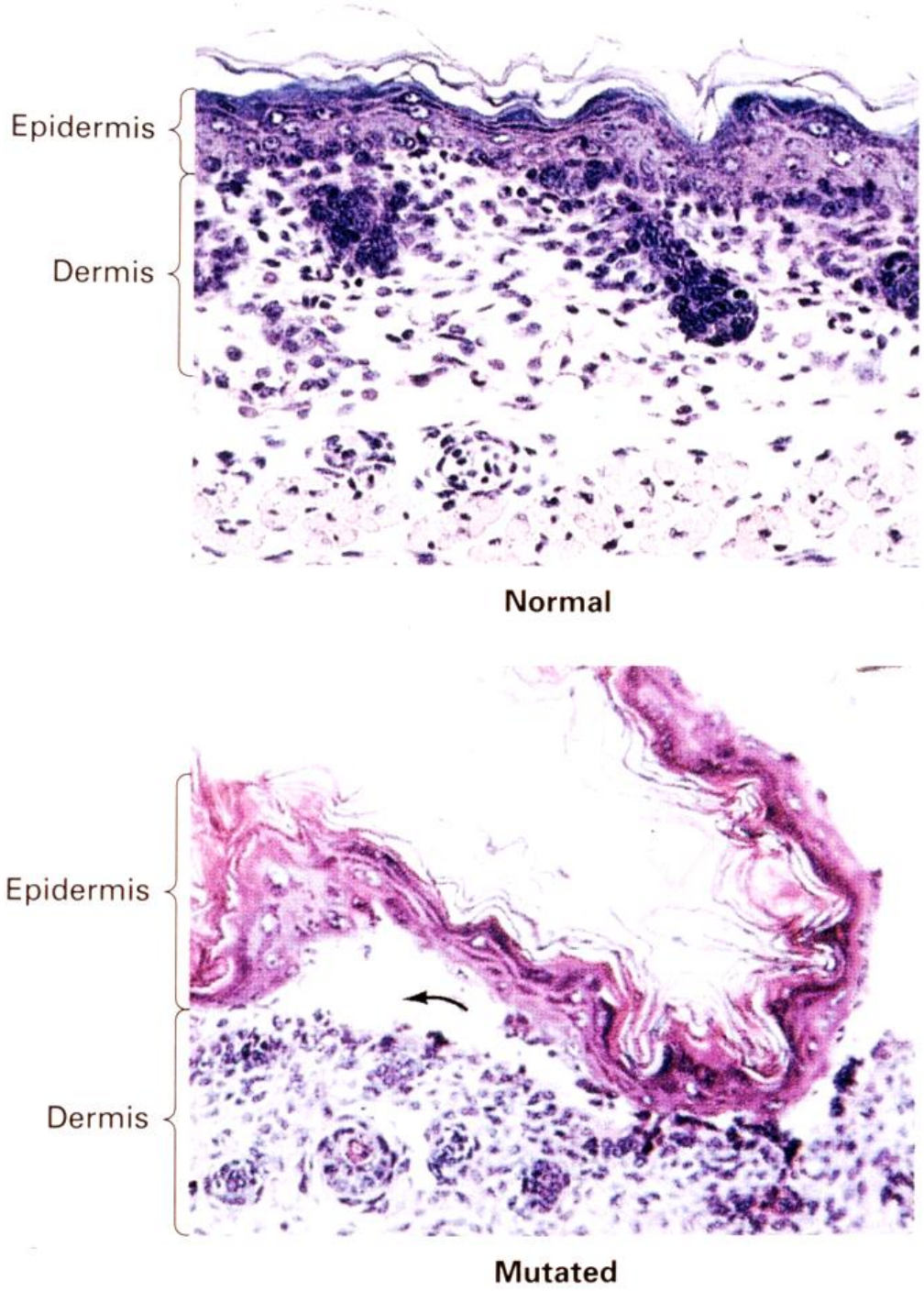

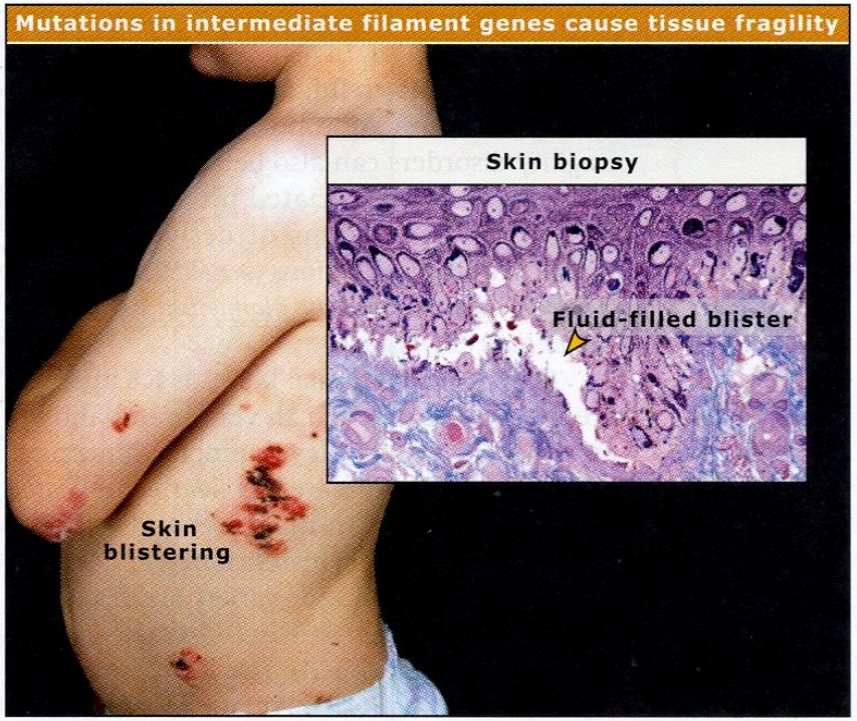

FIGURE 9.11 The condition illustrated here is *epidermolysis bullosa simplex* (EBS), the first disorder linked to intermediate filament gene mutations, caused by mutations in keratins K5 or K14. The main photo shows the characteristic skin blistering caused by scratching, rubbing, or tight clothing. The inset shows a section through a diagnostic skin biopsy taken after rubbing the skin surface with a pencil eraser: the basal layer of epidermal keratinocytes has a fluid-filled blister due to rupturing of the cells. Photos courtesy of Robin A. Eady, St. John's Institute of Dermatology, St. Thomas' Hospital.

Human type III-VI intermediate filament proteins			
	Protein	**Tissue differentiation program**	**Assembly partners *(where known)***
Type III	Vimentin	Widespread	self
	GFAP	Astroglial cells	self
	Desmin	All muscle cell types	self
	Peripherin	Peripheral nervous system; some CNS; injured axons	self, NF-L
Type IV	NF-H	Neurons	NF-L
	NF-M	Neurons	NF-L
	NF-L	Neurons	self
	Nestin	Widespread: neuroepithelial stem cells, glial cells, muscle	type III
	α-internexin	Neurons	self
	Synemin α, Desmuslin/synemin β	Muscle cells	type III
	Syncoilin	Muscle cells	type III, IV
Type V	Lamin A	Nuclei: many cell types, differentiated	Lamin A, C
	Lamin C1,C2	Nuclei: many cell types, differentiated	Lamin A, C
	Lamin B1	Nuclei: many cell types, less differentiated	Lamin B
	Lamin B2, B3	Nuclei: from early development	Lamin B
Type VI	Filensin/ CP115	Eye lens	CP49
	CP49/ phakinin	Eye lens	Filensin

FIGURE 9.12 The human intermediate filament proteins in the types III-VI sequence homology groups.

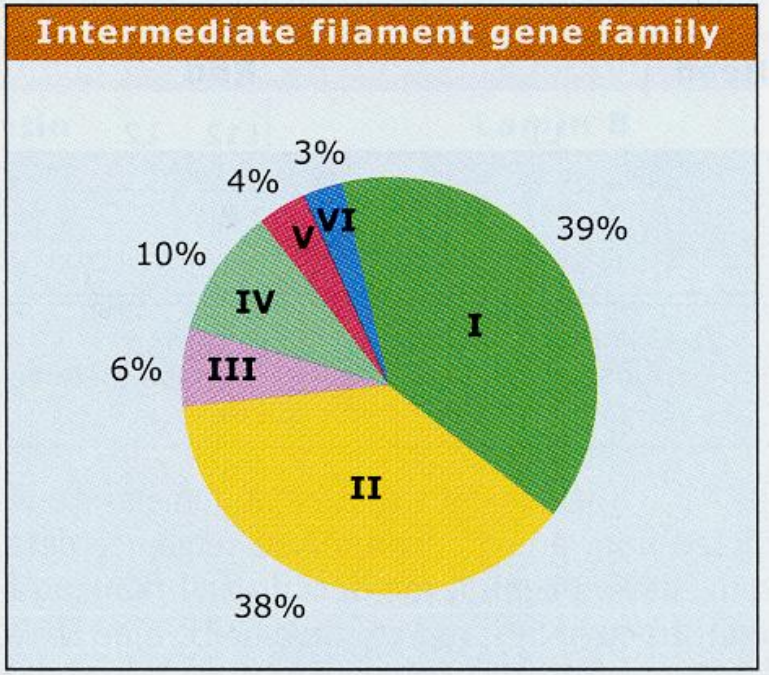

FIGURE 9.4 The intermediate filament genes can be divided into six groups based on sequence similarities. The type I and type II genes constitute the majority of intermediate filament genes (shown as percentages).

Lamins: Nuclear intermediate filaments

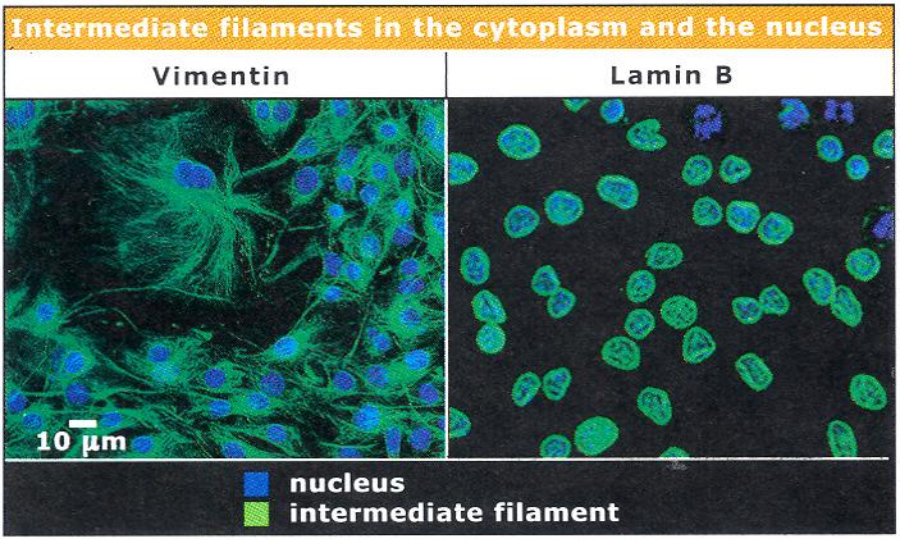

FIGURE 9.1 Immunofluorescence micrographs of vimentin and lamin B in cultured fibroblasts show the distribution of different types of intermediate filaments. Vimentin is restricted to the cytoplasm, whereas lamins are restricted to the nucleus. Photos courtesy of John Common and Birgit Lane, Centre for Molecular Medicine, Singapore.

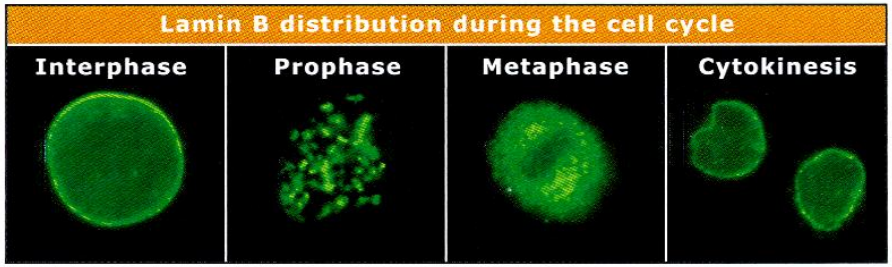

FIGURE 9.14 Immunofluorescence labeling of lamin B in fibroblast cells at progressive stages of the cell cycle. Lamin B staining localized to the nuclear envelope appears veil-like in interphase but fragments as the lamins become phosphorylated in prophase. Lamin B stays dispersed through metaphase and reassociates with chromatin in telophase to produce a new nuclear envelope around each daughter nucleus at cytokinesis. Photos courtesy of John Common and Birgit Lane, Centre for Molecular Medicine, Singapore.

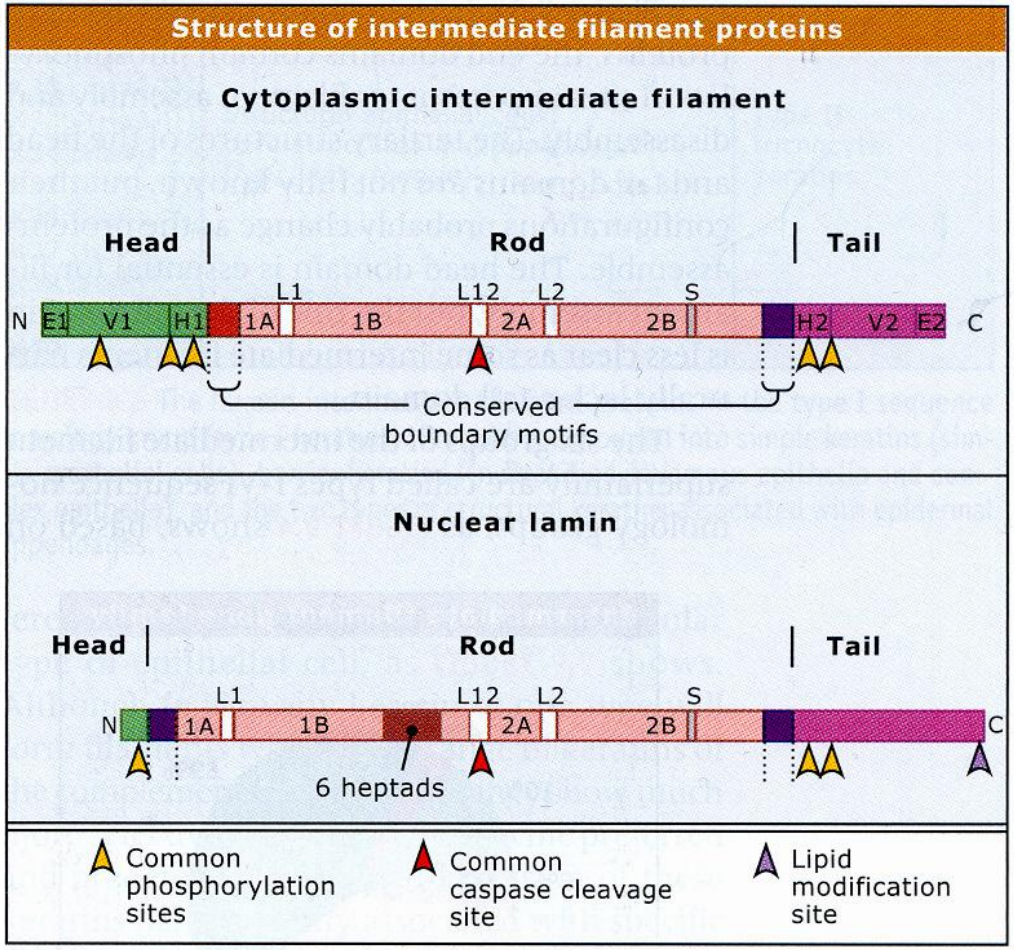

FIGURE 9.3 The general structure of human intermediate filament proteins, as predicted from primary amino acid sequence data. All intermediate filament proteins have a central rod domain and flanking head and tail domains. This general structure best represents type II, type III, and type VI proteins, as type I proteins lack H1/H2 regions and type V proteins lack the E/V domains. For the lamin protein, the position of the additional amino acids lengthening the rod domain in vertebrate lamins and invertebrate filaments is shown. Arrowheads denote common phosphorylation sites (some intermediate filament proteins have additional phosphorylation sites), the common caspase cleavage site, and the common lamin lipid modification site.

Nuclear Lamin Filaments (L) Interacting with Chromatin (C), Various Regulatory Proteins (R), and a Variety of Lamin Binding Proteins (yellow), which Link Lamins to Chromatin or to the Inner Membrane (IM).

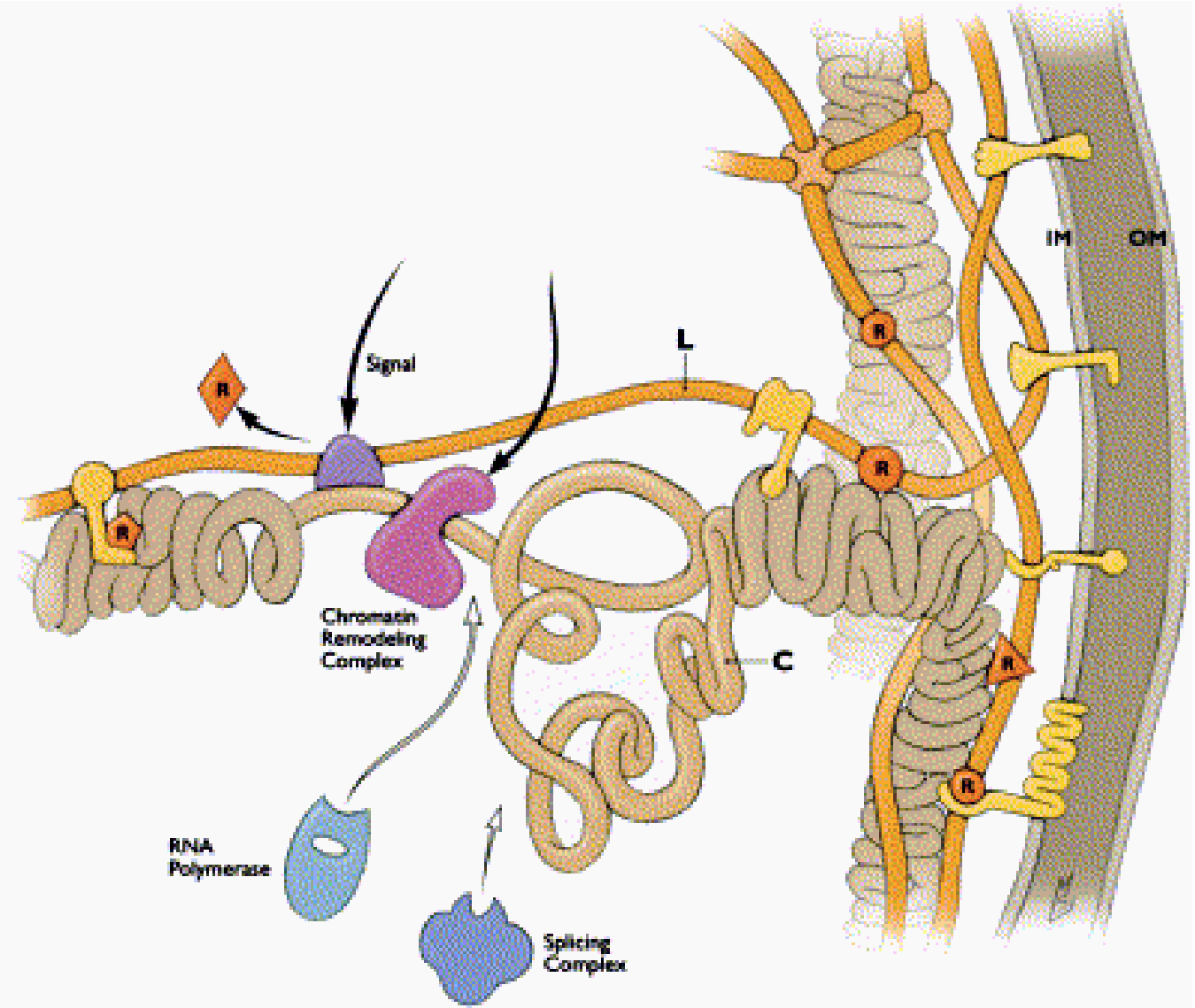

Lamins and actin and some of their proposed interactions

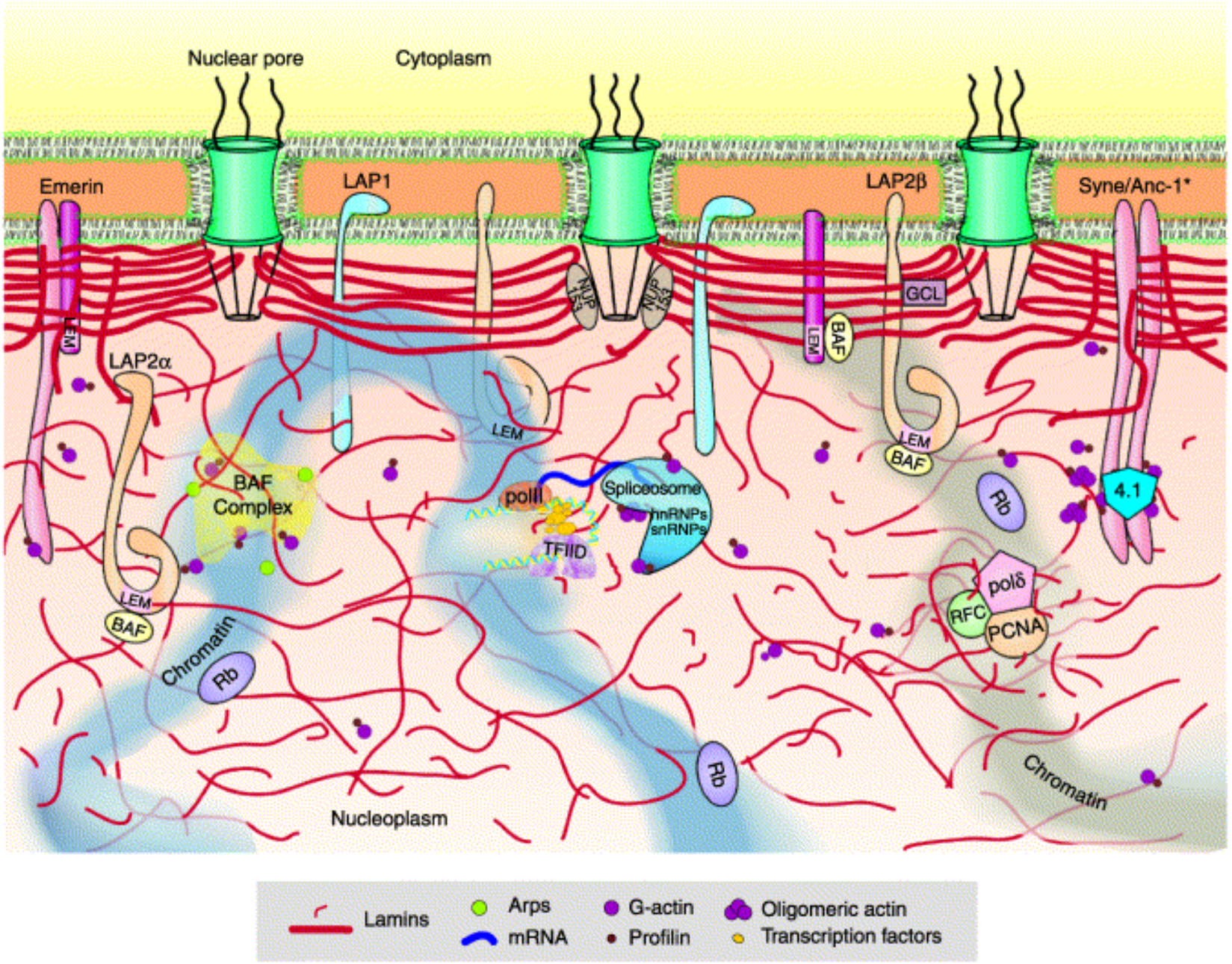

Intermediate Filament Proteins are good markers for determining the differentiation status of neural stem cells

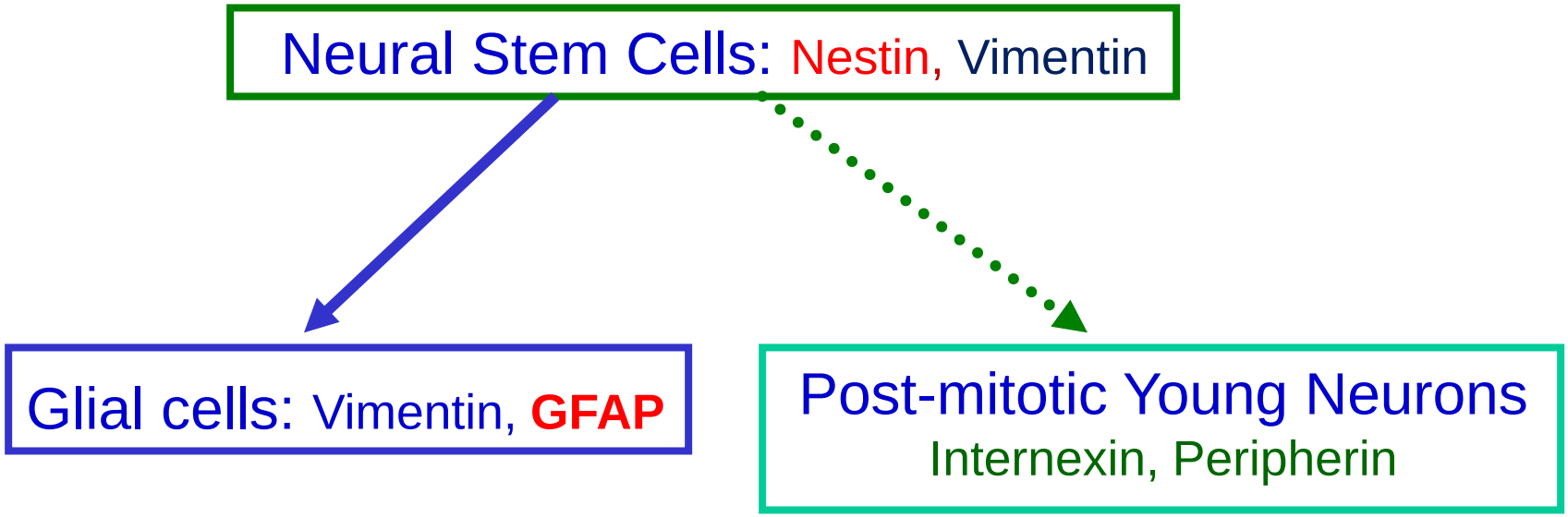

*Muscular cells:
Nestin, Vimentin,and Desmin

Differentiated Mature Neurons
Internexin, Peripherin
Neurofilament triplet Proteins
(NF-L, NF-M, and NF-H)

Desmin

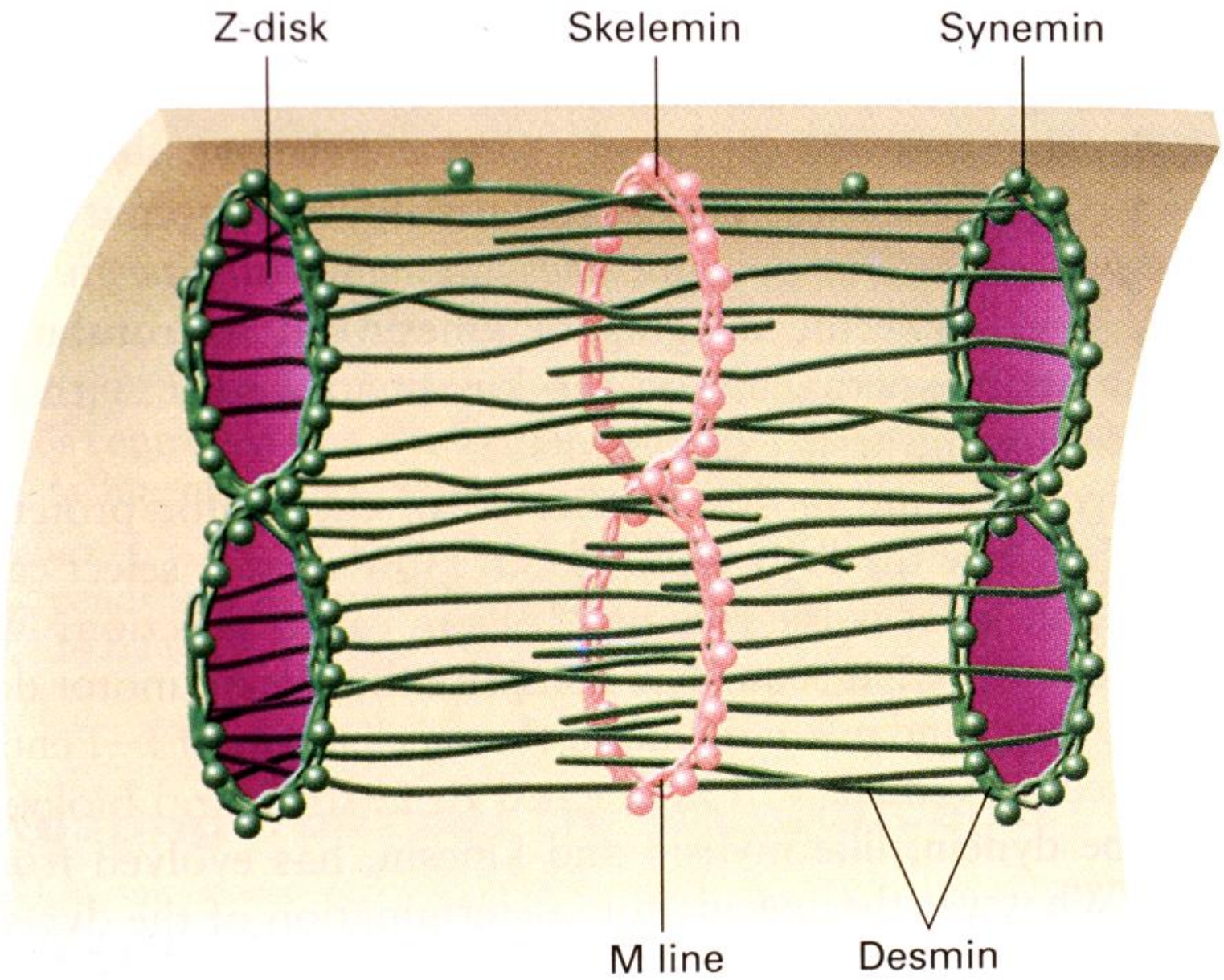

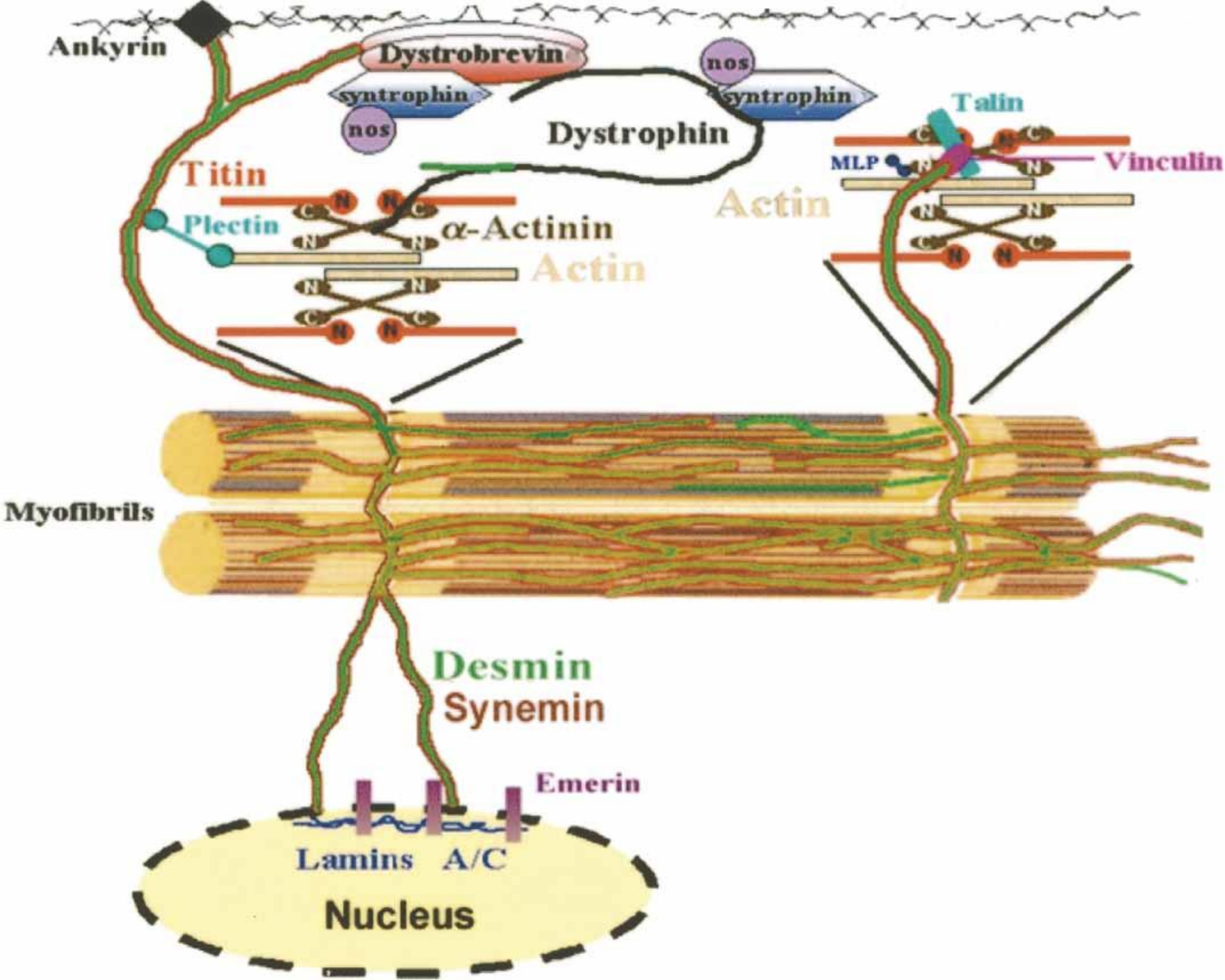
Ankyrin
Dystrobrevin
syntrophin
nos
nos
syntrophin
Dystrophin
Talin
MLP
Vinculin
Titin
Plectin
α-Actinin
Actin
Actin
Myofibrils
Desmin
Synemin
Emerin
Lamins A/C
Nucleus

Immuno-characterization of desmin in striated muscle.
Left: transversal section; right: longitudinal section

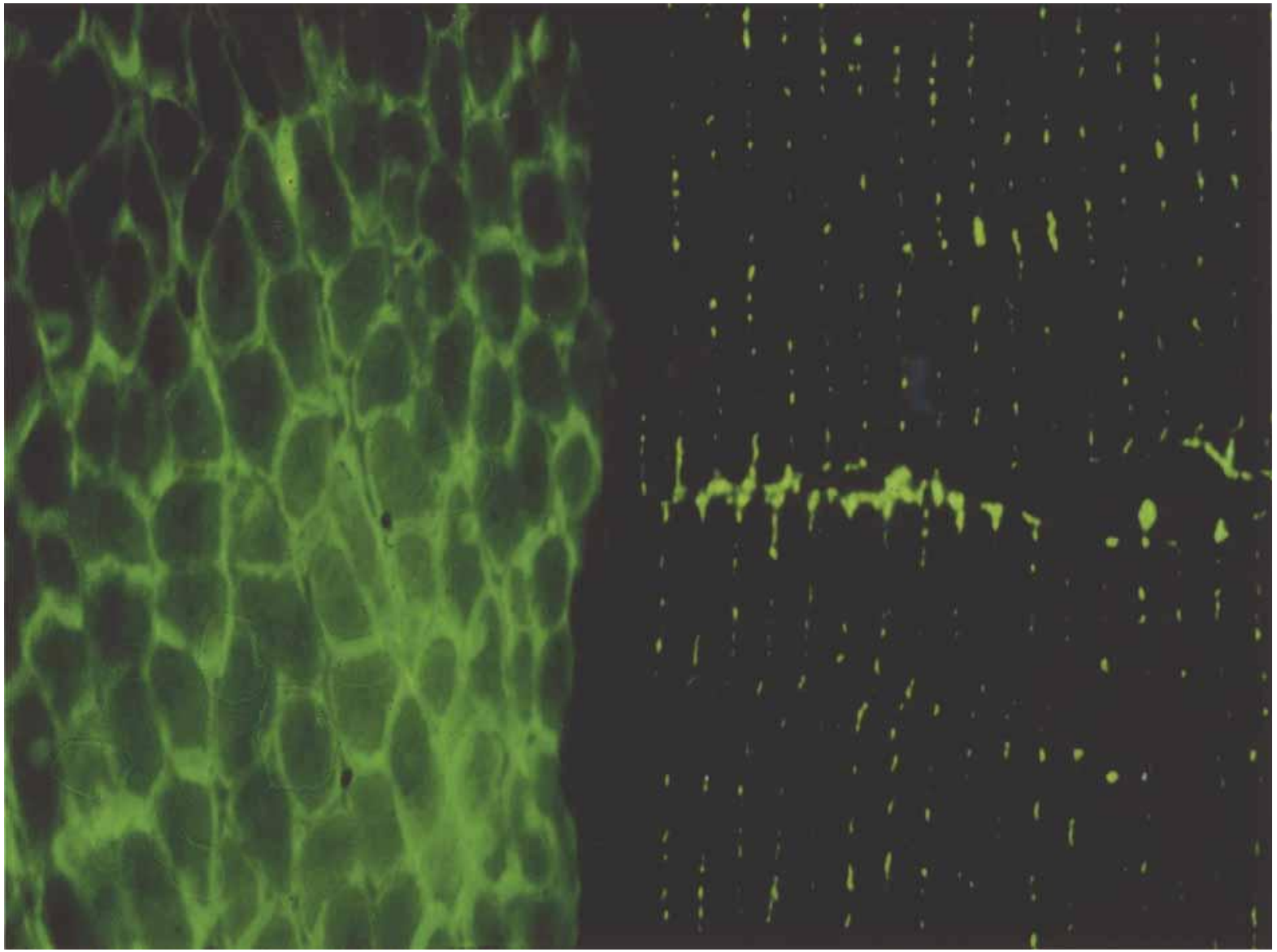

Disorganization of intercalated discs in desmin knockout (KO) mice. Des +/+ = desmin normal mice; Des -/- = desmin KO mice. Arrows point to the intercalated discs.

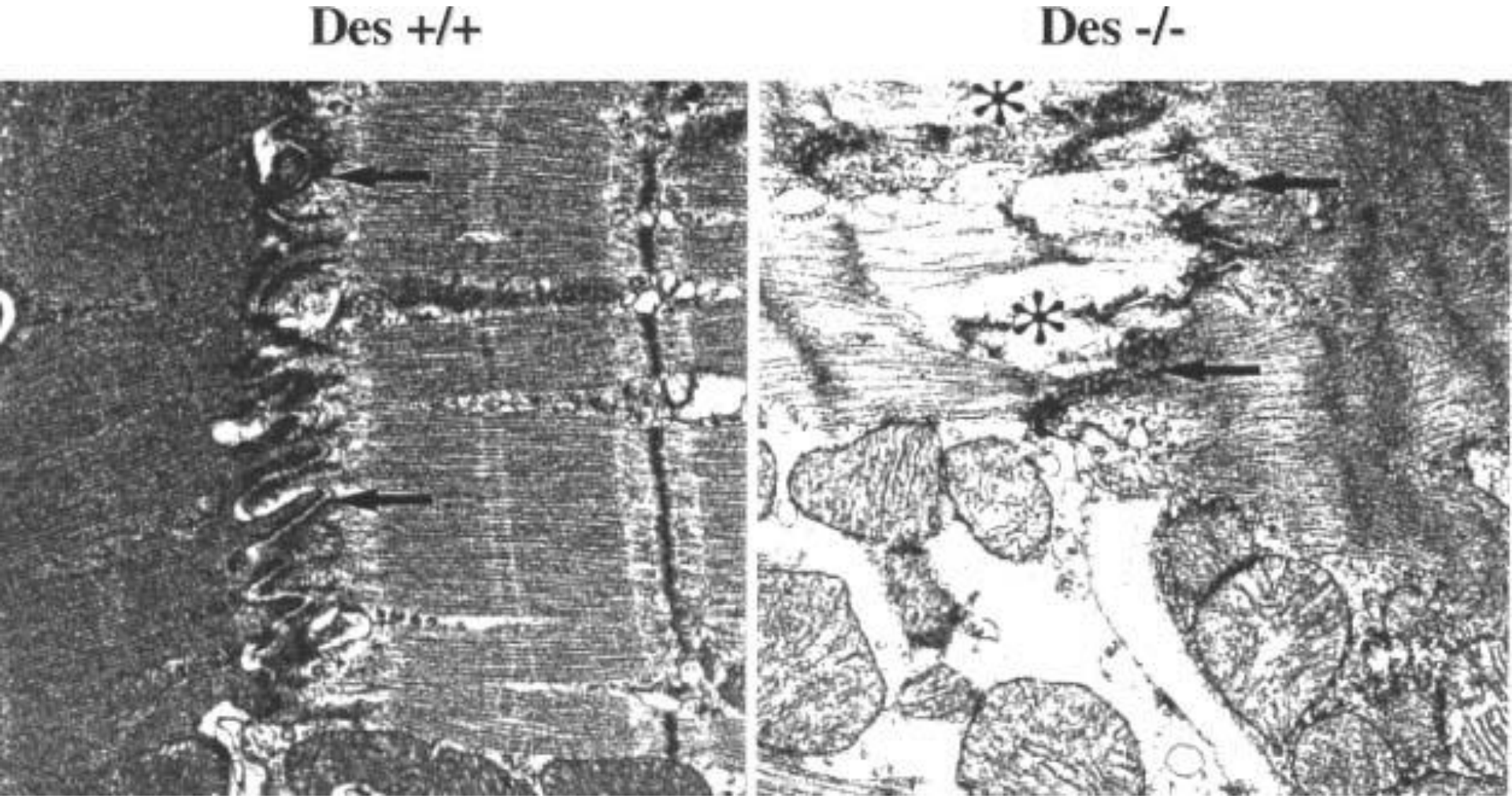

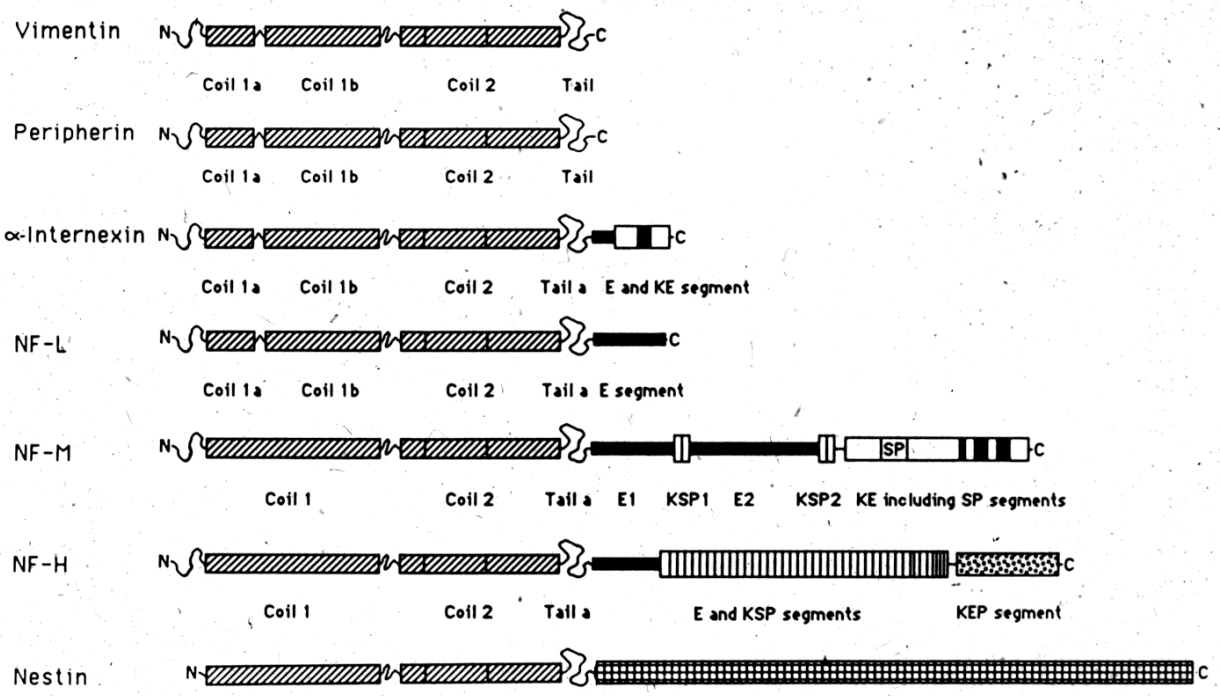
Vimentin
N
C
Coil 1a
Coil 1b
Coil 2
Tail
Peripherin
N
C
Coil 1a
Coil 1b
Coil 2
Tail
∝-Internexin
N
C
Coil 1a
Coil 1b
Coil 2
Tail a
E and KE segment
NF-L
N
C
Coil 1a
Coil 1b
Coil 2
Tail a
E segment
NF-M
N
SP
C
Coil 1
Coil 2
Tail a
E1
KSP1
E2
KSP2
KE including SP segments
NF-H
N
C
Coil 1
Coil 2
Tail a
E and KSP segments
KEP segment
Nestin
N
C

Axon

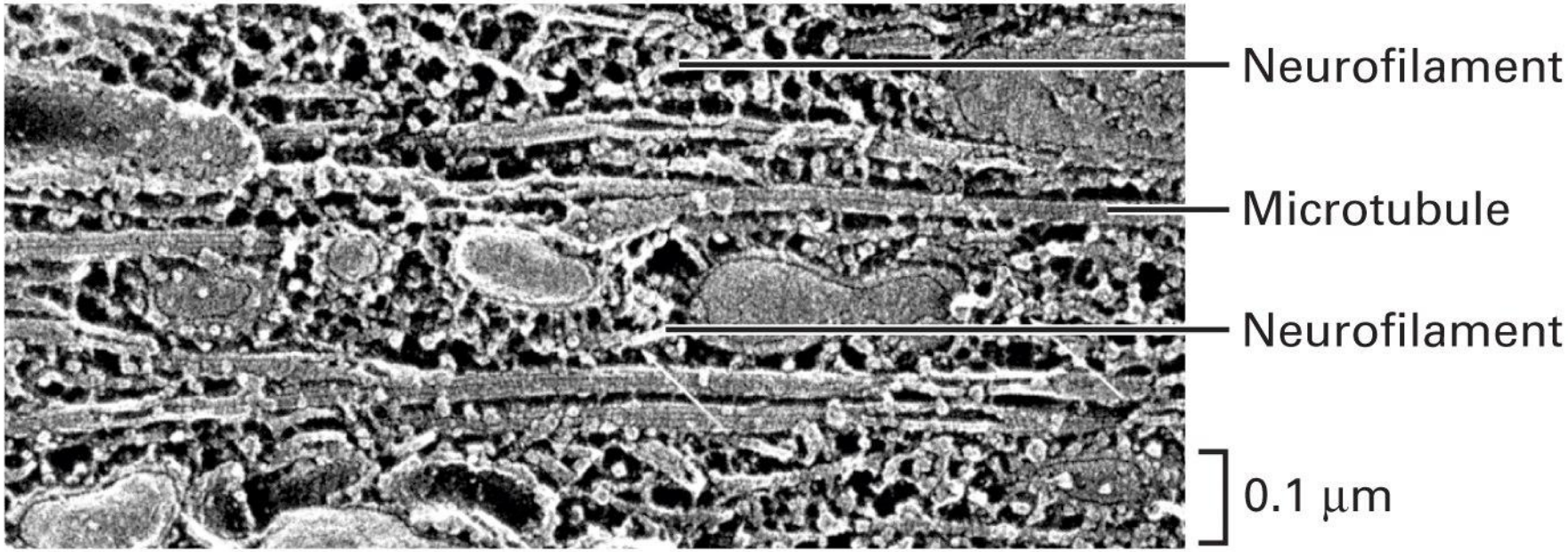
Neurofilament
Microtubule
Neurofilament
0.1 μm

Primary culture of embryonic hippocampal cells

α-internexin: a 66 kD protein,

the first neuronal intermediate filament protein expressed in the post-mitotic neurons of developing mammalian central nervous system

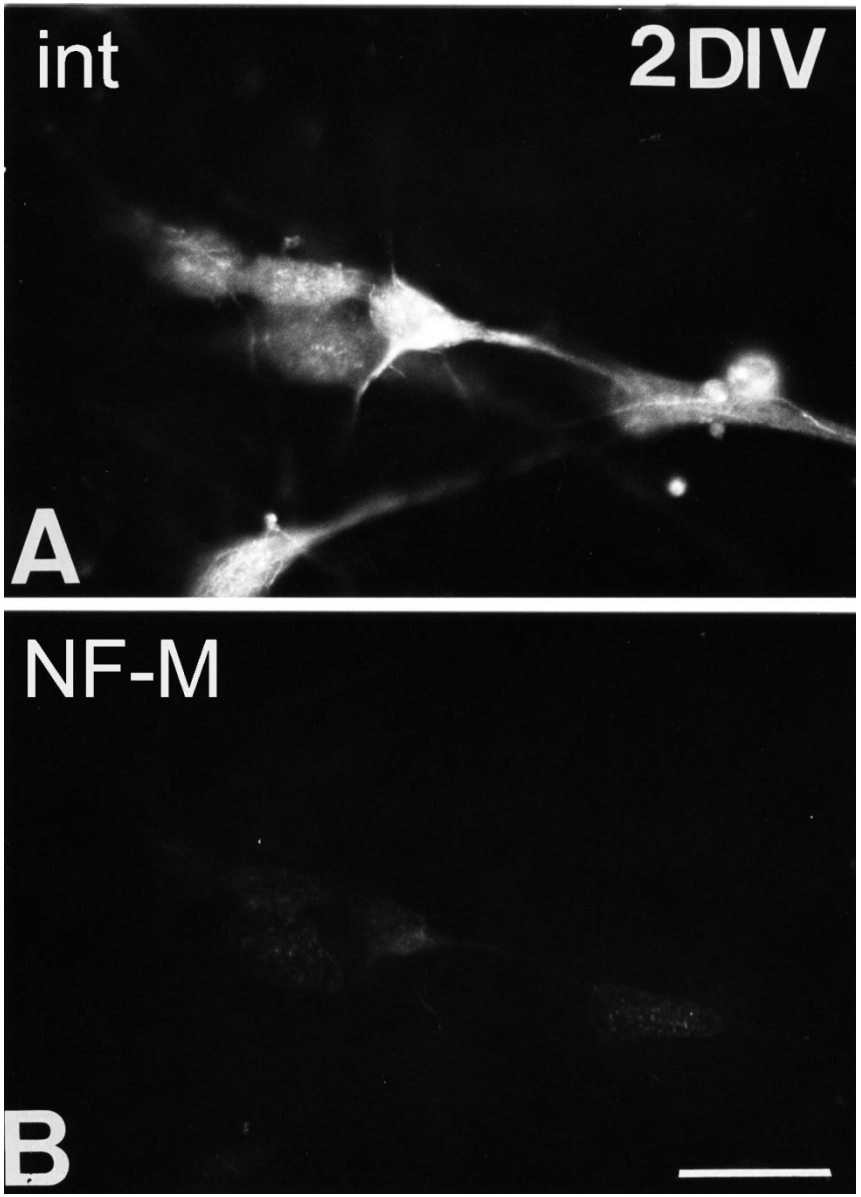

Internexin, NF-M, NF-L but not NF-H expressed in the 6 days *in vitro* (DIV) culture of hippocampal neurons

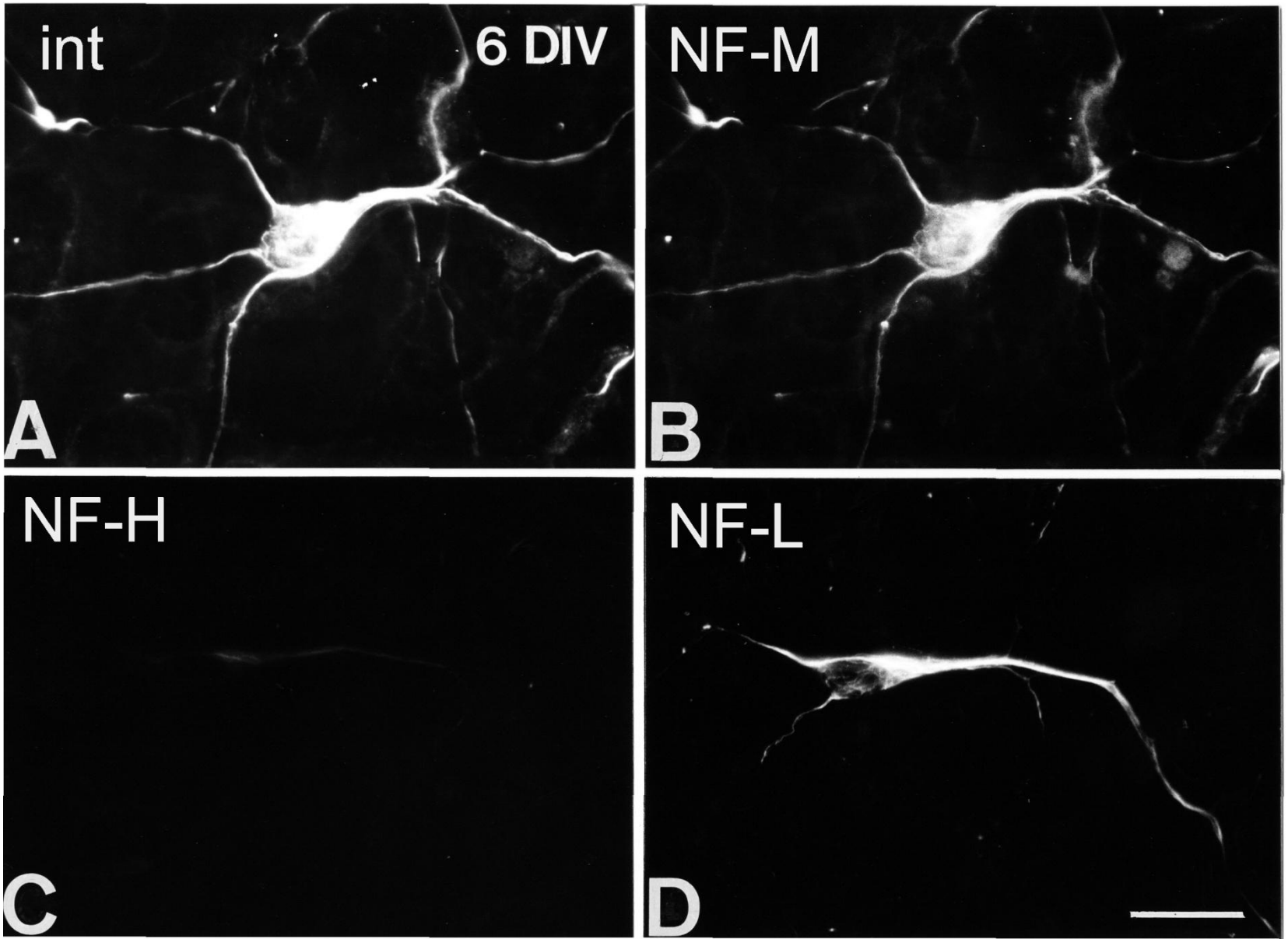

Internexin and Neurofilament Triplet Proteins (NF-L, NF-M and NF-H) all expressed in the 13 DIV hippocampal neurons

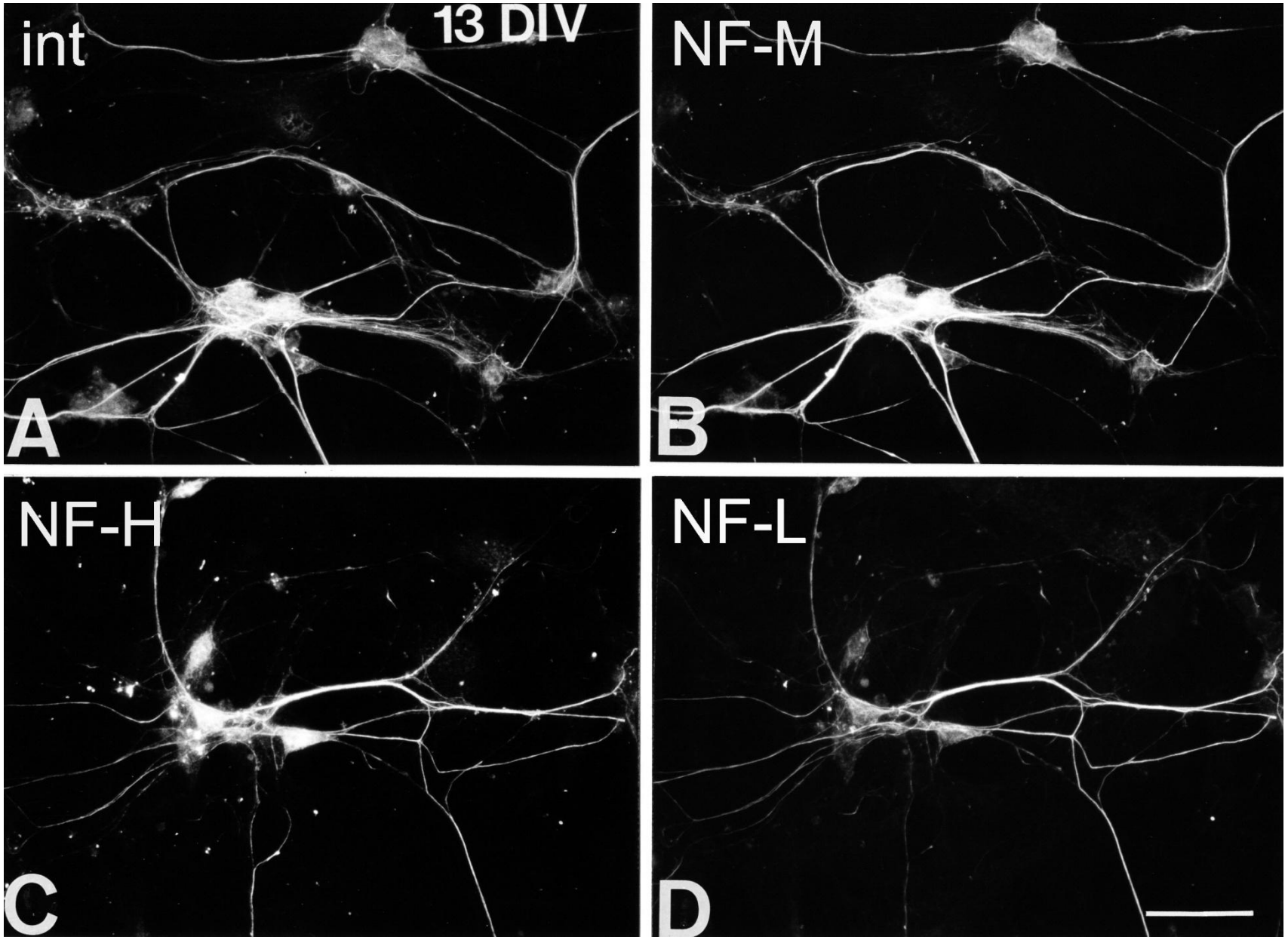

Neurofilaments and GFAP

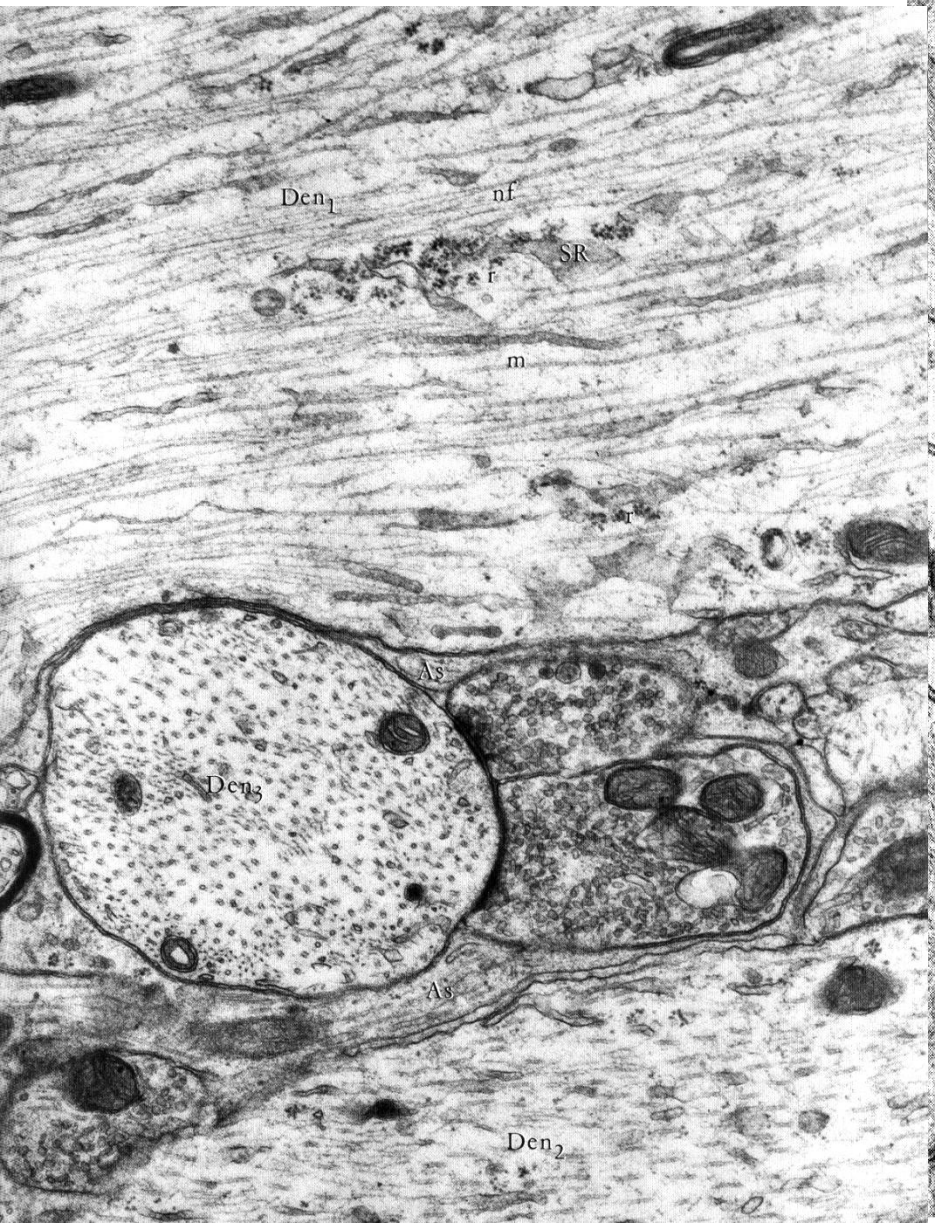

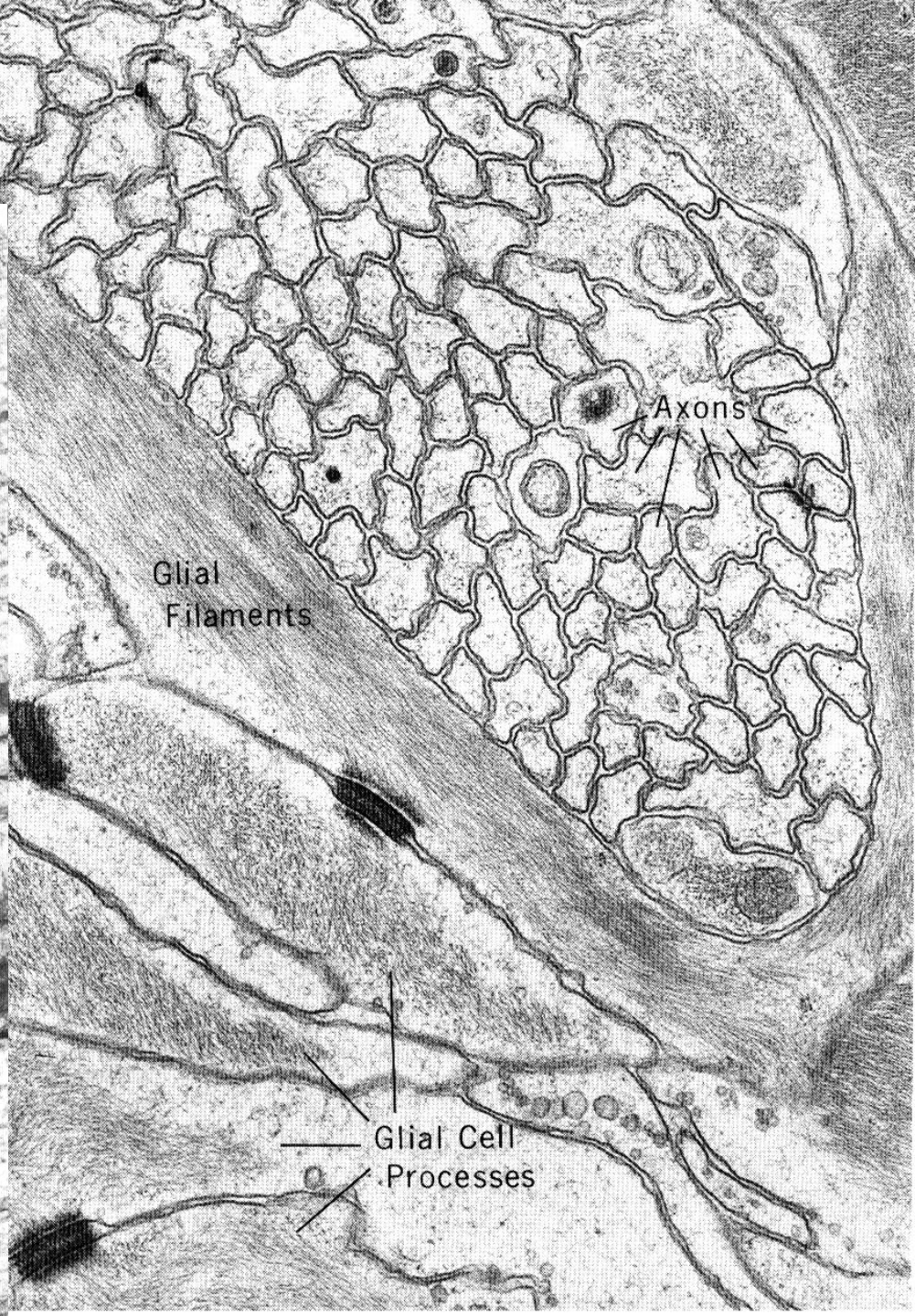

Primary culture of early postnatal cerebellar cells

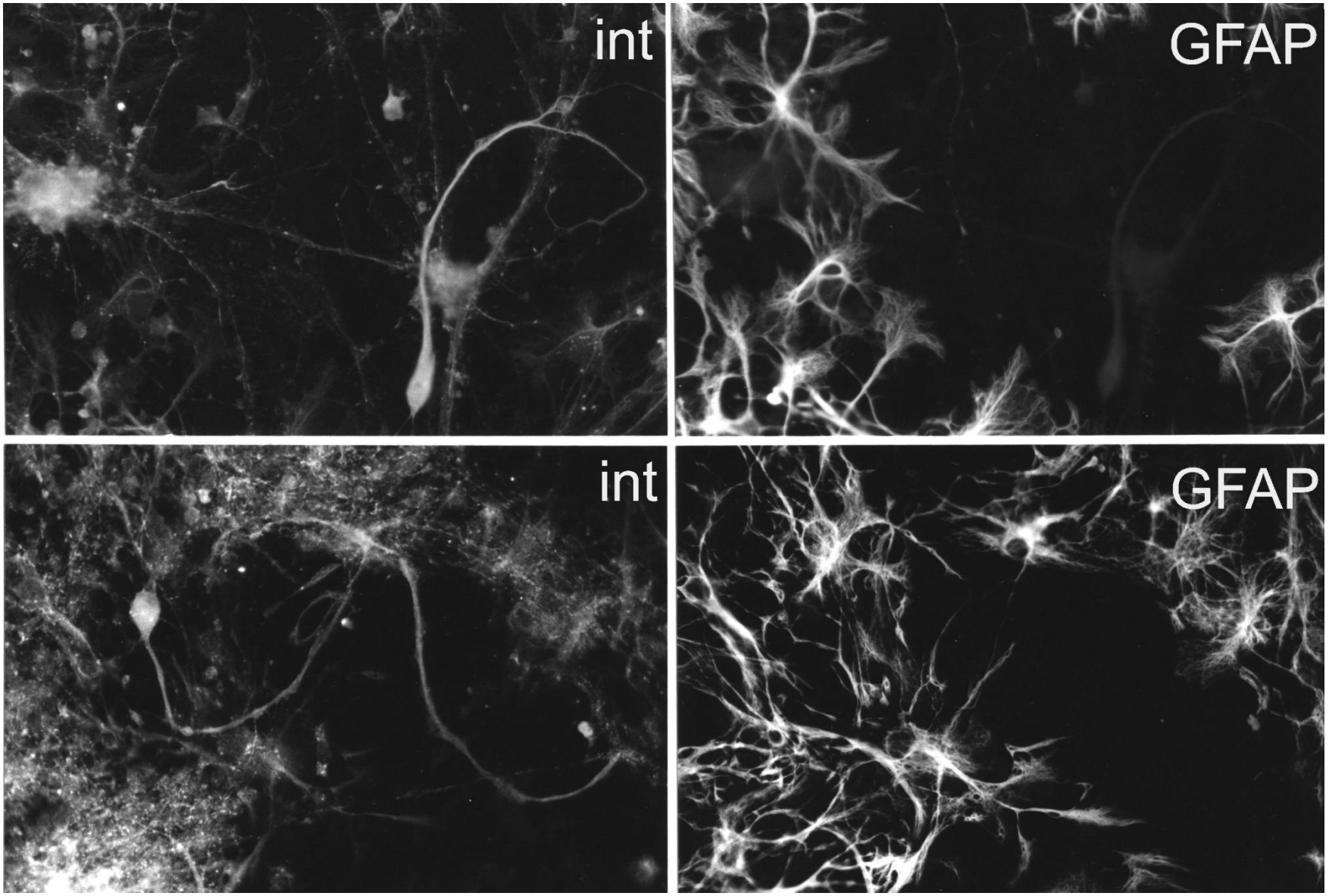

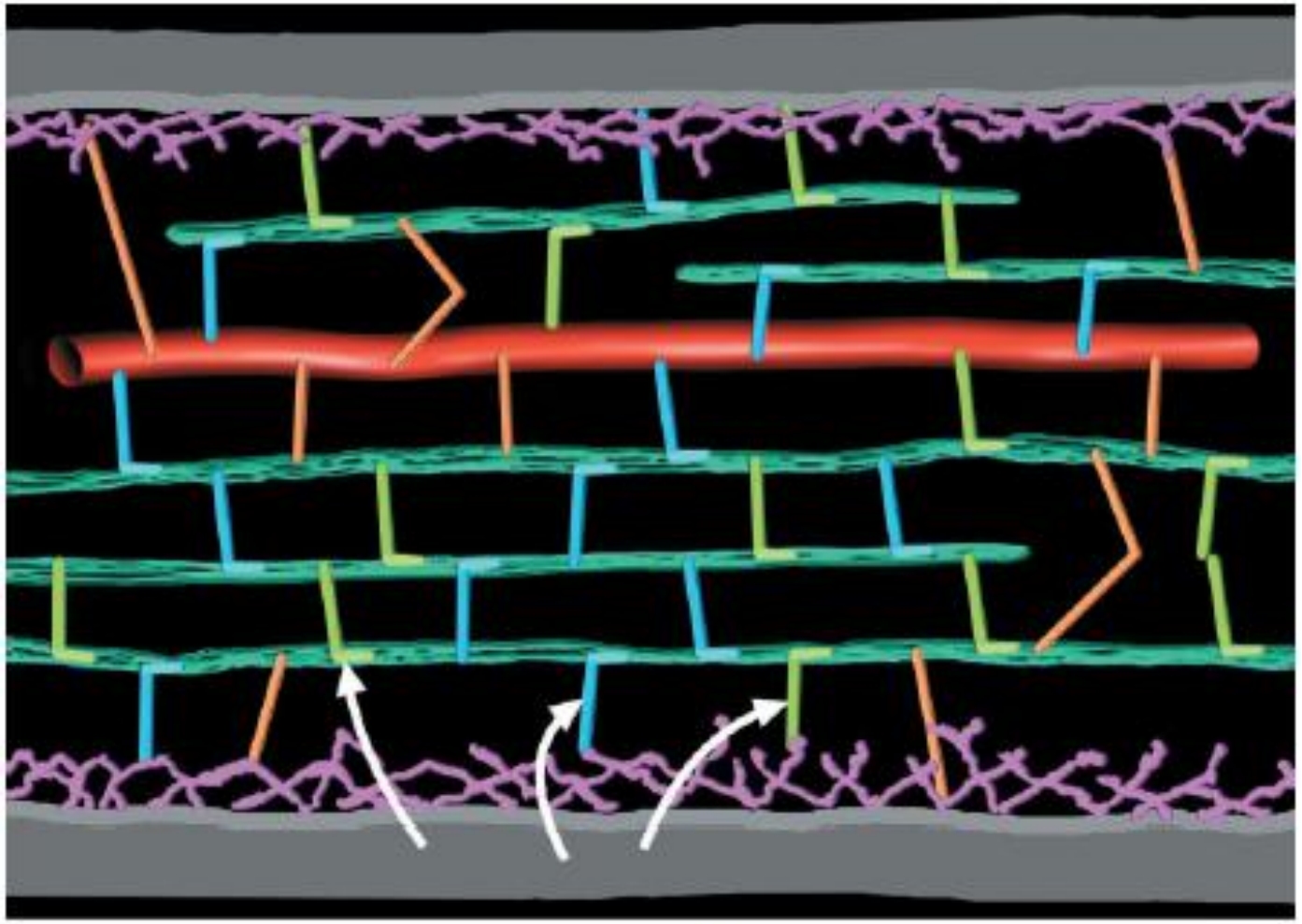
NF
MT
Plakin
Actin
NF-H tails
NF-M tails
Myelin
Axolemma

Plectin cross-links between IF and microtubules

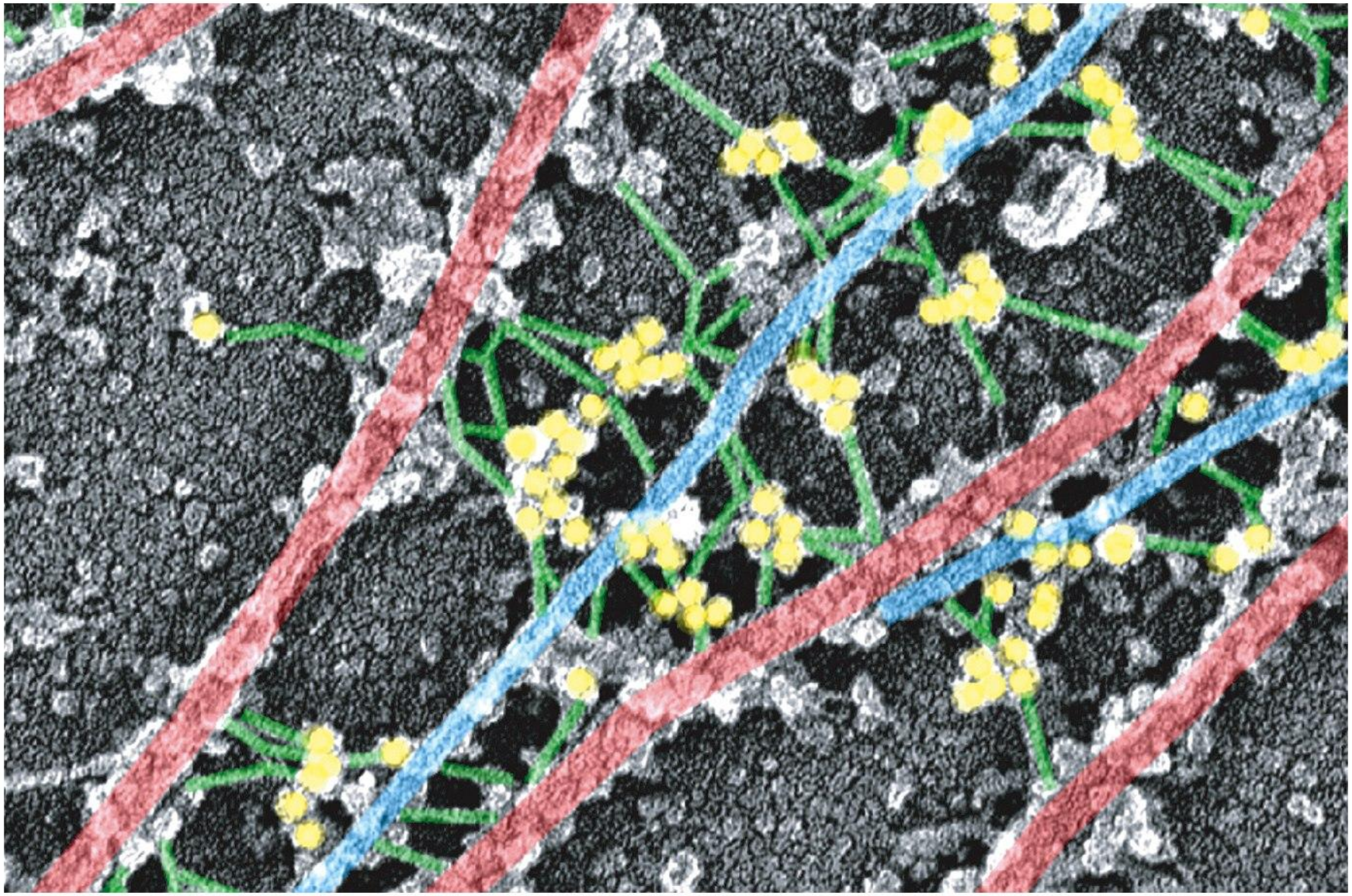

Plakins: linker proteins

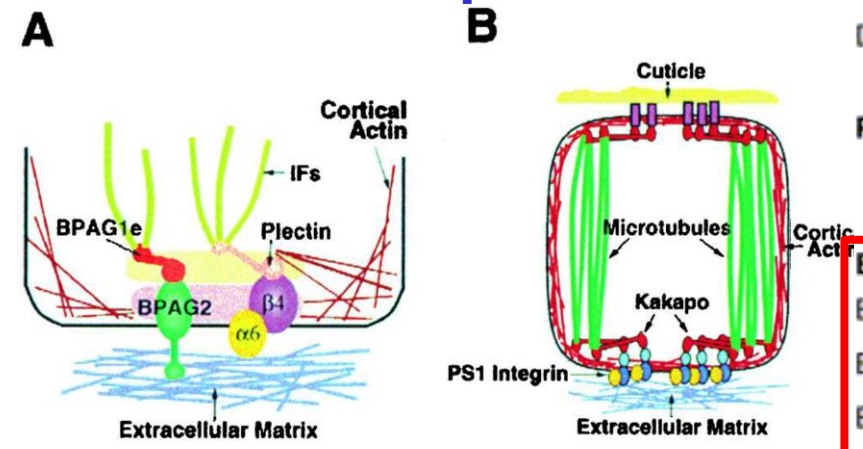

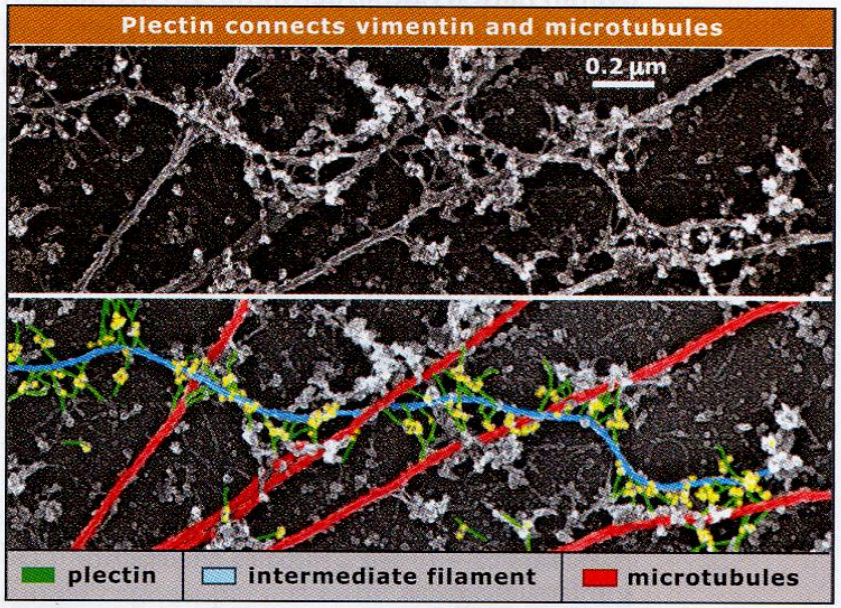

FIGURE 9.19 Plakins bind to intermediate filaments and integrate them with actin filaments and microtubules. These scanning electron micrographs show microtubules and intermediate filaments interacting with the large plakin protein, plectin. The bottom image is a false colored version of the top micrograph. Plectin has been conjugated to gold particles (yellow). Photos courtesy of Tatyana M. Svitkina, University of Pennsylvania. Reproduced from *The Journal of Cell Biology*, 1996, vol. 135, pp. 991-1007, by copyright permission of The Rockefeller University Press.

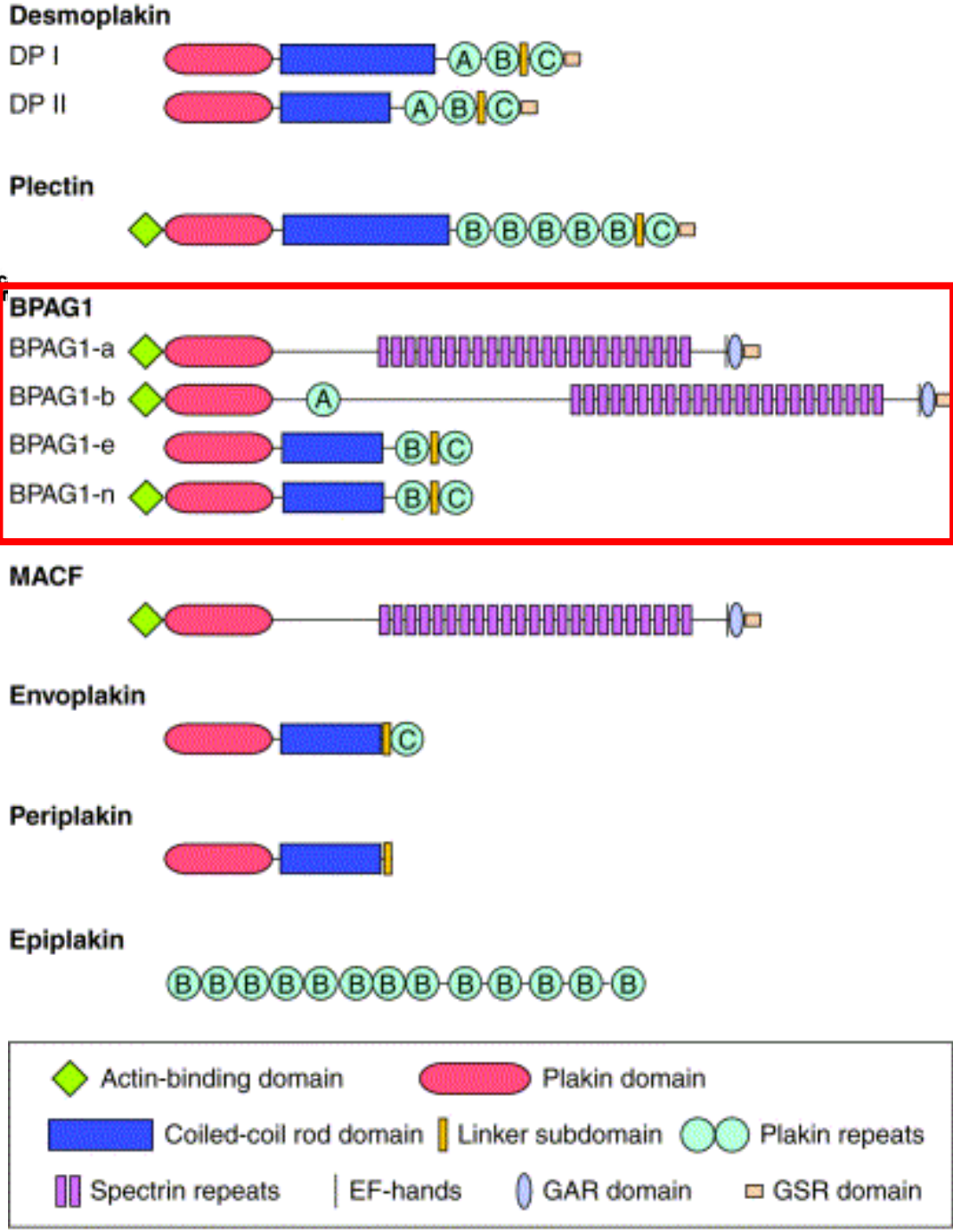

TRENDS in Cell Biology

Nature Mutant for Neuronal Degeneration

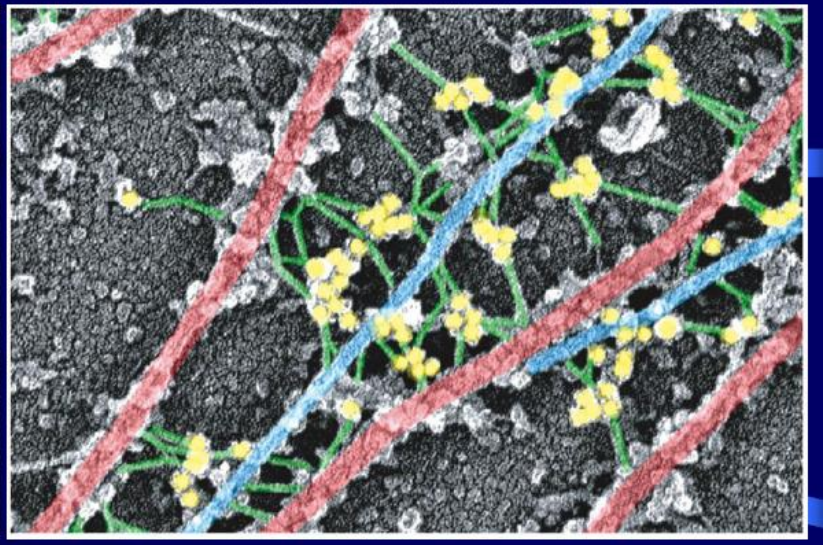

- *Dystonia musculorum (dt)* mouse is a recessive hereditary sensory neuropathy of the mutant mouse, which is defective in *BPAG1* gene.
- Mice affected with *dt* are seemingly normal at birth, but by 10–12 days they begin twitching, writhing, and exhibiting uncoordinated movements.
- **BPAG1** cross-links the intermediate filaments and other cytoskeletons.

(J. Neuropathol. Exp. Neurol. 65:336-347 , 2006)

Summary I

- The interaction between BPAG1 and α-internexin may be one of the key factors involved in the neuronal degeneration of DRG in the *dt* mutant.
- Abnormal accumulation of α-internexin and other cytoskeletal components may impair the axonal transport and subsequently turn on the cascade of neuronal apoptosis during development.

(J. Neuropathol. Exp. Neurol. 65:336-347 , 2006)